AFRL-VA-WP-TR-2002-3047

INTEGRATED HYPERSONIC AEROTHERMOELASTIC METHODOLOGY FOR TRANSATMOSPHERIC VEHICLE (TAV)/THERMAL PROTECTION SYSTEM (TPS) STRUCTURAL DESIGN AND OPTIMIZATION

D.D. Liu
P.C. Chen
Lei Tang
K.T. Chang

ZONA Technology, Inc.
7430 E. Stetson Drive, Suite 205
Scottsdale, AZ 85251

Adel Chemaly
Hilmi Kamhawi

TechnoSoft, Inc.
4434 Carver Woods Drive
Cincinnati, OH 45242-5545

JANUARY 2002

FINAL REPORT FOR 30 MARCH 2001 – 30 DECEMBER 2001

THIS IS A SMALL BUSINESS INNOVATION RESEARCH (SBIR) PHASE 1 REPORT

AIR VEHICLES DIRECTORATE
AIR FORCE MATERIEL COMMAND
AIR FORCE RESEARCH LABORATORY
WRIGHT-PATTERSON AIR FORCE BASE, OH 45433-7542

NOTICE

Using government drawings, specifications, or other data included in this document for any purpose other than government procurement does not in any way obligate the U.S. Government. The fact that the government formulated or supplied the drawings, specifications, or other data does not license the holder or any other person or corporation; or convey and rights or permission to manufacture, use, or sell any patented invention that may relate to them.

This report has been reviewed by the Office of Public Affairs (ASC/PA) and is releasable to the National Technical Information Service (NTIS). At NTIS, it will be available to the general public, including foreign nations.

This technical report has been reviewed and is approved for publication.

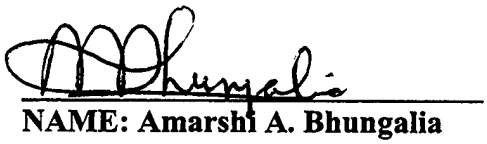

NAME: Amarshi A. Bhungalia
Project Engineer
Structural Design & Development Branch

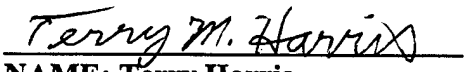

NAME: Terry Harris
Chief
Structural Design & Development Branch

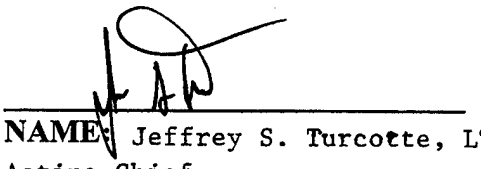

NAME: Jeffrey S. Turcotte, LTC, USAF
Acting Chief
Structures Division

Copies of this report should not be returned unless return is required by security considerations, contractual obligations, or notice on a specific document.

REPORT DOCUMENTATION PAGE

Form Approved
OMB No. 0704-0188

1. REPORT DATE *(DD-MM-YY)*	2. REPORT TYPE	3. DATES COVERED *(From - To)*
January 2002	Final	03/30/2001 – 12/30/2001

4. TITLE AND SUBTITLE

Integrated Hypersonic Aerothermoelastic Methodology for Transatmospheric Vehicle (TAV)/Thermal Protection System (TPS) Structural Design and Optimization

5a. CONTRACT NUMBER
F33615-01-M-3131

5b. GRANT NUMBER

5c. PROGRAM ELEMENT NUMBER
65502F

6. AUTHOR(S)

D.D. Liu (Zona)
P.C. Chen (Zona)
Lei Tang (Zona)
K.T. Chang (Zona)
Adel Chemaly (TechnoSoft)
Hilmi Kamhaw (TechnoSoft)

5d. PROJECT NUMBER
3005

5e. TASK NUMBER
42

5f. WORK UNIT NUMBER
2B

7. PERFORMING ORGANIZATION NAME(S) AND ADDRESS(ES)

ZONA Technology, Inc.
7430 E. Stetson Drive, Suite 205
Scottsdale, AZ 85251

TechnoSoft, Inc.
4434 Carver Woods Drive
Cincinnati, OH 45242-5545

8. PERFORMING ORGANIZATION REPORT NUMBER
ZONA 02-01

9. SPONSORING/MONITORING AGENCY NAME(S) AND ADDRESS(ES)

Air Vehicles Directorate
Air Force Research Laboratory
Air Force Materiel Command
Wright-Patterson AFB, OH 45433-7542

10. SPONSORING/MONITORING AGENCY ACRONYM(S)
AFRL/VASD

11. SPONSORING/MONITORING AGENCY REPORT NUMBER(S)
AFRL-VA-WP-TR-2002-3047

12. DISTRIBUTION/AVAILABILITY STATEMENT
Approved for public release; distribution is unlimited.

13. SUPPLEMENTARY NOTES
This is a Small Business Innovation Research (SBIR) Phase 1 report.

14. ABSTRACT

The adaptation of ZONA unified hypersonic/supersonic method ZONA7U and its integration/development into a ZONA aerothermoelastic software system for transatmospheric vehicle (TAV)/thermal protection system (TPS) design/analysis was proven a successful tool through feasibility study with cases of a CKEM body, blunt cones, and a modeled X-34 wing body. Preceding the feasibility study, substantial effort was directed toward further development of a new code, ZSTREAM, and using it and ZAERO to replace the outdated modules in SHVD, thus to couple them with SHABP for aerothermoelastic applications. In the feasibility study, the cases are well validated with FD solutions. Next, computed heat rates by applying ZONA aerothermoelastic software to X-34 through two assigned hypersonic trajectories were shown and found to agree with those using MINIVER. A potential TPS design procedure was established using the obtained heat rates as an input to MINIVER, resulting in a minimum weight TPS per hot-wall consideration. With FEM/TRIM modules, ASTROS* yields the trim solution and stress distribution for a flexible X-34 at a typical trajectory point, demonstrating the multifunctionality in MDO for the aerothermoelastic software.

15. SUBJECT TERMS

SBIR report, transatmospheric vehicle (TAV), thermal protection system (TPS) design, aerothermoelastic analysis, hypersonic aerodynamics/aeroheating, high-fidelity panel method (ZONA7U) with unified AIC, structural FEM in ASTROS*

16. SECURITY CLASSIFICATION OF:			17. LIMITATION OF ABSTRACT:	18. NUMBER OF PAGES	19a. NAME OF RESPONSIBLE PERSON (Monitor)
a. REPORT	b. ABSTRACT	c. THIS PAGE			Amarshi A. Bhungalia
Unclassified	Unclassified	Unclassified	SAR	124	19b. TELEPHONE NUMBER *(Include Area Code)* (937) 255-8335

TABLE OF CONTENTS

TABLE OF CONTENTS (cont.)

LIST OF FIGURES/TABLES

LIST OF FIGURES/TABLES (cont'd)

LIST OF FIGURES/TABLES (cont'd)

FOREWORD

This report was prepared by ZONA Technology, Inc., the prime contractor, and its Team member, Technosoft, Inc. for AFRL/VASD, WPAFB, Ohio. It describes the work performed under the Phase I contract of AF/SBIR No. F33615-01-M-3131 in response to the Topic No. AF01-252 entitled "Integrated Hypersonic Aerothermodynamic Methodology for TAV/TPS Structural Design and Optimization." The contractual period was from March 30, 2001 through December 30, 2001. Lt Mark Stevenson of AFRL/VASD was the technical monitor.

The contributors of this report are: Dr. D.D. Liu (P.I.), Mr. P.C. Chen, Dr. Lei Tang and Dr. K.T. Chang of ZONA Technology; Mr Adel Chemaly and Mr. Hilmi Kamhawi of Technosoft, Inc (Subcontractor).

ZONA Technology wishes to thank the technical support rendered by: Mr David Adamczak of AFRL/VASD (AEROHEAT); Dr. William Wood and Dr Steven Alter (X-34 Data and Grid Organization); Ms. Katheryn Wurster (MINIVER) of NASA-LaRC; Dr. Christ Riley of CFDesign (LATCH) and Dr. Harry Fuhrman of Orbital/OSC (X-34 and Data release), during the course of Phase I R&D. Technical management/advice received from Lt. Mark Stevenson and Dr. Jeffery Zweber is gratefully acknowledged.

SECTION 1

INTRODUCTION

Summary

- *Define Objective and Block Diagram of Integrated Hypersonic Aerothermoelastic Program Architecture*
- *Background*
- *A Supersonic-Hypersonic Vehicle Design System: SHVD*
- *ZONA7U: A Unified Unsteady Hypersonic/Supersonic Panel Method for Arbitrary Wing-Body Configurations*
- *Optimization Test-Bed of ZONA7U for TAV:ASTROS**
- *Other Related Disciplines for TAV Design*
- *Description of the following sections*

This final technical report describes work done by the ZONA team (ZONA Technology, Inc. and TechnoSoft, Inc.) under SBIR Phase I contract F33615-01-M-3131, entitled *"Integrated Hypersonic Aerothermoelastic Methodology for TAV/TPS Structural Design and Optimization."*

The overall Phase I technical objective is to develop a hypersonic aerothermoelastic methodology for Trans Atmospheric Vehicle (TAV)/Thermal Protection System (TPS) structural design/optimization with a view to integrate it with Adaptive Modeling Language (AML) (Ref 1) into a preliminary TAV design software system.

Specific objectives include:

- Establish interfaces between all key analysis software tools of the preliminary software system (see Figure 1.1)
- Validate the proposed software system by a feasibility study on a selected TAV configuration (*e.g.*, X-34)

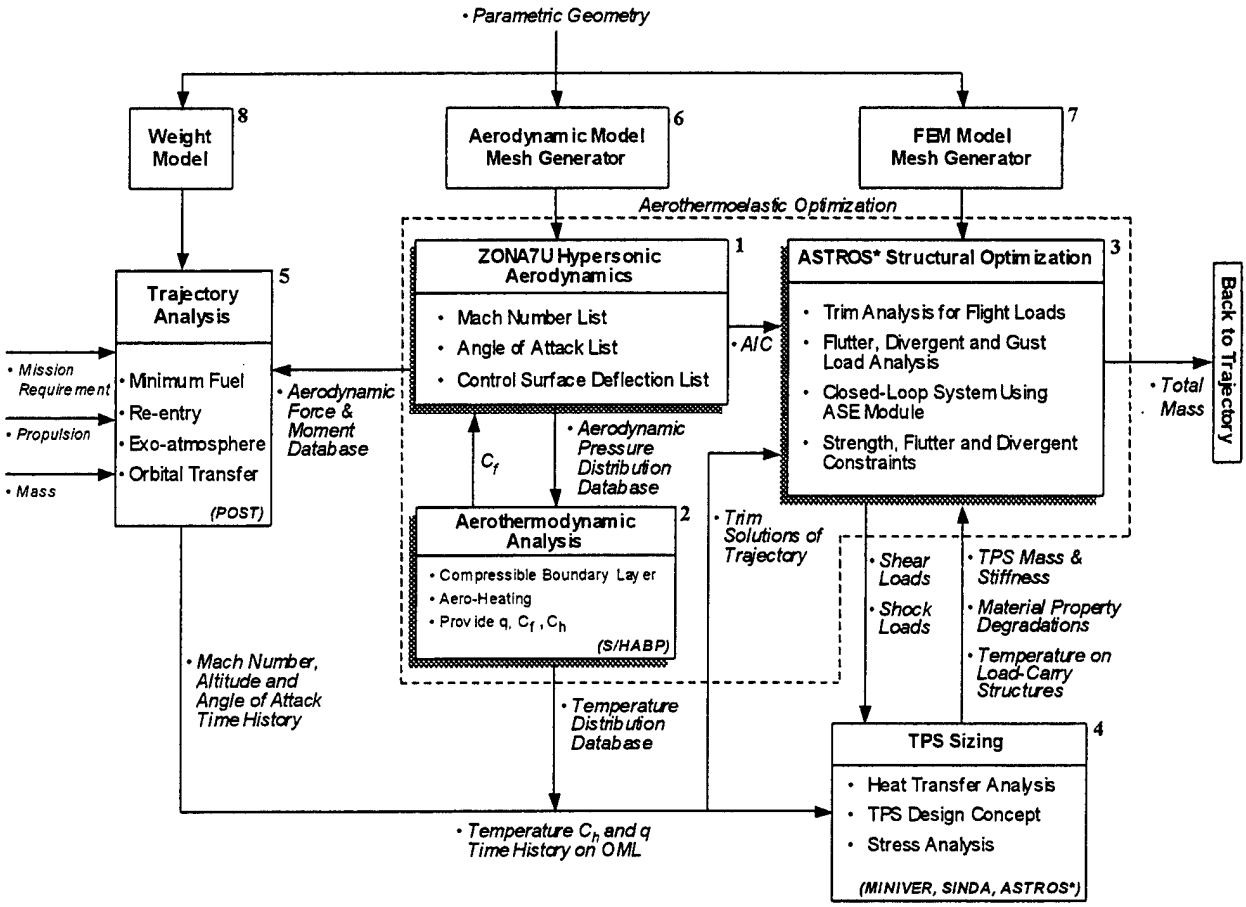

Figure 1.1 Block Diagram of Integrated Hypersonic Aerothermoelastic Program Architecture

In this Phase I effort, we have accomplished the following:

- Developed blunt-nose aerodynamic methodology, based on a Strained-Coordinate technique analytically applied to the local panel by matching the Chernyi's similarity solution (Ref 2), including Lees' hemisphere solution (Ref 3), with ZONA's unified hypersonic/supersonic pulsating-cone solution (Ref 4) on downstream panels
- Seamlessly integrated the SHABP module of the MARKV code (Ref 5) into ZONA7U for aeroheating analysis
- Developed a finite element based streamline code called ZSTREAM that adopts the inviscid surface velocities generated by ZONA7U as input to yield high quality streamline solutions
- Integrated the EXITS module of MINIVER (Ref 6) with ZONA7U+SHABP for TPS sizing
- Demonstrated the integrability and the trim analysis capability of ASTROS* for a flexible X-34 in hypersonic maneuver and re-entry phase.
- Validated *Central Methodologies (Blocks 1-5 in Figure 1.1)* required for aerothermodynamic optimization individually for X-34, a selected TAV configuration for methodology demonstration.

1.1 Background

Aerothermoelastic analysis has become a required discipline for TAV design. Aerothermoelasticity is a synergic disciplinary of aerothermodynamics and aeroelasticity. In a hypersonic extreme environment, aerothermoelastic effects will strongly influence the TPS sizing and the integrated TAV/TPS structural design. During the hypersonic flight phase, the aerothermoelastic load will cause TAV deformation, which in turn will impact the structural integrity of the TAV/TPS system. If designed properly with the main structures, the TPS will serve as a part of the load-carrying structure, thus helping further reduce the total weight of the TAV. For this reason, both the TAV and its TPS require an accurate aerothermodynamic loads prediction method to couple with an optimization method in order to achieve a viable TAV/TPS structural design.

Other important disciplines that will influence TAV/TPS design are the trajectory analysis, the TPS sizing and thermal analysis. To integrate all these disciplines and turn them into a Multidisciplinary Design and Optimization (MDO) design tool for TAV/TPS presents great challenges. A series of Computational Fluid Dynamics (CFD) works and test data were directed towards the X-34 research and developed by NASA and Orbital Sciences Corporation in the last decade (Refs 7-12). Adopting the CFD approach for an effective TAV/TPS design tool in a hypersonic environment is prohibited by the slow CFD turn around time. On the other hand, other more expedient computational methods (e.g., Refs 13-14) utilized in treating all these required disciplines have been developed individually to a certain extent including the focused aerothermodynamic program. Nonetheless, all these previous computational approaches lack a main design-oriented program with data management capability and multidisciplinary design/optimization perspective. An MDO oriented program such as ASTROS* (Automated STRuctural Optimization System) or NASTRAN should be the central piece of a valid TAV/TPS design tool. If ASTROS* is selected then a compatible aerothermodynamic program must be a high-fidelity one in order to interface with a structural FEM module. This requirement will probably rule out the existing efficient but non-FEM compatible types of aerodynamic prediction programs such as APAS (Ref 15), Datcom (Ref 16), or AP98 (Ref 17). Clearly, a high fidelity, computationally efficient hypersonic aerothermoelastic methodology is lacking.

1.2 A Supersonic-Hypersonic Vehicle Design System: SHVD (Ref 18)

Adaptive Modeling Language (AML), developed by TechnoSoft, Inc., offers the advanced, object-oriented engineering modeling language to enable the modeling and simulation of the entire product development. Based on AML, TechnoSoft and Lockheed Martin are developing a Supersonic-Hypersonic Vehicle Design (SHVD) system, which is an object-oriented, web-enabled distributed framework environment for design analysis and simulation of TAV. The SHVD system automates and manages the data transfer between various design, analyses and simulation tools, including aerodynamics, aero-heating, Thermal Protection System (TPS), propulsion system, trajectory analysis, structural weight optimization and cost. The SHVD system builds upon, and leverages years of software development and TAV design domain knowledge offered by the entire SHVD team: 1) AML, a web-enabled Adaptive Modeling Language from TechnoSoft; 2) IMD, an Interactive Missile Design system from Lockheed Martin Missile and Fire Control; 3) Numerous aerodynamic, aero-thermal, propulsion and

trajectory codes and detailed domain knowledge offered by Lockheed Martin Aeronautics Company (Forth Worth, Skunk Works and Marietta); 4) Structural/TPS sizing, optimization applications and domain knowledge offered by Collier Research; 5) Software support/validation for TAV design by NASA/Langley and NASA/Marshall.

The SHVD development resulted in an advanced multidisciplinary capability for TAV design/simulation under hypersonic extreme environment; the enabling software methodologies include:

- Aerodynamic Analysis: S/HABP, APAS, PANAIR, VUAERO
- Thermal Analysis: MINIVER, FEM/SINDA
- Boundary Layer/Aero-Heating Analysis: S/HABP MarkV
- Trajectory Analysis: POST
- Structural Analysis: NASTRAN

For realistic TAV design/analysis in an extreme hypersonic environment, aero-heating problems related to aerothermodynamic and aerothermoelasticity will strongly impact the TAV/TPS structural design compatibility, hence the vehicle structural integrity. Further, the aeroelastic instability induced by aero-heating could lead to serious divergence or flutter problems in its hypersonic flight phase. Close examination of the aerodynamic software capability of SHVD (e.g., Ref 18) reveals that:

- S/HABP-APAS does not have unsteady aerodynamic capability needed for flutter, divergence and ASE instability analysis
- It does not generate Aerodynamic Influence Coefficient (AIC) matrices needed for sensitivity analysis to avoid repetitive aerodynamic computation in an optimization procedure
- It is not a PANAIR-level high-fidelity panel method; hence, it offers no solution refinement from conceptual to preliminary design stage

On the other hand, unsteady aerodynamics-structural dynamics coupling via Panel-FEM interface has been a widely practiced methodology in both loosely or tightly-coupled levels. Only until the recent ZONA unsteady-hypersonic development, such a Panel-FEM methodology for hypersonic TAV design has not been available due to the lack of a suitable hypersonic aerodynamic panel method.

For decades, the difficulty that has hampered the development of a viable hypersonic panel method lies in the following:

- *Superinclined Panel*: Supersonic kernel integral becomes singular at a Mach number at which the inclined panel slope exceeds that of the Mach wave. Computation breaks down beyond this Mach number
- *Flow Rotationality*: Strong shock induced flow rotationality cannot be included in the conventional potential flow-based panel method. Accuracy will deteriorate rapidly as the supersonic Mach number increases toward the hypersonic range

1.3 ZONA7U: A Unified Unsteady Hypersonic/Supersonic Panel Method for Arbitrary Wing-Body Configurations

With continuous R&D in hypersonics since 1995, ZONA Technology, Inc. (ZONA) has made major breakthroughs in overcoming the above two issues. The result is a unique software product ZONA7U, a high-fidelity unified unsteady hypersonic panel method (Ref 4). ZONA7U (U stands for unified) has the following capabilities:

- It is a frequency-domain and s-domain aerodynamic for unified supersonic/hypersonic Mach numbers up to the Newtonian limit, hence capable of performing hypersonic aeroelasticity/aerothermoelastic applications including flutter, divergence, gust and aeroservoelasticity (ASE) instability
- It provides unified supersonic/hypersonic AIC matrix, hence is readily applicable for structural optimization procedure with aeroelastic constraints
- It can aerodynamically model complex air vehicles such as conventional aircrafts, blended wing-body and TAV configurations, hence a high-fidelity panel method

Based on the formulation of strained coordinates in conjunction with the local pulsating body analogy, ZONA7U can accurately approximate the nonlinear thickness effect and the shock-induced rotationality in the unified supersonic/hypersonic Mach range up to the Newtonian limit. Both of these effects are ignored by the linear theory and are overestimated by the Piston theory (Refs 19, 20, 21). In the following examples, it can be seen that the ZONA7U results agree well with the Euler solutions for various classes of wings and bodies.

- *ZONA7U for Various Wing Planforms*

Figures 1.2-1.5 present the ZONA7U unsteady damping derivative, generalized aerodynamic forces and flutter solutions for various wing planforms at hypersonic Mach numbers showing comparable accuracy.

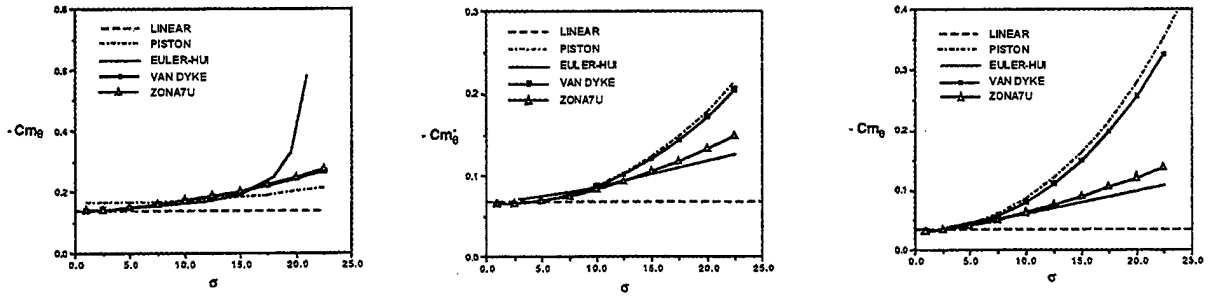

Figure 1.2 ZONA7U Damping-in-Pitch Derivatives of a Rectangular Wing with a Diamond Profile versus Airfoil Thickness (σ) at: (a) M=2.0, (b) M=5.0, and (c) M=10.0.

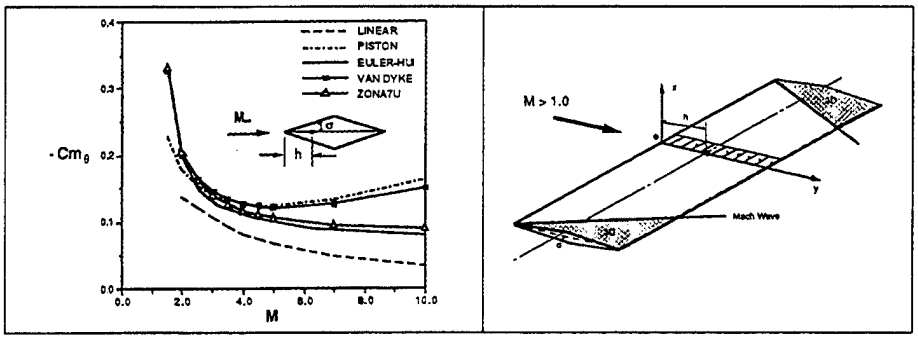

Figure 1.3 ZONA7U Damping-in-Pitch Derivatives of a Rectangular Wing with a Diamond Profile versus Mach Number (σ=15°, h/c=0.5).

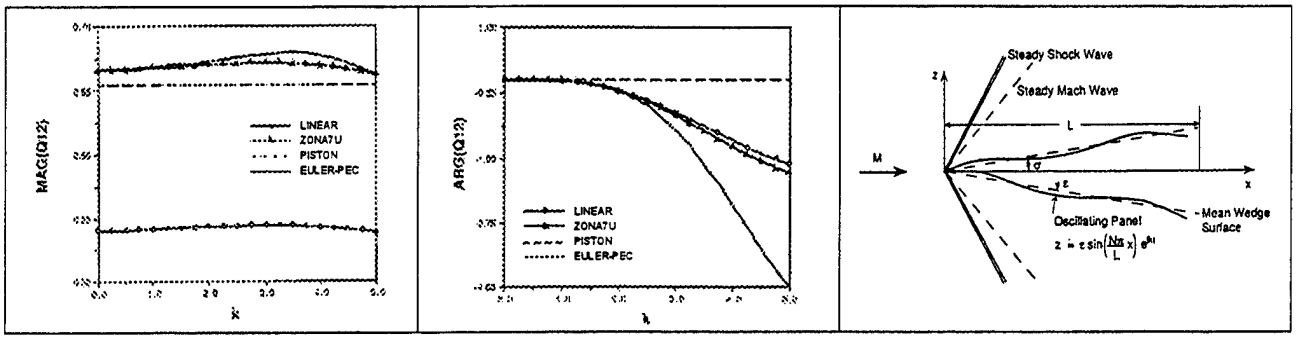

Figure 1.4 Effect of Reduced Frequency on Generalized Aerodynamic Forces for Oscillating Panels ZONA7U at M = 5.0, σ = 2°, N = 2

Aerodynamic Method	Mach Number								
	5			10			15		
	q_r (psi)	ω_r (r/s)	h (Kft)	q_r (psi)	ω_r (r/s)	h (Kft)	q_r (psi)	ω_r (r/s)	h (Kft)
Piston Theory	129	78	18	184	78	42	250	72	51
QSCFD 2-D	169	80	11	331	81	28	982	224	22
QSCFD 3-D	---	---	---	330	82	28	981	224	22
ZONA7U									
- *V-g Method*	129	82	18	175	73	42	206	70	55
- *S-Domain*	130	82	18	184	71	41	213	68	54

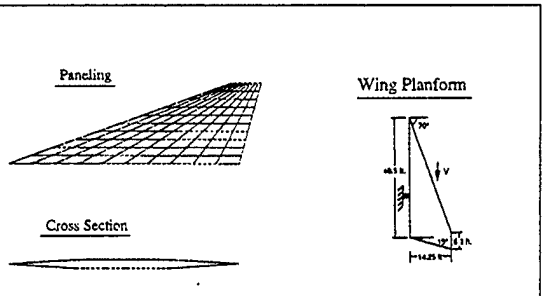

Figure 1.5 ZONA7U Flutter Results of the NASP Demonstrator Wing at Mach 5.0, 10.0, and 15.0.

- *ZONA7U for Bodies*

Figures 1.6-1.15 present the ZONA7U paneling, pressure distributions and unsteady stability derivatives for various bodies showing excellent agreement with CFL3D/Euler solutions (Ref 22) and measure data.

Under a recent Army/REDC support, ZONA has further extended ZONA7U to treat body-fin configurations at Mach 6.0. To circumvent the superinclined panel problem (i.e., when the Mach line cuts into the body panel due to high Mach number), we introduce an equivalent Mach number transformation to recast the physical problem into a new coordinate, whereby the body undergoes a compressibility stretch in the axial direction.

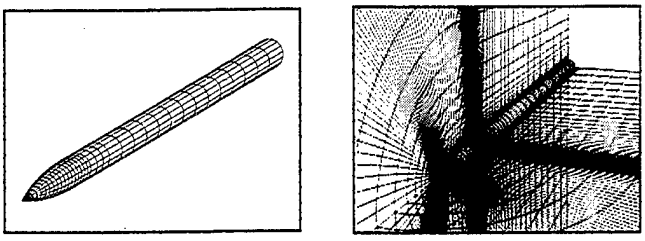

(a) ZONA7U Panel Model *(b) CFL3D Mesh*

Figure 1.6 ZONA7U and CFL3D Models of the CKEM Body

For the inclusion of flow rotationality effects, we have established a local pulsating body analogy to extend Sims' (Ref 23), Brong's (Ref 24), and Dorodnitsyn's (Ref 25) steady Euler solutions. A detailed theoretical formulation of ZONA7U can be found in References 4 and 26 (Chen and Liu).

Note that CFL3D requires over 2 hours of computer time for each bent-nose case whereas ZONA7U takes only 1 minute.

Undeflected Case, Body & Nose at the same AOA (Nose = Body = -2°, at M=6.0)

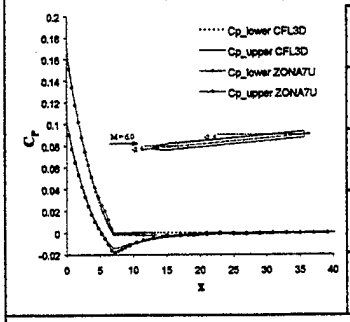

	CFL3D	ZONA7U
C_L	-0.118	-0.1125
C_m	-0.0549	-0.05588
C_D	0.0465	0.050
C_h	-0.00612	-0.00668

Positive 2° Deflection between Body & Nose (Nose = 0°, Body = -2°, at M=6.0)

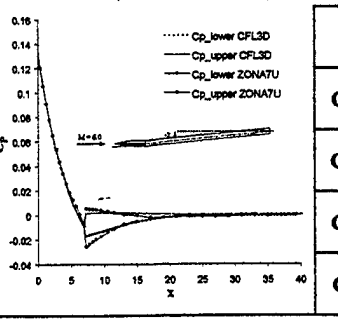

	CFL3D	ZONA7U
C_L	-0.076	-0.0712
C_m	-0.02552	-0.02776
C_D	0.0553	0.049
C_h	3.76e-7	0

Positive 2° Deflection between Body & Nose (Nose = 2°, Body = 0°, at M=6.0)

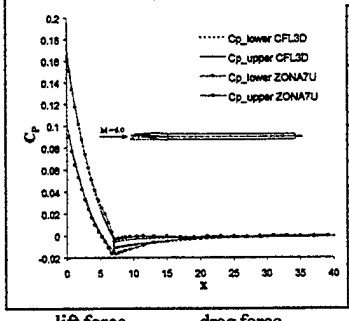

	CFL3D	ZONA7U
C_L	0.0437	0.0408
C_m	0.0292	0.02806
C_D	0.0492	0.0493
C_h	0.00612	0.00668

Positive 2° Deflection between Body & Nose (Nose = 4°, Body = 2°, at M=6.0)

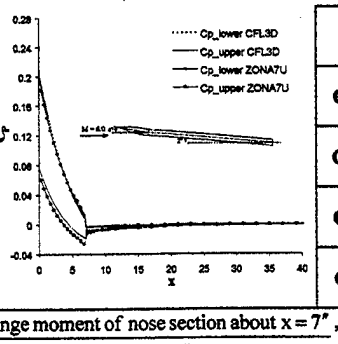

	CFL3D	ZONA7U
C_L	0.1637	0.1517
C_m	0.0857	0.08388
C_D	0.0537	0.057
C_h	0.0123	0.0133

$C_L = \frac{\text{lift force}}{q_\infty A_B}$, $C_D = \frac{\text{drag force}}{q_\infty A_B}$, $C_m = \frac{\text{pitch moment about C.G.}}{q_\infty A_B L}$, $C_h = \frac{\text{hinge moment of nose section about x = 7"}}{q_\infty A_B L}$, $A_B = 2.405$ in^2, $L = 40.25$ in

Figure 1.7 ZONA7U Pressure Distributions and Aerodynamic Force/Moments along the CKEM Body at M = 6.0 for Various Bent-Nose Angles and Angles of Attack

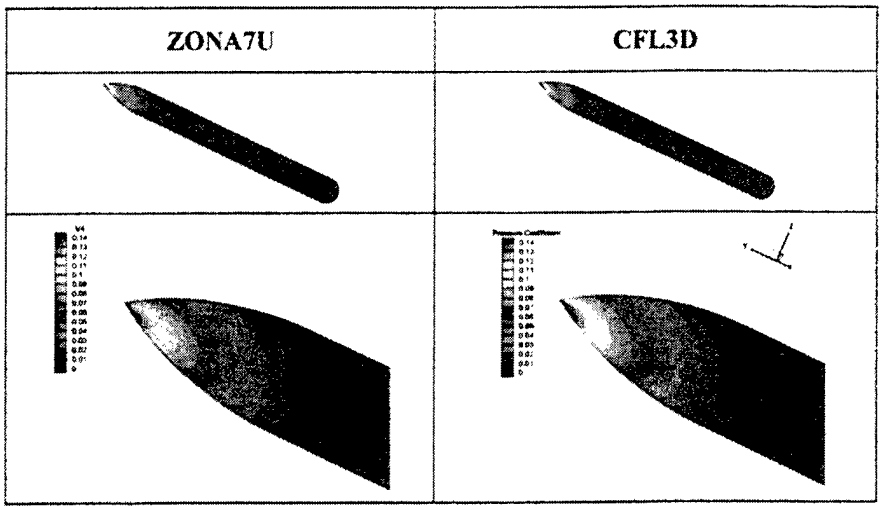

Figure 1.8 Pressure in Color Maps of CKEM Body at M = 6.0 and $\alpha = 2°$

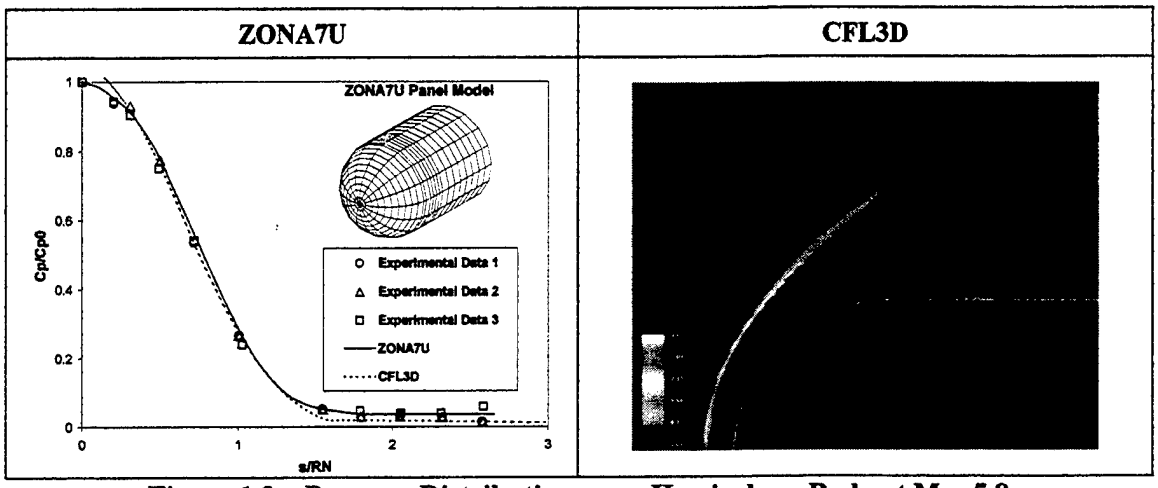

Figure 1.9 Pressure Distributions on a Hemisphere Body at M = 5.8

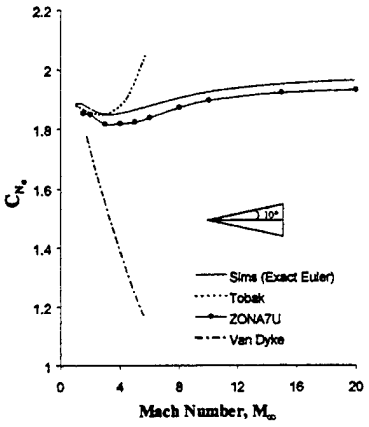

Figure 1.10 Variation with Mach Number of the Stability Derivative (at Cone Angle = 10°)

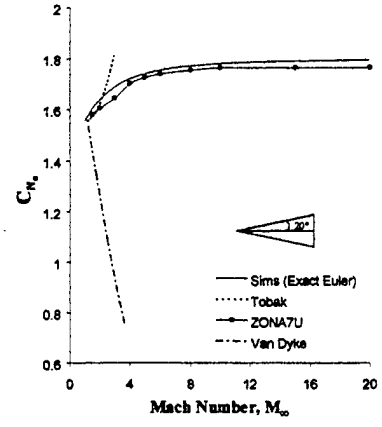

Figure 1.11 Variation with Mach Number of the Stability Derivative (at Cone Angle = 20°)

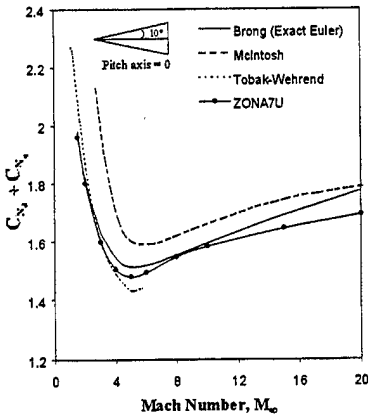

Figure 1.12 Variation with Mach Number of the Stability Derivative (at Cone Angle = 10°)

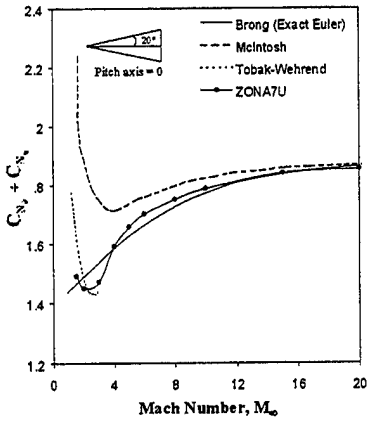

Figure 1.13 Variation with Mach Number of the Stability Derivative (at Cone Angle = 20°)

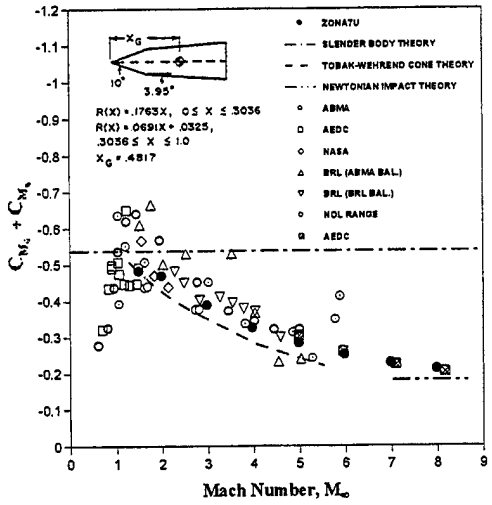

Figure 1.14 ZONA7U Damping-in-Pitch Moment Coefficients for a Cone Frustum

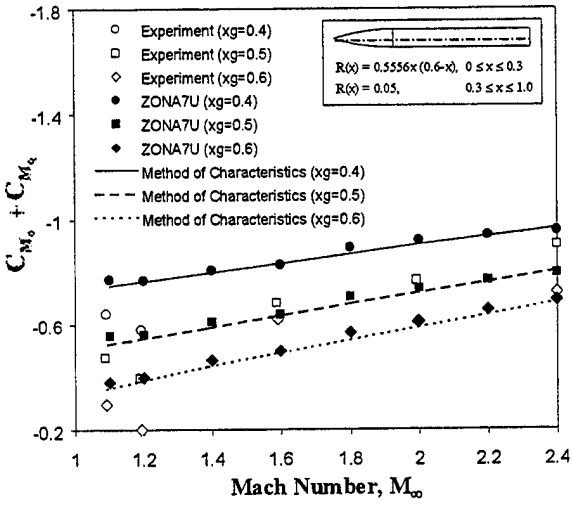

Figure 1.15 ZONA7U Damping-in-Pitch Moment Coefficients for an Ogive Cylinder at Various Pivot Locations

1.4 Optimization Test-Bed of ZONA7U for TAV: ASTROS*

Under recent Army/RDEC support, ZONA has successfully integrated ZONA7U with ASTROS* and performed structural optimization for a hypervelocity Compact Kinetic Energy Missile (CKEM) design with flexible body control at Mach 6.0 (Ref 26). ASTROS* is ZONA Technology's enhanced version of ASTROS that is seamlessly integrated with ZONA's Unified Aerodynamic ZEARO system and Aeroservoelasticity (ASE) module. ASTROS (Automated STRuctural Optimization System) is a proven engineering design/analysis and optimization software which includes most of the essential aerospace disciplines that impact an aircraft/missile structural design (isotropic or composites).

Under a two-year contract support by AFRL, ZONA Technology Inc. (ZONA) has further enhanced the software system by seamlessly integrating several additional engineering modules

into ASTROS (Refs 27, 28). Figure 1.16 shows all the essential modules of ASTROS*, including the ZAERO aerodynamic module, the smart structure module, the ASE module, the trim module and the aeroelastic stability module. The functionalities and features of each module are shown in Figure 1.16. Note that ASTROS* = ASTROS + ZAERO (Refs 29, 30)

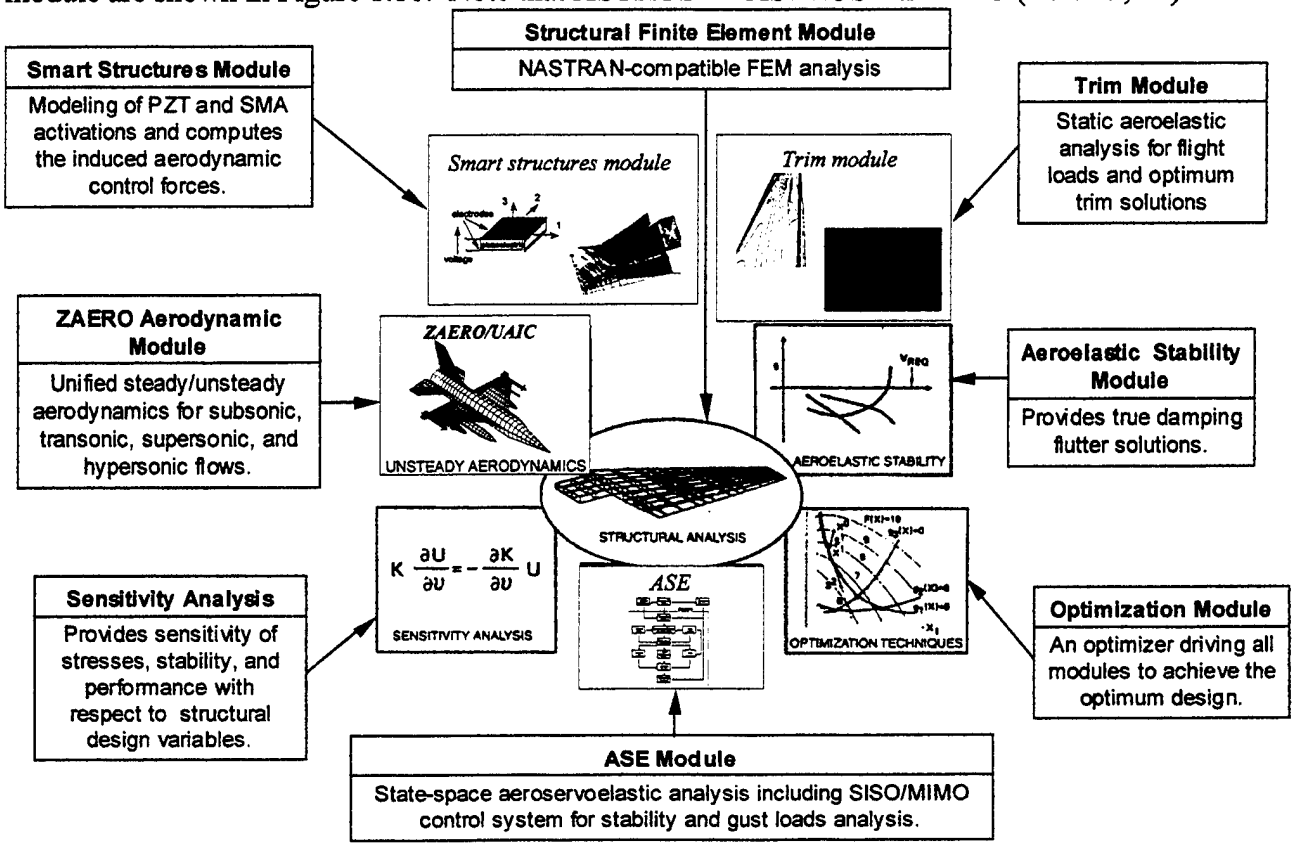

Figure 1.16 Engineering Modules in ASTROS*

ZONA plans to use ASTROS* as the ZONA7U test-bed for TAV structural design/optimization. Once shown successful, ZONA7U compatibility is assured for subsequent interface with other structural FEM codes such as NASTRAN.

1.5 Other Related Disciplines for TAV Design

Aerothermoelastic analysis is a major concern for load-carry structures and Thermal Protection System (TPS) structural design of TAV. In addition to the strength and flutter/divergence constraints, the thermal-stress and the material property degradations due to the aero-heating effects must also be taken into an account for designing the load-carry structures.

The TPS sizing is normally dominated by the boundary conditions of the thermal analysis. Petley et al. (Ref 31) outlined an excellent design procedure of TPS sizing in which they conducted a trajectory analysis to obtain a transient heating profile over a Mach 10 cruise vehicle. Two types of TPS design concepts were presented; one for the vehicle skin over the integral tank structure and the other for skin with no integral tank to provide the hydrogen heat sink capability. For TPS sizing, SHVD has MINIVER and FEM/SINDA as software tools for design/analysis.

Trajectory simulation/optimization is required for aero-heating analysis and vehicle mission closure for TAV. POST (Program to Optimized Simulated Trajectories) developed by NASA is included in SHVD for fuel minimization and other objectives for a given mission. Aerothermoelastic analysis requires local temperature gradient heat transfer and heat rate over the outer mold-line (OML) of the TAV. This in turn requires the hypersonic inviscid and compressible boundary layer interaction. ZONA7U will provide the edge pressure and velocity which will be coupled with the boundary layer/aero-heating module of S/HABP MarkV to replace MarkV's inviscid module. The output is the above local heat transfer quantities, heat transfer coefficients and equivalent skin friction coefficients. The last parameter will be a new trajectory input from the integrated ZONA7U.

1.6 Description of the Sections

There are 9 sections in the present report.

- Section 2 describes our methodology development of the hypersonic aerodynamics and aerothermodynamics for basic vehicle component.
- Section 3 describes our development of a surface streamline routine, ZSTREAM, which is essential in aerodynamics/aeroheating interface, and an integral part of the present methodology.
- Section 4 describes the application of the present hypersonic aerothermodynamics methodology to X-34, a selected TAV configuration.
- Section 5 describes how we employ ASTROS* to perform analysis for a flexible X-34, under aerothermodynamic loading, demonstrating the integrability of the present methodology with ASTROS* as a design/optimization central software.
- Section 6 describes the elementary TPS sizing procedure in anticipation to a proposed automated optimized procedure (See Section 8).
- Section 7 describes aeroheating history of the stagnation point of X-34 throughout two different trajectories and shows validation with that due to MINIVER.
- Section 8 is the phase I concluding researches/recommendation.
- Section 9 describes the proposed phase II plan.

The interfacing/interaction plan of AML without present hypersonic aerothermodynamics methodology is shown in the Appendix A.

SECTION 2

HYPERSONIC AEROTHERMODYNAMICS DEVELOPMENT: POINTED AND BLUNT BODIES

Summary
In this section, we describe ZONA's extended development of its unified hypersonic/supersonic aerodynamic tool ZONA7U to aerothermodynamic applications. In so doing, a new surface streamline method has been developed based on ZONA7U. ZSTREAM, the ZONA developed streamline scheme, is Mach number dependent and uniformly valid everywhere including the stagnation point. ZSTREAM is to replace the role of QUADSTREAM in SHABP. Thus ZONA unified hypersonic/supersonic aerothermodynamic methodology is developed by suitably coupling ZONA7U + ZSTREAM + SHABP. Two cases studied in hypersonic aerothermodynamics for pointed body (CKEM) and for a 15° blunt cone are shown to demonstrate the ZONA developed methodology. Our computed results in C_p and heat flux are validated with those obtained by a CFD method (CFL3D + LATCH, also worked out by ZONA). Overall good correlations are found except that the computing efficiency of the ZONA method is one to two orders faster than that of the CFD method.

2.1 ZONA7U Unified Hypersonic Aerodynamics (Block 1)

Previous description of ZONA7U capability includes:

- It generates unsteady aerodynamics, aeroelasticity and aeroservoelasticity instability solution for design constraints
- It provides Unified Mach number AIC Matrix readily to be integrated with structural FEM of ASTROS* for MDO
- It is generally applicable to arbitrary wing-body configuration

In addition to the above, ZONA7U can handle sharp nose as well as blunt nose bodies at arbitrary angles of attack up to flow separation. The blunt-nose aerodynamic methodology is based on a Strained-Coordinate technique analytically applied to the local panel by matching the Chernyi's similarity solution, including Lees hemisphere solution, with ZONA's unified hypersonic/supersonic pulsating-cone solution on downstream panels. In Phase I, a validation effort of the ZONA7U pressure solution was extensive showing good correlation with test data and CFD solution up to flow separation (see Figs 2.1 – 2.13).

2.2 ZSTREAM Development for Aerothermodynamics (Block 2)

In Phase I, we have seamlessly integrated the SHABP module of the MARKV code into ZONA7U for aeroheating analysis.

SHABP performs the boundary layer / aeroheating computations along each streamline using the empirical equations documented in the first Phase I progress report. In the original SHABP module, the Newtonian steepest decent method (called "QUADSTREAM") is employed for

streamline computation. However, it was found that the Newtonian steepest decent method experienced numerical problems on complex configurations that contain highly twisted panels. Because the four corner points of a twisted quadrilateral panel are not located on the same plane, a gap exists between two adjacent twisted panels. The streamline tracing procedure of the QUADSTREAM method is not robust enough to overcome this problem.

Another shortcoming of QUADSTREAM is its independence of Mach number. The only information needed to generate the streamline is the freestream velocity vector and a quadrilateral discretization of the geometry. Obviously, the accurate streamline locations should be determined by the local velocity vectors over the surface of the configuration. Because the aerodynamic methods in the SHABP code are all based on empirical methods, they do not generate the local velocity vectors over the surface; only the local pressure is computed. However, this is not the case if the ZONA7U code is used because of its hypersonic panel method formulation that generates the local velocity vectors.

In Phase I, we have developed a finite element based streamline code called ZSTREAM that adopts the inviscid surface velocities generated by ZONA7U as input to yield high quality streamline solutions. The details of the theoretical formulation of ZSTREAM will be described in Section 3 in detail.

To validate the ZONA7U/ZSTREAM/SHABP procedure, we have performed the aeroheating analysis on three configurations, namely the CKEM (Compact Kinetic Energy Missile) body at M=6.0 and α=2°, a 15° blunt cone at M=10.6 and α=0°, 5°, and 10° and the X-34 wing-body configuration at M=6.0, α=9° and 15.22°. These results are compared to the CFD results using CFL3D + LATCH (Ref 25). These comparisons on the inviscid C_p and heat transfer rates are shown as follows:

2.3 Case Study (A): CKEM Body at M = 6.0 and α = 2°

The CKEM body consists of a sharp ogive nose and a cylinder body. Fig 2.1 shows the inviscid surface pressure distribution computed by ZONA7U and the CFL3D Euler solver. Fig 2.2 depicts the comparison of the wind-side C_p distribution computed by ZONA7U and CFL3D. In both figures, excellent agreement between the ZONA7U results and the CFL3D results can clearly be seen. The streamlines computed by ZSTREAM using the ZONA7U generated surface velocities are shown in Fig 2.3. For clarity, only streamlines associated with panels at the rear of the CKEM body are shown. Based on these ZSTREAM results and the ZONA7U inviscid C_p results, the Laminar heat transfer rates ($\dot{q}$) distribution is shown in Fig 2.4 and compared with results computed by the CFL3D + LATCH code. It should be noted that the streamline computation procedure of LATCH is based on an integral method that contains a singularity at the stagnation point. Due to this singularity, LATCH cannot provide the heat transfer rate near the stagnation point resulting in a "cut-out" of $\dot{q}$ at the nose. The comparison of $\dot{q}$ on the wind-side surface between ZONA7U + SHABP and CFL3D + LATCH using the boundary condition T_w = 540°R is shown in Fig 2.5. At the ogive nose region, ZONA7U + SHABP slightly over-predicts the heat transfer rates when compared to CFL3D + LATCH. This discrepancy is probably caused by the shortcoming of the empirical-equation-based methodology in SHABP.

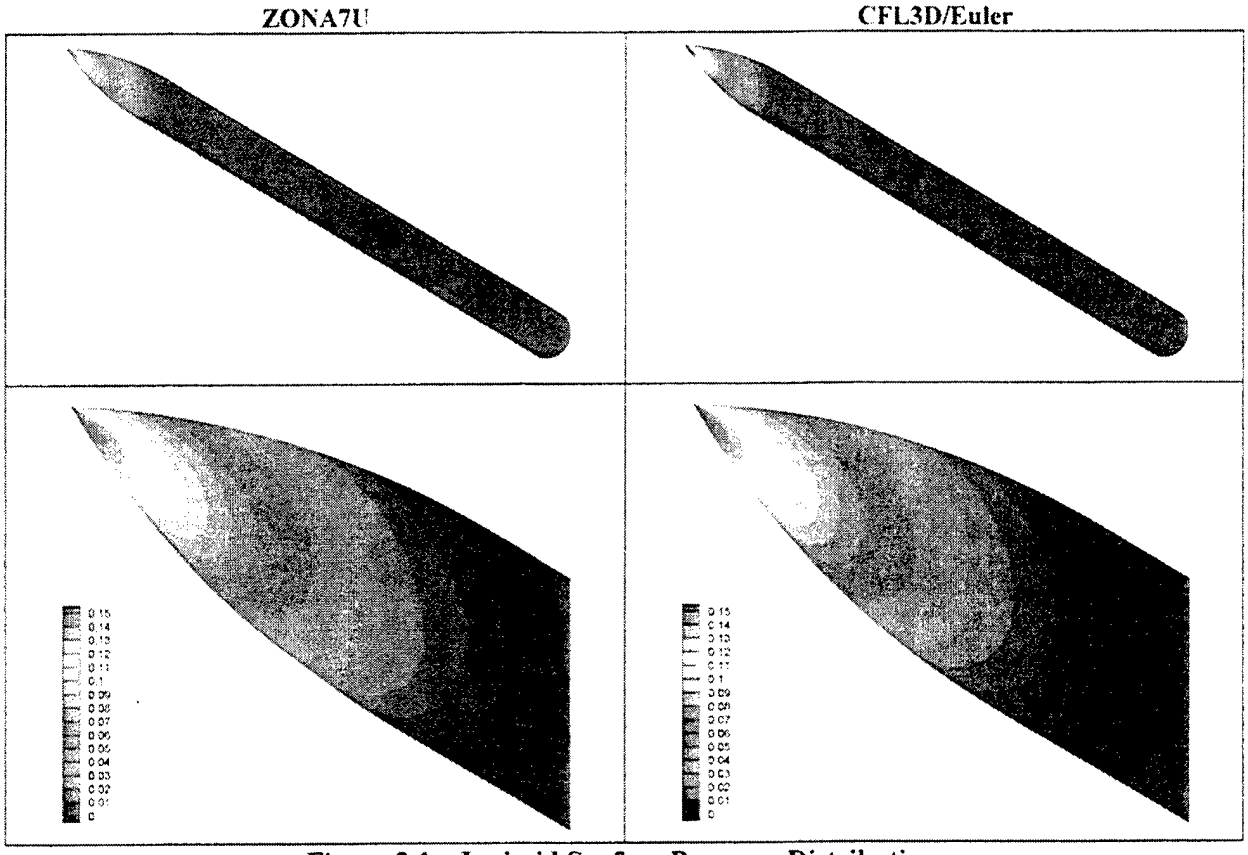

Figure 2.1 Inviscid Surface Pressure Distribution,
Sharp Cone/CKEM: M_∞=6.0, α=2°, p_∞=2.66 lb/ft^2, T_∞=89.971°R, T_w=540°R

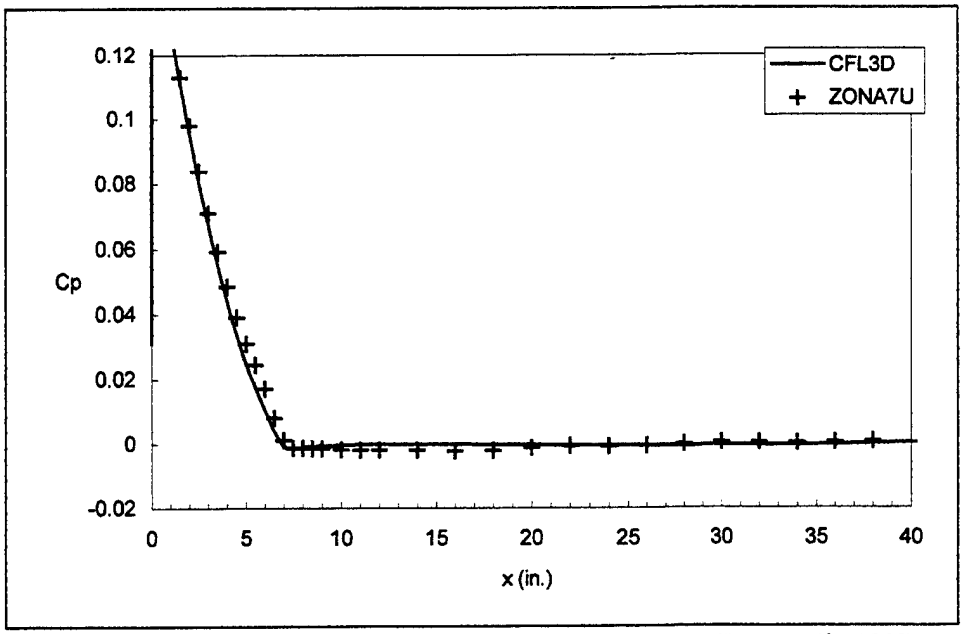

Figure 2.2 Wind-Side Inviscid Surface Pressure Distribution (ϕ=180°).

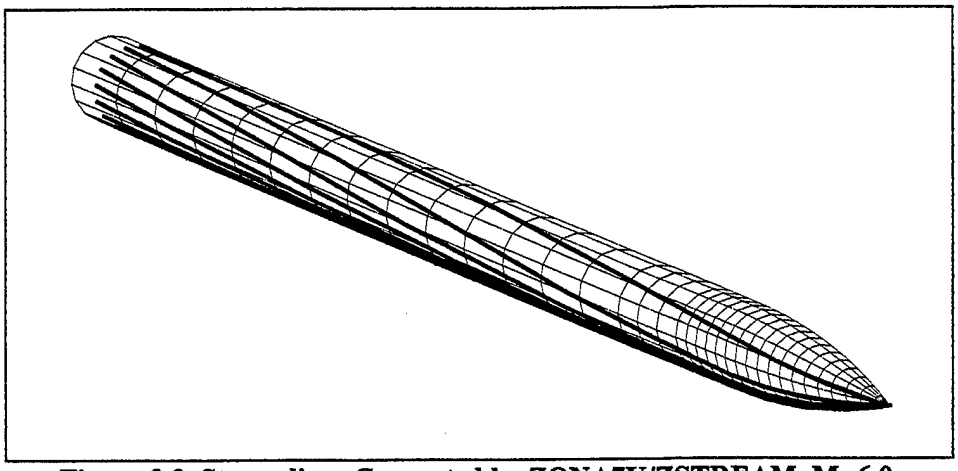

Figure 2.3 Streamlines Computed by ZONA7U/ZSTREAM, M=6.0.

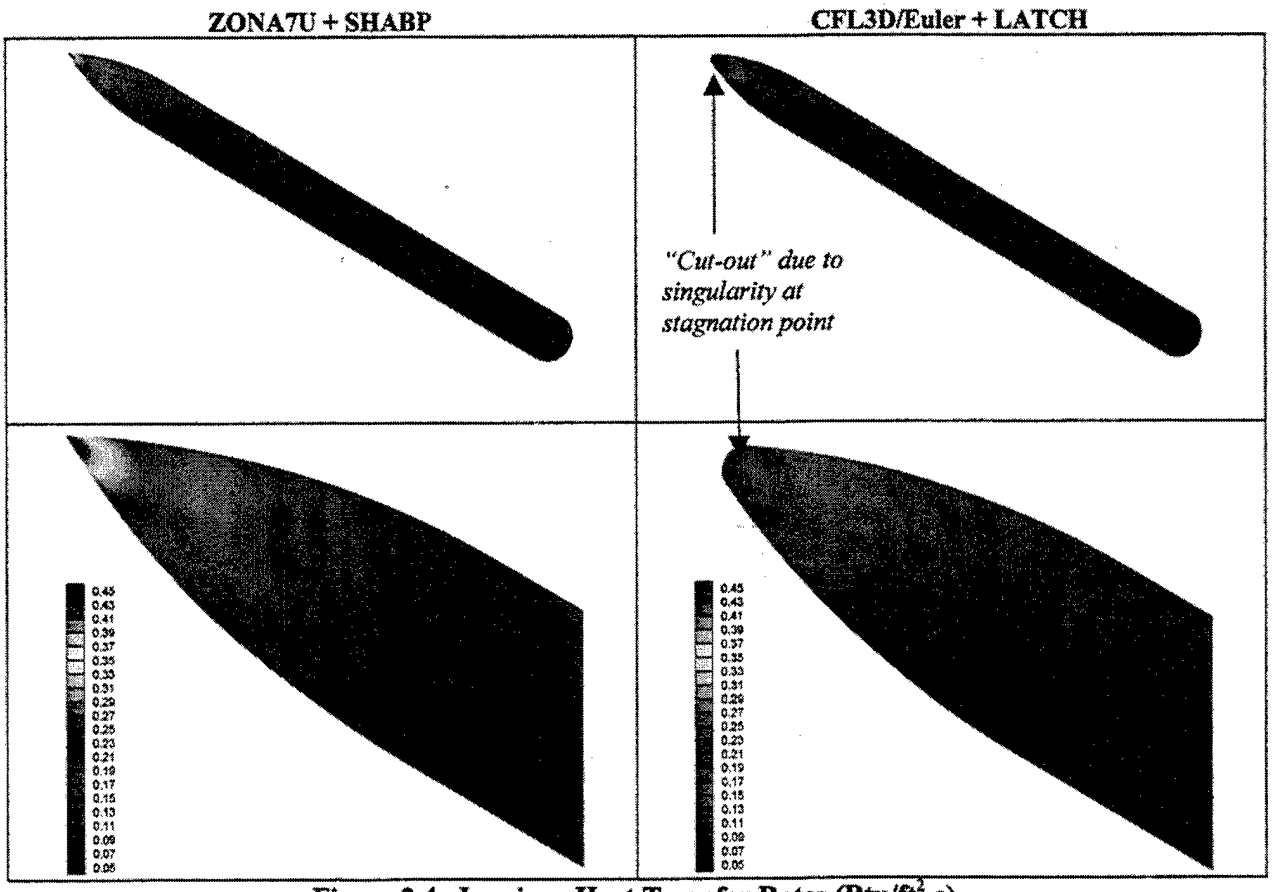

Figure 2.4 Laminar Heat Transfer Rates (Btu/ft^2-s).

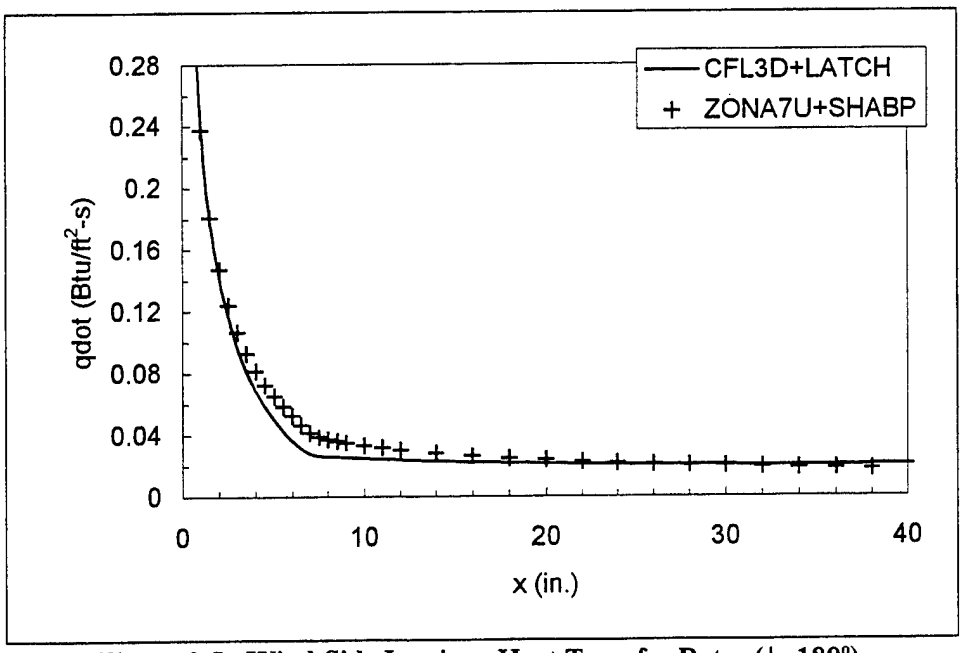

Figure 2.5 Wind-Side Laminar Heat Transfer Rates (ϕ=180°).

2.4 Case Study (B) 15° Blunt Cone at M=10.6, α=0°, 5°, and 10°

The *15°* blunt cone geometry consists of a 15° cone with a round nose of 1.1" radius. The inviscid surface C_p distributions computed by ZONA7U and CFL3D are presented in Fig 2.6 for α = 0°, 2.7 for α = 5°, and 2.8 for α = 10° where good correlations near the nose region can be seen. Note that at α = 0°, the CFL3D result shows some numerical oscillation while ZONA7U remains smooth. The comparisons of the inviscid C_p between the test data and the computed results of ZONA7U and CFL3D are depicted in Figs 2.9, 2.10, and 2.11 for the α = 0°, 5°, and 10° cases, respectively. At α = 0°, both the ZONA7U and CFL3D results correlate well with the test data. At α = 5° and 10°, the CFL3D results give a better correlation with the test data than ZONA7U. This is expected since CFL3D solves the Euler's equations; whereas, ZONA7U suffers from the attached-flow assumption and consequently loses its accuracy at high angles-of-attack. However, CFL3D requires much longer computing time than ZONA7U. For the present case, CFL3D requires 30 hours of computing time whereas ZONA7U requires only 10 minutes.

Based on the surface velocities generated by ZONA7U, the streamline computed by ZSTREAM at α = 0°, 5°, and 10° are presented in the Fig 2.12. The Laminar heat transfer rates computed by ZONA7U + SHABP and CFL3D + LATCH at α = 0°, 5°, and 10° are depicted in Figs 2.13, 2.14, and 2.15, respectively. Again, due to the singularity in the integral method, the CFL3D + LATCH cannot provide $\dot{q}$ at the stagnation point near the nose whereas ZONA7U + SHABP does not have such a problem. Figs 2.16, 2.17, and 2.18 present the comparison of $\dot{q}$ between the computed results of ZONA7U + SHABP, of CFL3D + LATCH and the test data for the α = 0°, 5°, and 10° cases, respectively. The temperature on the wall is fixed at 540°R. In general, the CFL3D + LATCH results correlate better with the test data than those of the ZONA7U + SHABP results. Again, the discrepancy of the ZONA7U + SHABP is probably due to the

inaccurate C_p at high angles of attack and the shortcoming of the empirical-equation-based methodology in SHABP.

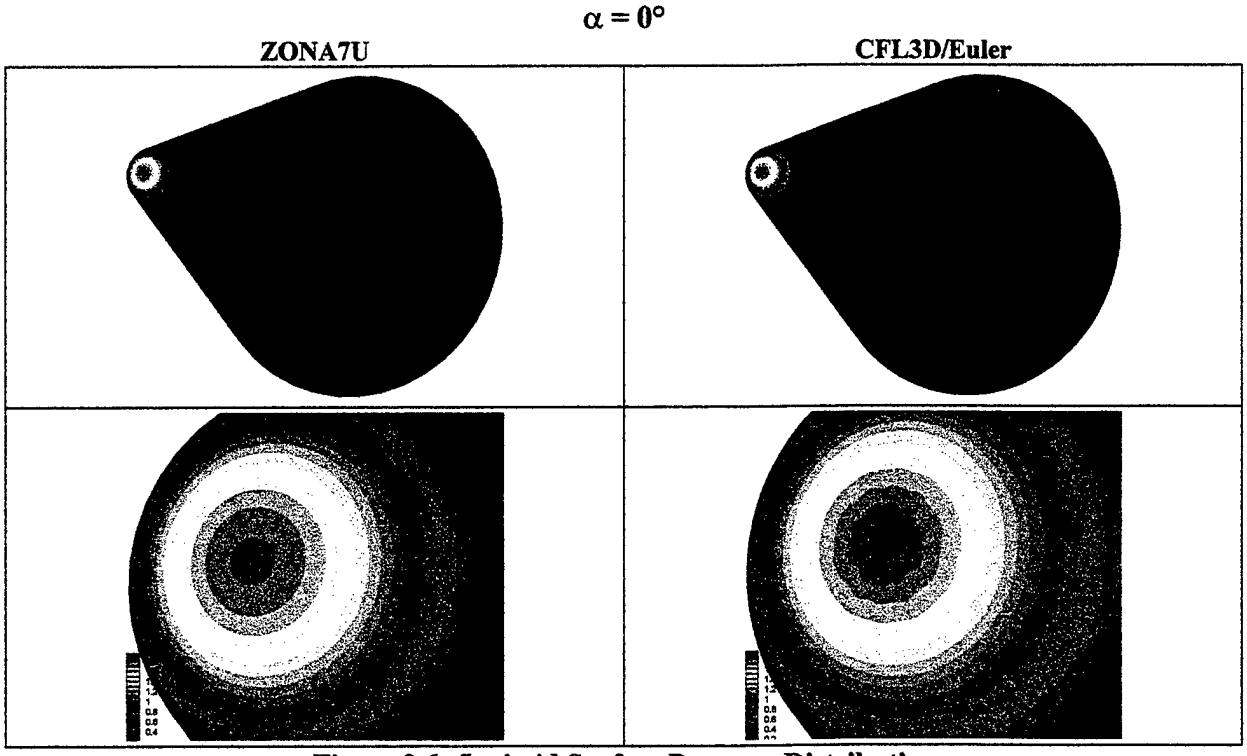

Figure 2.6 Inviscid Surface Pressure Distribution
15° Blunt Cone at M_∞ =10.6, α=0°, p_∞ =2.66 lb/ft^2, T_∞ =89.971°R, T_w =540°R

$\alpha = 5°$

ZONA7U CFL3D/Euler

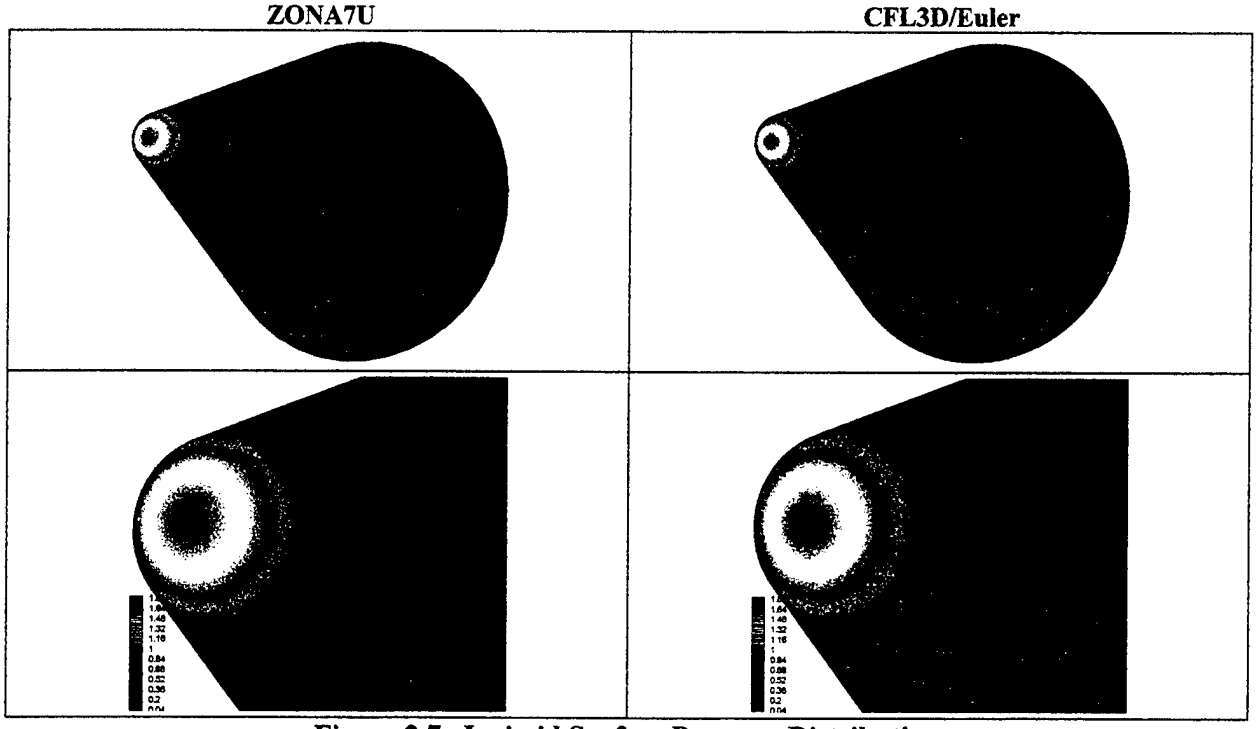

Figure 2.7 Inviscid Surface Pressure Distribution
15° Blunt Cone at M_∞ =10.6, α=5°, p_∞ =2.66 lb/ft^2, T_∞ =89.971°R, T_w =540°R

$\alpha = 10°$

ZONA7U CFL3D/Euler

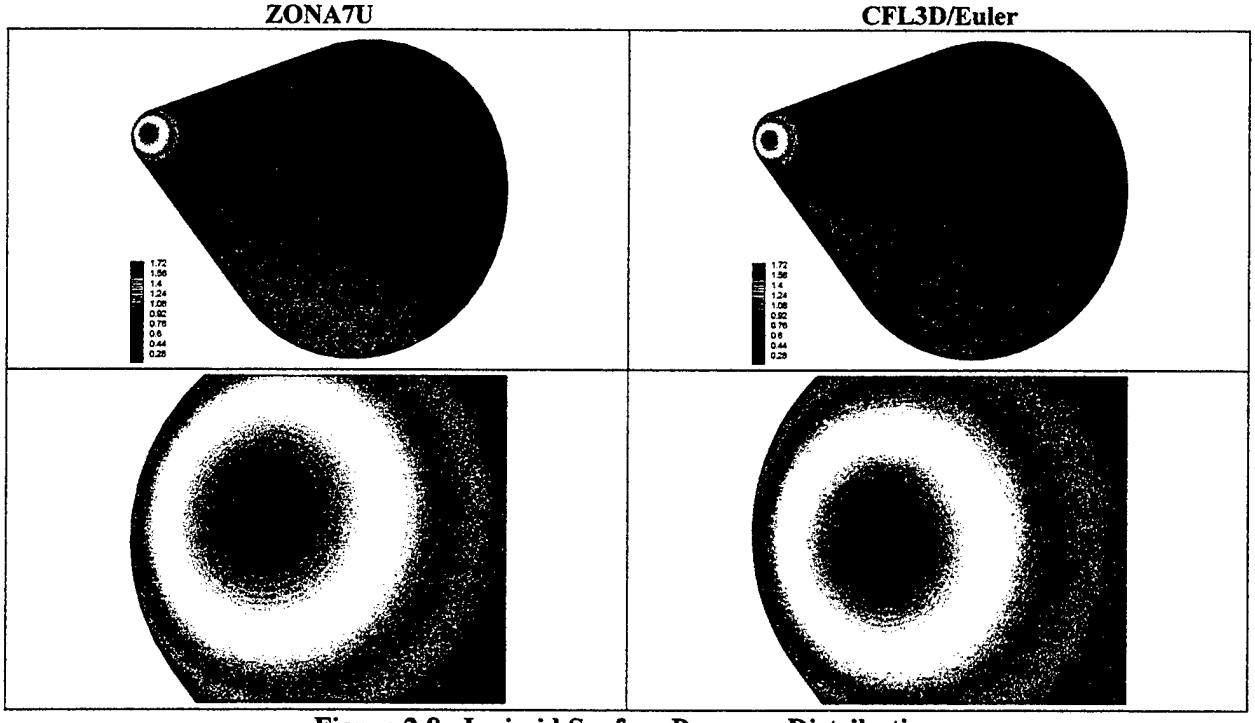

Figure 2.8 Inviscid Surface Pressure Distribution
15° Blunt Cone Case at M_∞ =10.6, α=10°, p_∞ =2.66 lb/ft^2, T_∞ =89.971°R, T_w =540°R

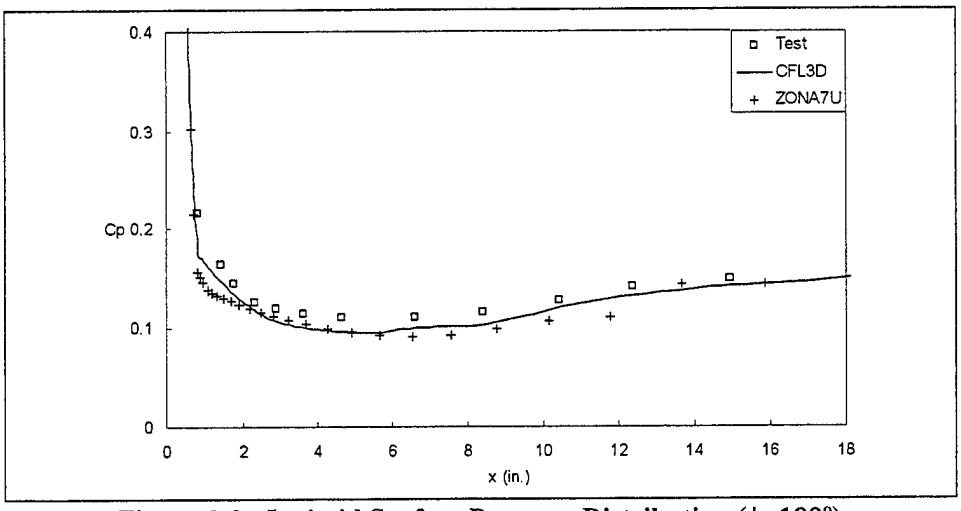

Figure 2.9 Inviscid Surface Pressure Distribution (ϕ=180°) on a 15° Blunt Cone at M=10.6 and α=0°.

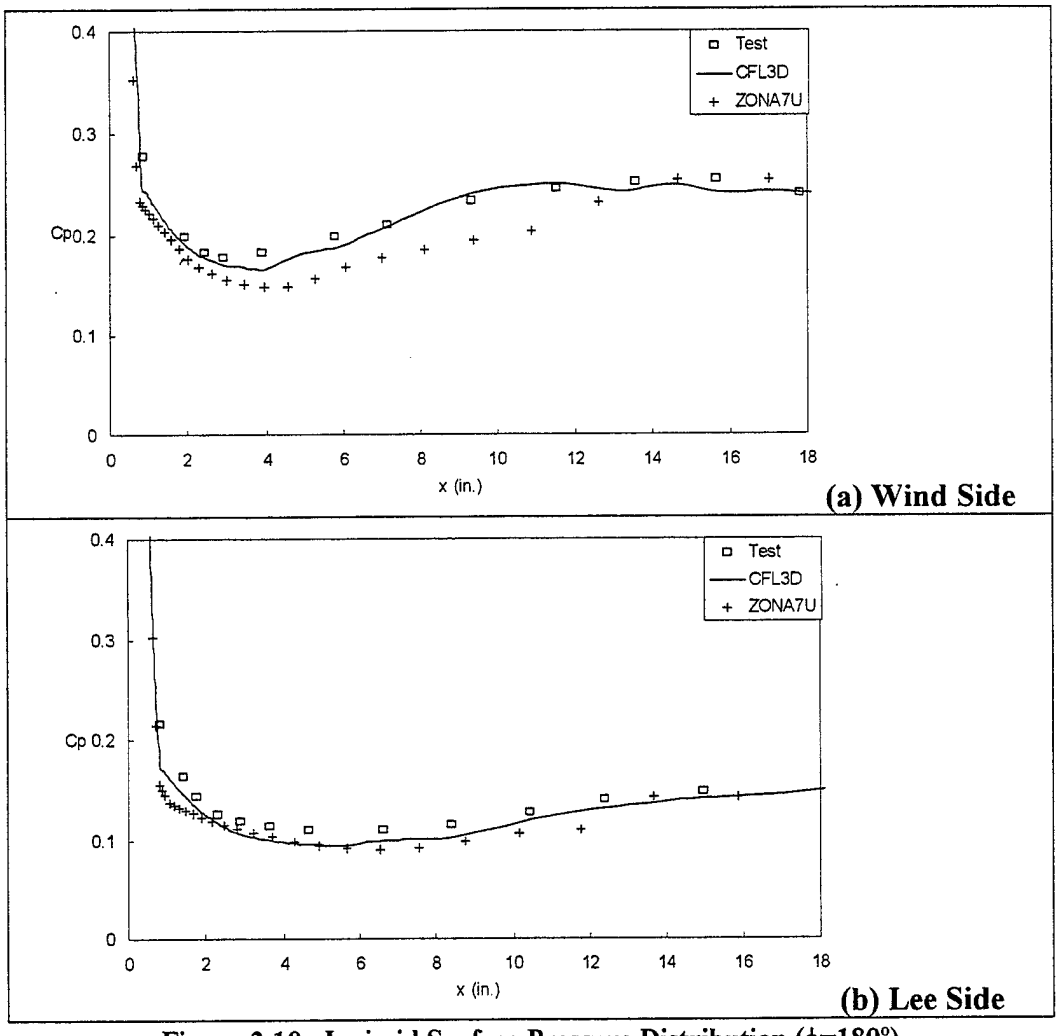

Figure 2.10 Inviscid Surface Pressure Distribution (ϕ=180°) on a 15° Blunt Cone at M=10.6 and α=5°.

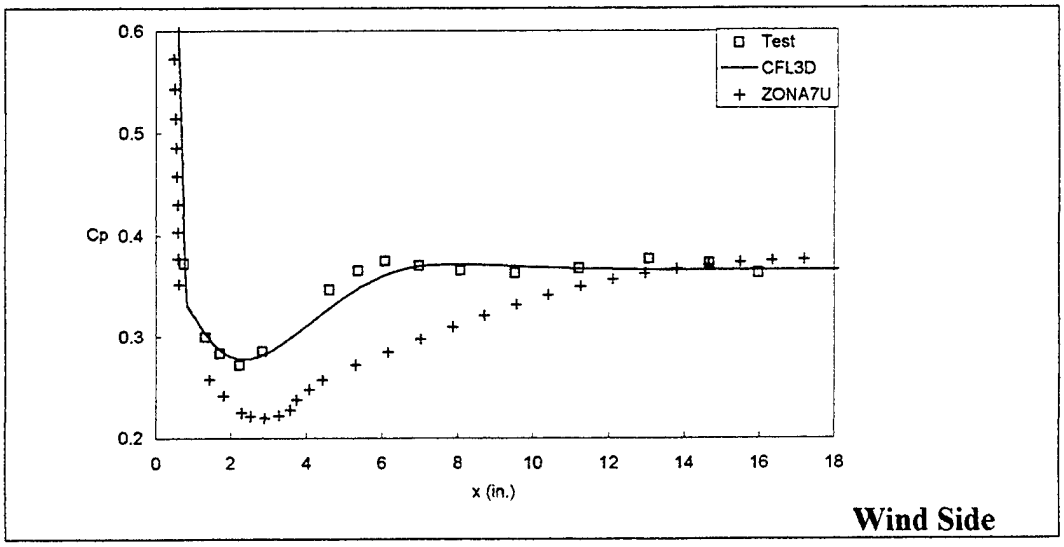

Figure 2.11 Inviscid Surface Pressure Distribution (ϕ=180°) on a 15° Blunt Cone at M=10.6 and α=10°.

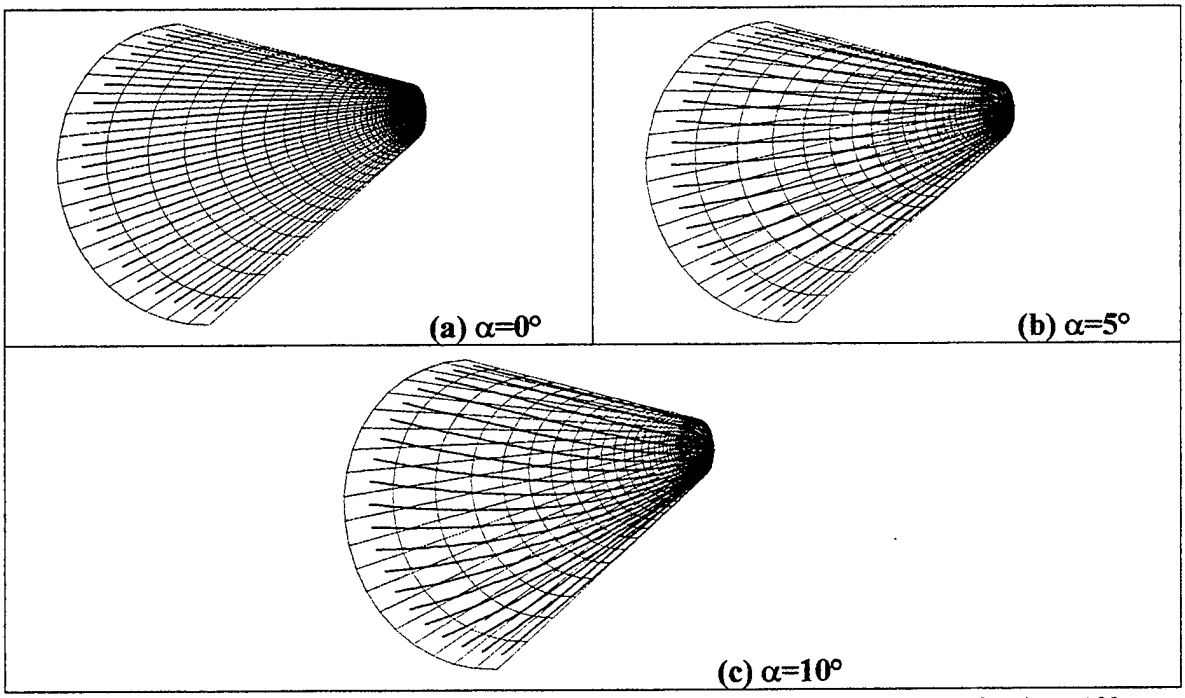

Figure 2.12 Streamlines on a 15 Blunt Cone at M=10.6; (a) α=0°, (b) α=5°, (c) α=10°.

$\alpha = 0°$

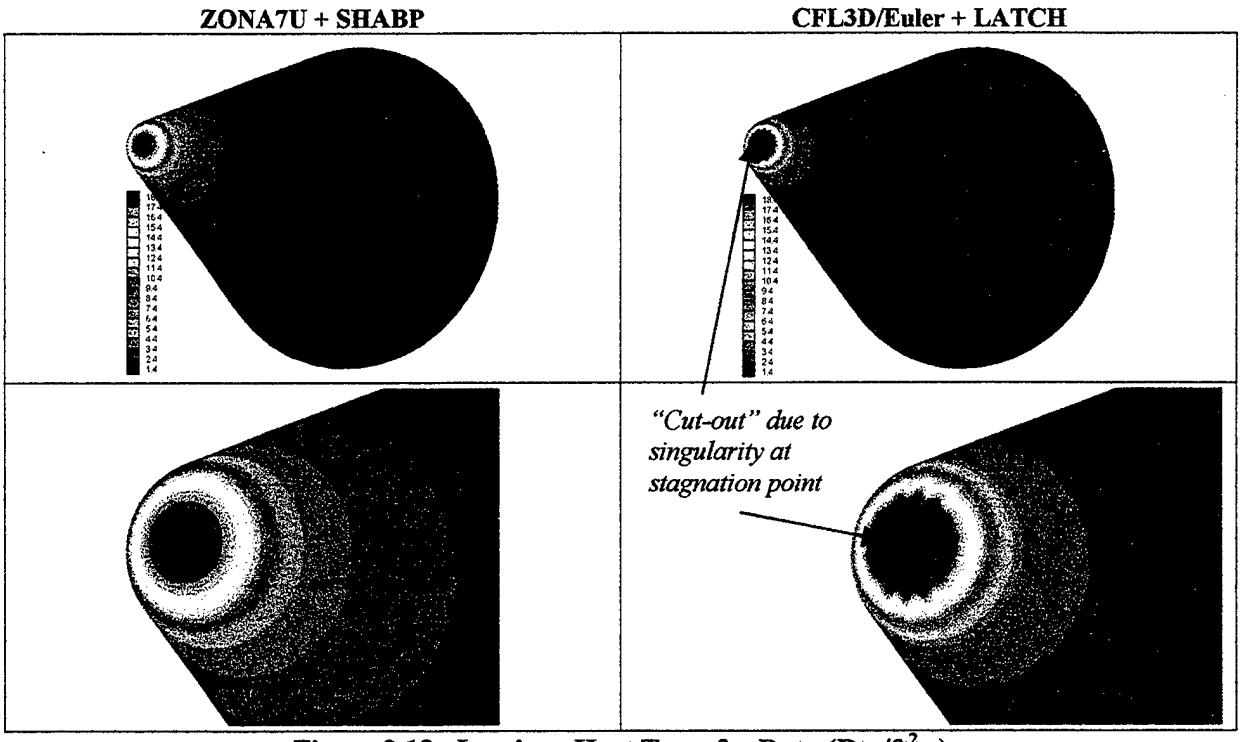

Figure 2.13 Laminar Heat Transfer Rates(Btu/ft^2-s)
15° Blunt Cone at M_∞=10.6, α=0°, p_∞=2.66 lb/ft^2, T_∞=89.971°R, T_w=540°R

$\alpha = 5°$

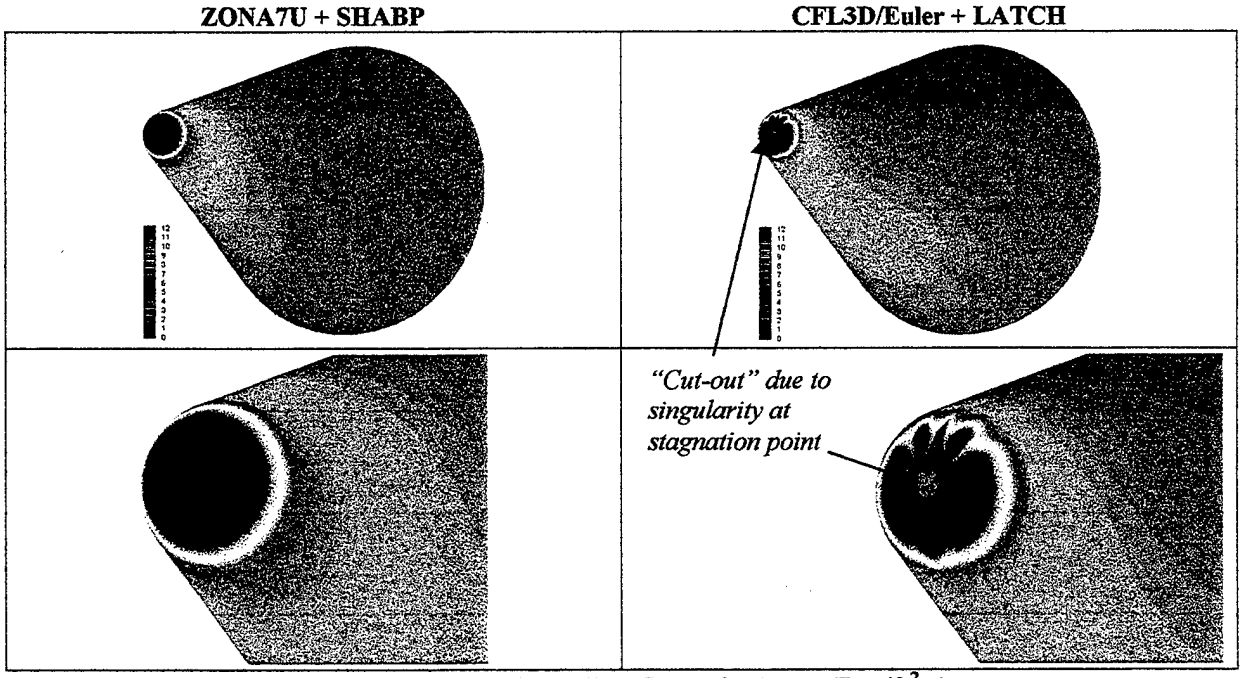

Figure 2.14 Laminar Heat Transfer Rates(Btu/ft^2-s)
15° Blunt Cone at M_∞=10.6, α=5°, p_∞=2.66 lb/ft^2, T_∞=89.971°R, T_w=540°R

$\alpha = 10°$

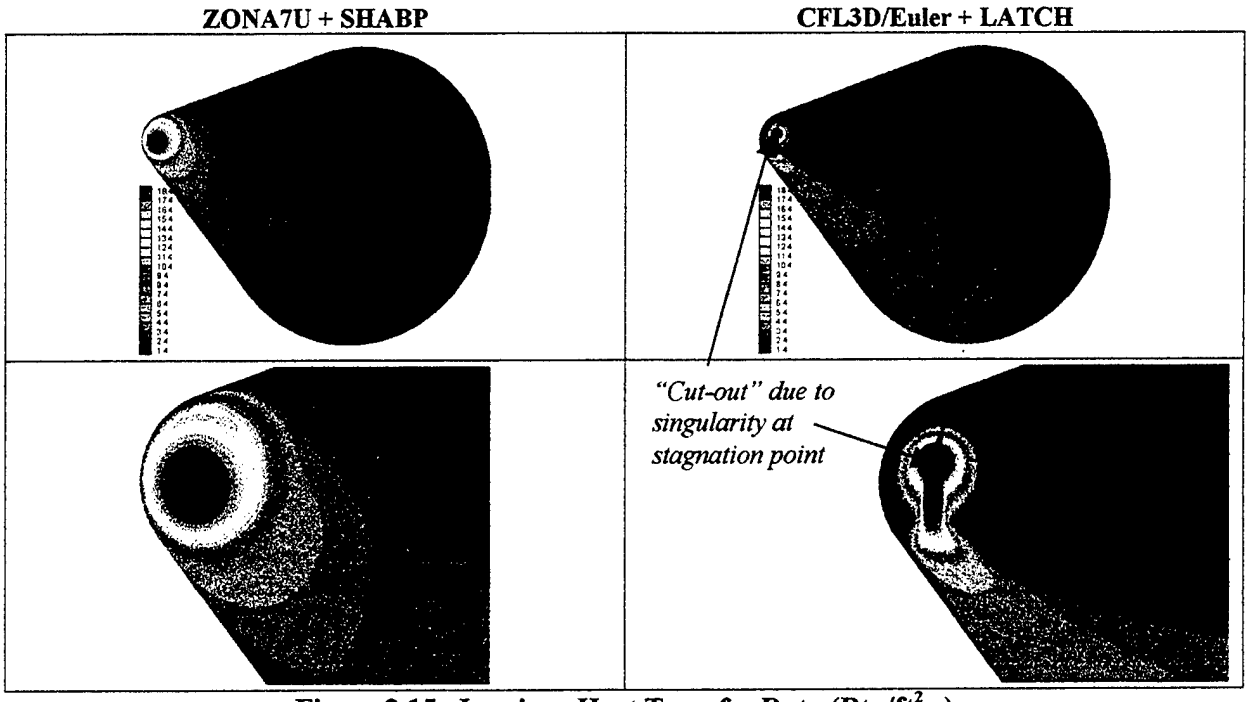

Figure 2.15 Laminar Heat Transfer Rates(Btu/ft^2-s)
15° Blunt Cone at M_∞=10.6, α=10°, p_∞=2.66 lb/ft^2, T_∞=89.971°R, T_w =540°R

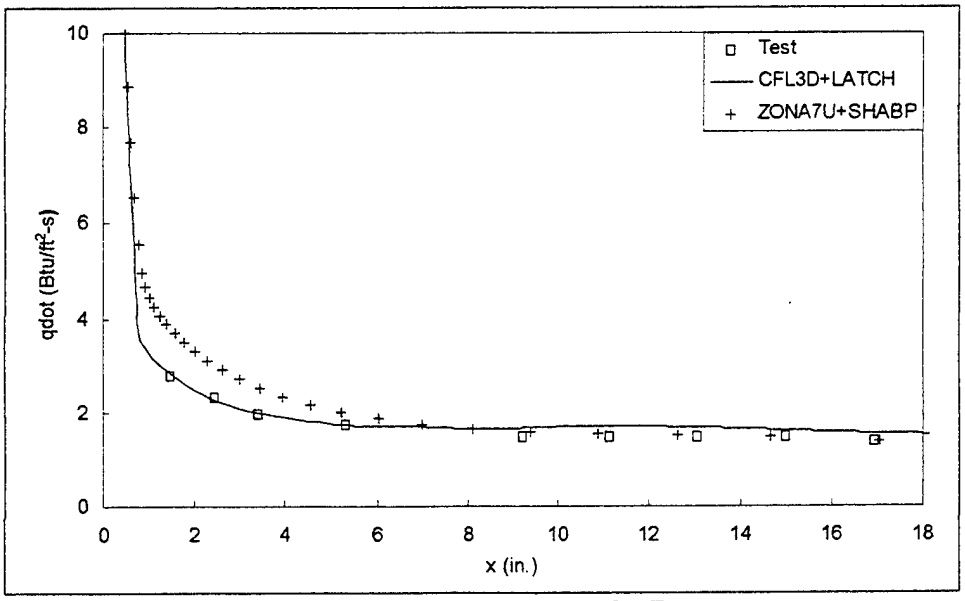

Figure 2.16 Laminar Heat Transfer Rates on a
15° Blunt Cone at M_∞=10.6, α=0°, p_∞=2.66 lb/ft^2, T_∞=89.971°R, T_w =540°R

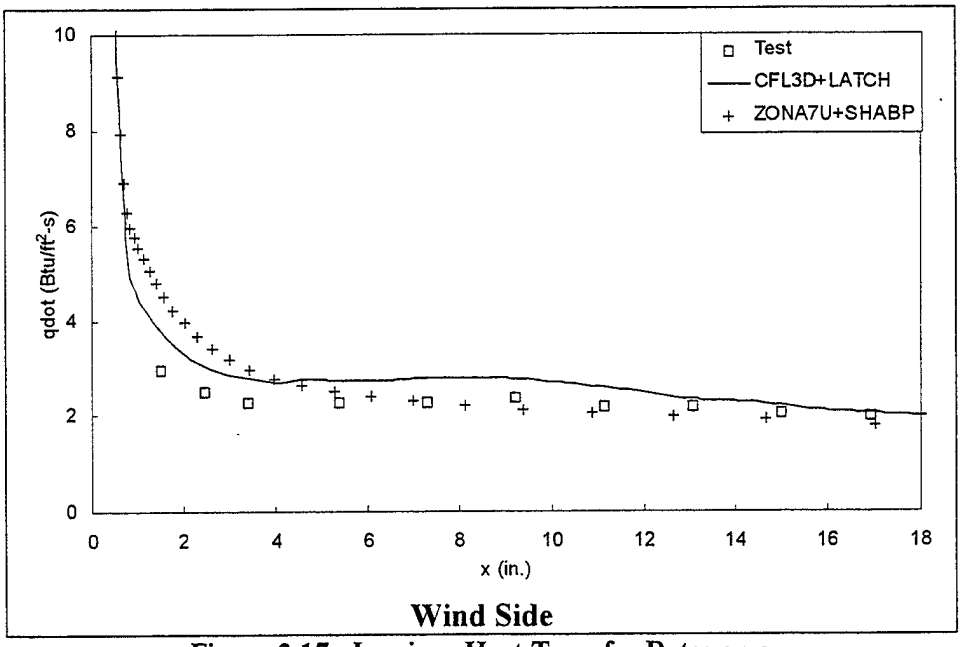

Figure 2.17 Laminar Heat Transfer Rates on a 15° Blunt Cone at M_∞=10.6, α=5°, p_∞=2.66 lb/ft^2, T_∞=89.971°R, T_w=540°R

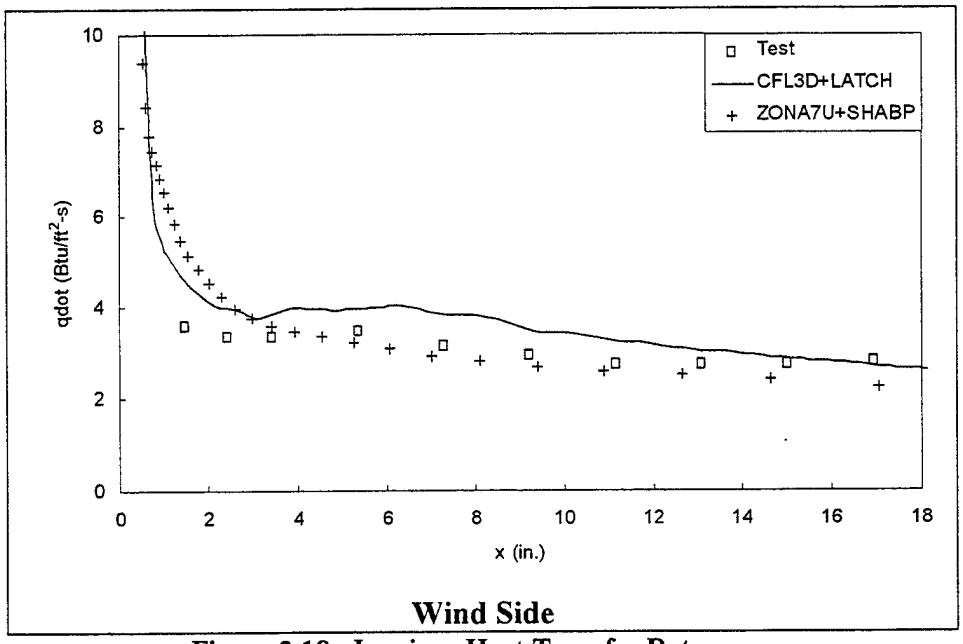

Figure 2.18 Laminar Heat Transfer Rates on a 15° Blunt Cone at M_∞=10.6, α=10°, p_∞=2.66 lb/ft^2, T_∞=89.971°R, T_w=540°R

SECTION 3

ZSTREAM for Hypersonic Aerothermodynamic Methodology

Summary
The ZONA development of ZSTREAM was prompted by the breakdown of QUADSTREAM at the stagnation points and its independency of freestream mach numbers. ZSTREAM is a finite element based streamline code, which is Mach number dependent and uniformly valid everywhere on the body surface. It is capable to define/plot the complete streamline domain on body surface, including the stagnation point, according to surface flow solutions given by a panel code (for example, ZONA7U) or a CFD code (For example, CFL3D).

The input required is the surface velocities at each grid/element points. The output is the surface streamlines. ZSTREAM functionality is to provide streamlines input for Aeroheating/Heat-transfer programs such as SHABP/MARKV[1] or MINIVAR for computations of the heat-transfer rate at the body surface.

Two test cases are presented to demonstrate the resulting streamlines and the developed aeroheating procedure using ZONA7U + ZSTREAM + SHABP for C_p and heat-transfer rate predictions. These cases are:

A) 3D Validation: Blunt Cone Case and
B) 2D Verification: Blunt Wedge Case

Given flow condition reads:
M=10.6, δ_c = 15° and α = 10°. Solution outputs for validation are the pressure coefficent C_p and the heat-transfer rate, $\dot{q}$.

3.1 ZSTREAM Development

Several problems were found in the QUADSTREAM code of SHABP/MARKV. First, the code only works for quadrilateral elements. Second, the Newtonian steepest decent method used in QUADSTREAM calculates streamlines only based on the freestream velocity vector and the normal vector of the element. No local flowfield variables are involved. We found the method is not accurate, nor is it uniformly valid throughout the surfaces.

By contrast, there are two other approaches that will yield more accurate streamline solutions that the Newtonian steepest decent method used in QUADSTREAM. One is to use the inviscid surface pressure, and the other is to use the inviscid surface velocity. Both can yield streamlines that are mach number dependent and uniformly valid throughout. ZSTREAM adopts the latter as input to yield higher quality streamline solutions.

3.2 Methodology of Tracing Streamlines

A streamline on a three-dimensional surface is traced by a step-marching method using the flow velocity on the tangential plane of the surface. In order to define the tangential plane at a point, the geometry of the body surface is approximated by a number of four-noded quadrilateral elements (Fig 3.1) and the surface close to the nose is modeled by some three-noded triangular elements (Fig 3.2)

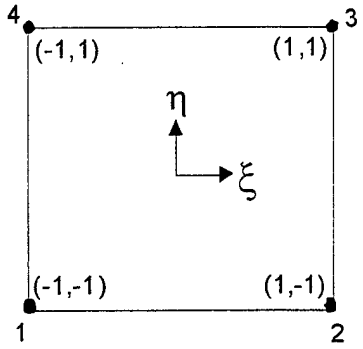

Fig 3.1 Quadrilateral Isoparameter Element

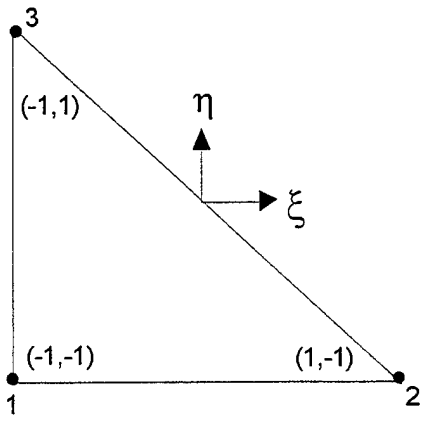

Fig 3.2 Triangular Isoparameter Element

Over an element, coordinates can be determined using the following equation

$$x_i(\xi,\eta) = \sum_{\alpha=1}^{N_e} N_\alpha(\xi,\eta) x_i^\alpha \tag{1}$$

where N_e is the number of element nodes (4 for quadrilateral elements and 3 for triangular elements), x_i^α are the coordinates at the node α, ξ and η are parameters ranged from -1 to 1, and $N_\alpha(\xi,\eta)$ are shape functions given by

$$
\begin{aligned}
N_1(\xi,\eta) &= \frac{1}{4}(1-\xi)(1-\eta) \\
N_2(\xi,\eta) &= \frac{1}{4}(1+\xi)(1-\eta) \\
N_3(\xi,\eta) &= \frac{1}{4}(1+\xi)(1+\eta) \\
N_4(\xi,\eta) &= \frac{1}{4}(1-\xi)(1+\eta)
\end{aligned}
\tag{2}
$$

for quadrilateral elements, and

$$
\begin{aligned}
N_1(\xi,\eta) &= -\frac{1}{2}(\xi+\eta) \\
N_2(\xi,\eta) &= \frac{1}{2}(1+\xi) \\
N_3(\xi,\eta) &= \frac{1}{2}(1+\eta)
\end{aligned}
\tag{3}
$$

for triangular elements.

A local Cartesian coordinate system x_i' is defined on the element with x_1' along ξ direction and x_3' along the normal direction (see Fig. 3.3).

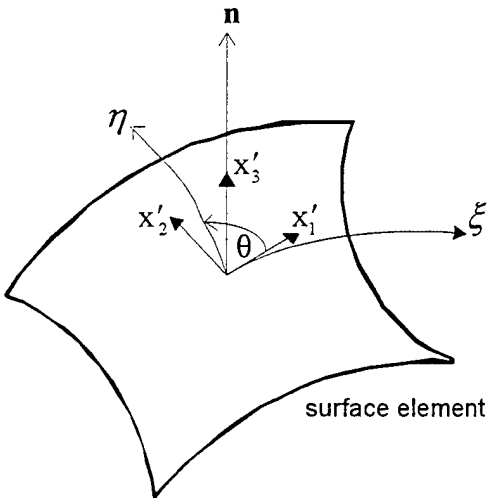

Fig. 3.3 Local Coordinate System

Based on this coordinate system, coordinates (x, y) and velocity (u, v) at the element nodes on the tangential plane can be calculated in terms of their global values by

$$x^{\alpha} = \sum_{j=1}^{3} L_{1j} x_j^{\alpha}$$
$$y^{\alpha} = \sum_{j=1}^{3} L_{2j} x_j^{\alpha} \tag{4}$$

$$u^{\alpha} = \sum_{j=1}^{3} L_{1j} g_j^{\alpha}$$
$$v^{\alpha} = \sum_{j=1}^{3} L_{2j} g_j^{\alpha} \tag{5}$$

where g_j^{α} are the global components of the velocity and L_{1j} and L_{2j} are the direction cosines of the local coordinate axes x_1' and x_2' with respect to the global coordinate system.

The streamline marches from a beginning point towards the stagnation point along the negative direction of the tangential velocity (u, v). Denoting the current position with (x_0, y_0) and the velocity at this point with (u_0, v_0) and referring to Fig. 3.4, the new position (x, y) can be determined using the relation:

$$(x - x_0)v_0 = (y - y_0)u_0 \tag{6}$$

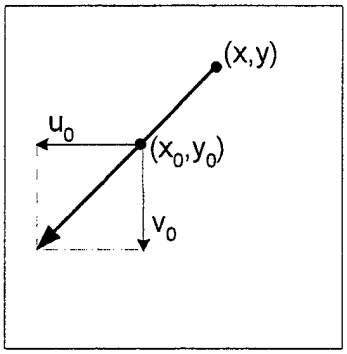

Fig. 3.4 Marching from position (x_0, y_0) to (x, y)

In equation (6), the coordinates x and y in the tangential plane can be calculated using shape functions as follows

$$x = \sum_{\alpha=1}^{N_e} N_{\alpha}(\xi,\eta) x^{\alpha}$$
$$y = \sum_{\alpha=1}^{N_e} N_{\alpha}(\xi,\eta) y^{\alpha} \tag{7}$$

The distance between the current position (x_0, y_0) to the new position (x, y) is controlled by step size $\Delta\xi$ or $\Delta\eta$. Using (ξ_0, η_0) to denote the parameters at the current position, their values at the new position can be written as

$$\begin{aligned} \xi &= \xi_0 + \Delta\xi \\ \eta &= \eta_0 + \Delta\eta \end{aligned} \tag{8}$$

Thus, for a given step size $\Delta\xi$, we can solve equation (6) for $\Delta\eta$ and vice versa. This task is accomplished by using the software *Mapple*. For quadrilateral elements, the results are:

```
dxi = [v0 * (4 * x0 - (-1 + deta + et0) * x1 * (-1 + xi0) + (-1 + deta + et0) * x2 * (1 + xi0) -
        (1 + deta + et0) * (x3 + x4 + x3 * xi0 - x4 * xi0)) +
      u0 * (-4 * y0 + (-1 + deta + et0) * (-1 + xi0) * y1 - (-1 + deta + et0) * (1 + xi0) * y2 +
        (1 + deta + et0) * (y3 + xi0 * y3 + y4 - xi0 * y4))] / [v0 *
       ((-1 + deta + et0) * x1 + x2 + x3 - x4 - (deta + et0) * (x2 - x3 + x4)) + u0 * y1 -
      u0 * (y2 + y3 + (deta + et0) * (y1 - y2 + y3)) + (1 + deta + et0) * u0 * y4]
```

(9)

for the given step size $\Delta\eta$ (here denoted by deta), and

```
deta = -[v0 (-4 x0 + (-1 + et0) x1 (-1 + dxi + xi0) - (-1 + et0) x2 (1 + dxi + xi0) +
          (1 + et0) (x4 - x4 (dxi + xi0) + x3 (1 + dxi + xi0))) -
        u0 (-4 y0 + (-1 + et0) (-1 + dxi + xi0) y1 + (1 + dxi + xi0) (y2 - et0 y2 + y3 + et0 y3) -
          (1 + et0) (-1 + dxi + xi0) y4)] / [v0 (-x2 + x3 + x4 + x1 (-1 + dxi + xi0) -
         (x2 - x3 + x4) (dxi + xi0)) + u0 (-(-1 + dxi + xi0) y1 + (1 + dxi + xi0) (y2 - y3) +
         (-1 + dxi + xi0) y4)]
```

(10)

for the given step size $\Delta\xi$ (here denoted by dxi).

The results for a triangular element are:

```
dxi = [v0 * (-2 * x0 + x2 - (deta + et0) * (x1 - x3) + x3 + (-x1 + x2) * xi0) +
       u0 * (2 * y0 + deta * y1 + et0 * y1 + xi0 * y1 - y2 - xi0 * y2 -
         (1 + deta + et0) * y3)] / [v0 * (x1 - x2) + u0 * (-y1 + y2)]
```

(11)

for the given step size $\Delta\eta$, and

```
deta = [v0 * (-2 * x0 - dxi * x1 - et0 * x1 + x2 + dxi * x2 + x3 + et0 * x3 -
         x1 * xi0 + x2 * xi0) + u0 * (2 * y0 + dxi * y1 + et0 * y1 + xi0 * y1 -
         y2 - dxi * y2 - xi0 * y2 - (1 + et0) * y3)] / [v0 * (x1 - x3) + u0 * (-y1 + y3)]
```

(12)

for the given step size $\Delta\xi$.

Once $\Delta\xi$ and $\Delta\eta$ are obtained, the new position can be determined by equation (7) and the tangential velocity at the new position can be calculated by

$$u = \sum_{\alpha=1}^{4} N_\alpha(\xi,\eta)u^\alpha$$
$$v = \sum_{\alpha=1}^{4} N_\alpha(\xi,\eta)v^\alpha \qquad (13)$$

This process is repeated until the element boundary is reached. On the element boundary, ξ and/or η equal(s) ± 1. Once this condition is satisfied, the next nearest element is considered in a similar way, until the stagnation point, characterized by u=v=0, is encountered. Here are some examples:

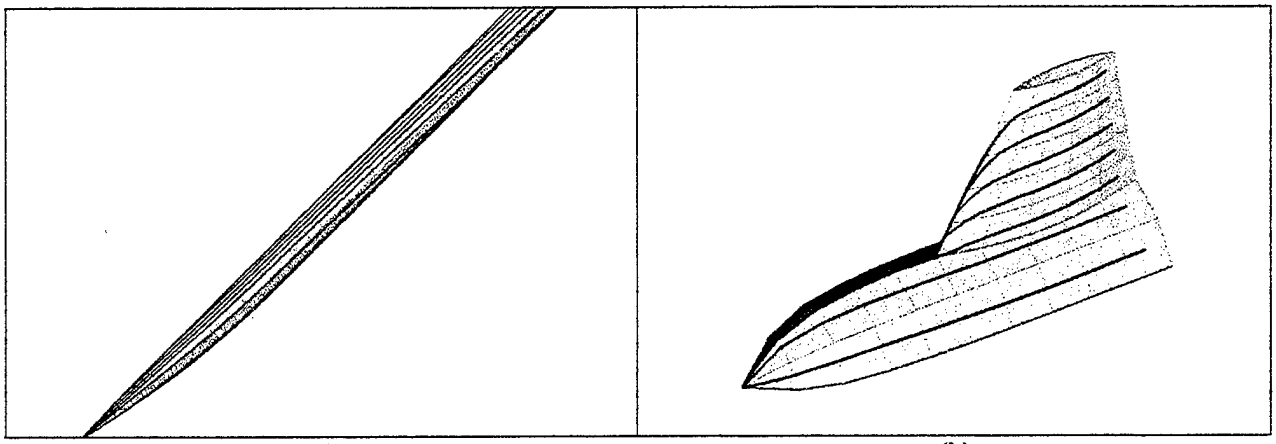

(a) (b)

Fig. 3.5 Body and Wing Streamlines Produced by ZAERO/ZSTREAM
(a) Ogive-Cylinder Body (M=6.0, α=2°, τ=0.022) (b) Simple Wing Body Combination at α=0

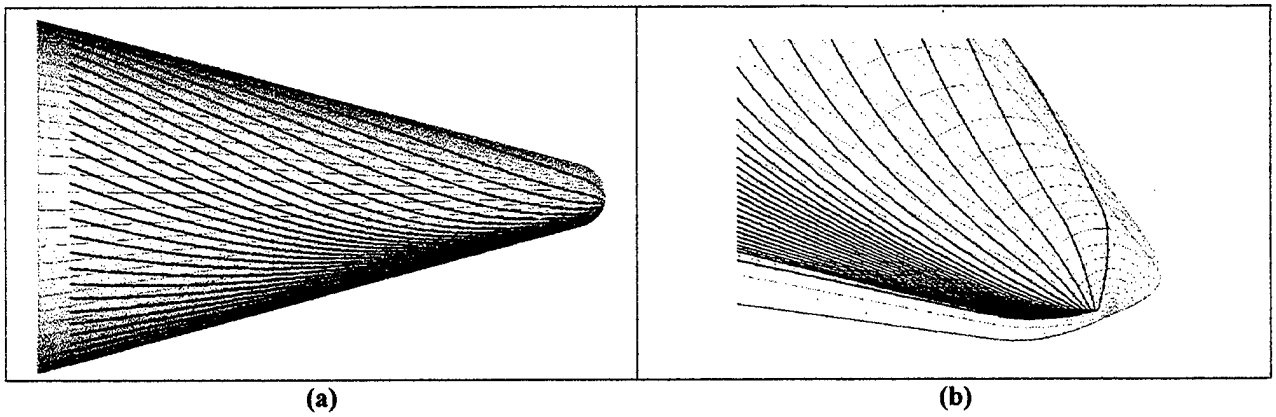

(a) (b)

Fig. 3.6 Blunt-Nose Cone Streamlines Produced by ZSTREAM
(Two different views with flow condition at M=10.6, α=10°, δ_c=15°, R_N=1.1^{in})

3.3 Aeroheating Procedure Demonstration

Two cases are selected for case study; namely, the 15°-Blunt Cone and the 15°-Blunt Wedge with the given conditions below.

Given Hypersonic Flow Conditions for Blunt Cone/Wedge	
Mach No.	**M = 10.6**
Wedge/Cone angle	**$\delta_c = 15°$**
AoA	**$\alpha = 10°$**
Meridian Plane	**$\varphi = 180°$**
Nose Radius	**$R_N = 1.1''$**
Freestream Pressure	**$P_\infty = 2.66^{psf}$**
Freestream Temperature	**$T_\infty = 89.971^{°R}$**
Wall Temperature	**$T_\omega = 540^{°R}$**

Our objective is to validate/verify the results obtained with existing results/test data as collected by Moore (Ref 32, See Fig. 3.1)

3.4 Pressure Distributions, C_p

Case A: Blunt-Nose Cone

To validate the computation procedure with the existing data, we select the CFL3D code, for flow accuracy, to generate the surface pressure. Fig. 3.4.2 shows C_p versus surface distance, at the meridian plane $\varphi = 180°$, up to 18 times of nose radius. The demarcation points on the body exhibit the following:

- Sonic Point θ^* at $x = 0.4\ R_N$
- Tangent Point θ_1 at $x = 0.74\ R_N$
- First Minimum Pressure at $x = 2.6\ R_N$
- Sharp Cone Pressure Restored at (C_{pc}=0.378) $x = 12\ R_N$

Accordingly, several observations can be made:

i) In the nose region, the CFL3D result checks quite well with the Newtonian-Lees distribution+ (Ref 3). One exception is that the flow characteristics at θ_1 does not reflect a kink in C_p.

ii) In the aft-body downstream an asymptotic matching point exists (say, $X/R_N = 12$), the C_p recovers the value of that due to a sharp cone of the same angle δ_c (called equivalent cone). It is known that the sharp cone C_p typically serves as an asymptotic pressure for the blunt-nose cone problem.

iii) The relaxation distance, defined as the distance from the first minimum C_p location to the asymptotic matching point, is not known in advance.

Case B: Blunt-Nose Wedge

The present 2D case is a heuristic study with the goal of understanding the physics of the blunt-nose body flow characteristics while keeping a relatively low CFD computing level. Further, the C_p obtained could be immediately linked with the Heat-Transfer code (MARKV). No coupling with the QUADSTREAM is needed, since the 2D body shape is the basic streamline itself.

Fig. 3.9 presents C_p versus X/R_N up to $x = 4.0\ R_N$, where C_p converges to the asymptotic matching value of an equivalent wedge of the same δ_w ($\delta_w = 15°$). The demarcation points on the wedge exhibit the following:

- Sonic Point θ^* at $x = 0.47\ R_N$
- Tangent Point θ at $x = 0.74\ R_N$
- First Minimum Pressure at θ_1 or $x = 0.74\ R_N$
- Sharp Wedge Pressure Restored at $x = 3\ R_N$ ($C_{pw} = 0.45$)

Similarly, observations can be made:

i) Similar to the Blunt-Cone Case, the NLD-C_p formula should be applicable to the wedge case up to θ.

ii) The asymptotic matching value in the aft body is indeed the sharp wedge value.

iii) Again the relaxation distance is better defined in this case, as its starting point is the tangent point (defined by the body symmetry) θ_1

+ Also known as the improved modified Newtonian approach

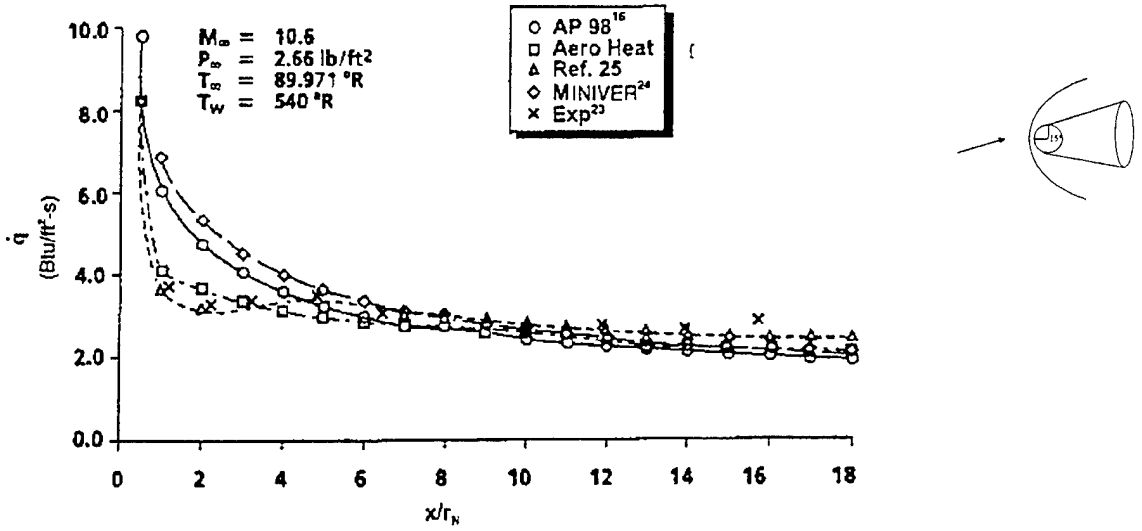

Fig. 3.7 Heat Transfer Rates for 1.1-in. Nose Radius
15° Half-Angle Cone at α=10°and φ=180°

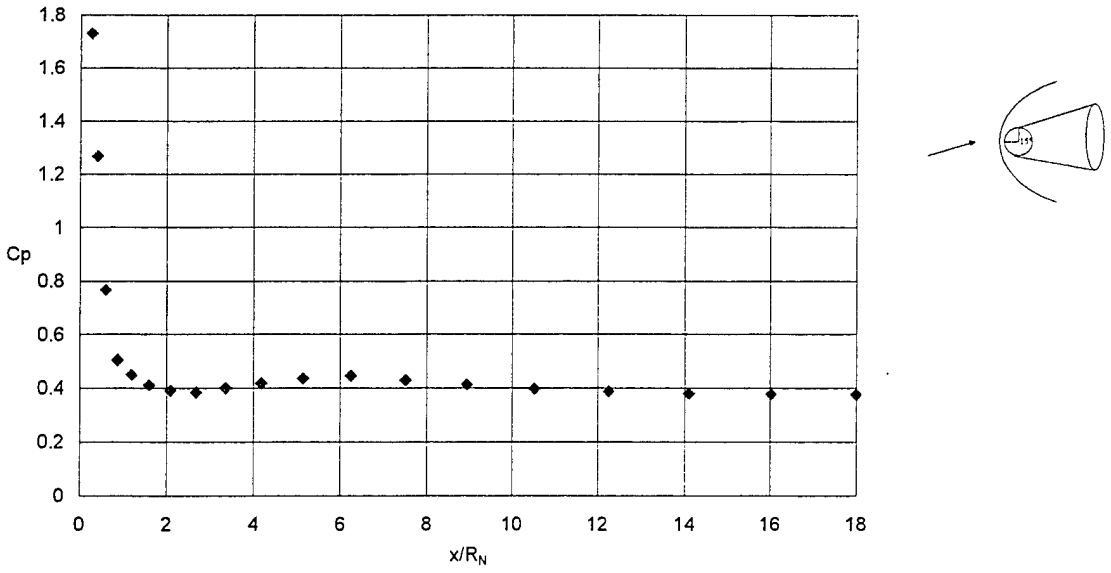

Fig. 3.8 C_p for 1.1-in. Nose Radius 15° Half-Angle Cone at M_∞= 10.6, α= 10°, φ= 180°

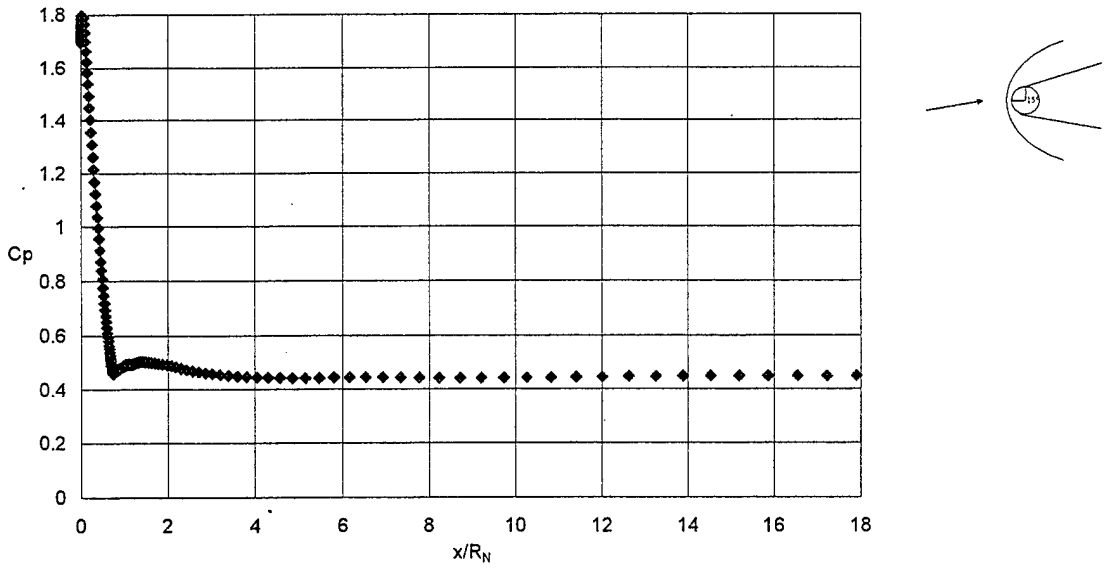

Fig. 3.9 C_p for 1.1-in. Nose Radius 15° Half-Angle Wedge at M_∞=10.6, α= 10°,φ=180°

3.5 Heat Transfer Rates, $\dot{q}$

With the computed pressures, we then used the ZSTREAM to couple them with the MARKV of SHABP. Shown in Figs. 3.10 and 3.11 are the Heat Transfer Rates, $\dot{\mathbf{q}}$, for a 15°-Blunt Cone (Case A) and for a 15°- Blunt Wedge (Case B). Comparisons of the present results with that of the existing methods (MINIVAR (Ref 33), AEROHEAT (Ref 34)) and Cleary's test data (Ref 35) are made. A fairly good trend is found between the present result and the test data. However, in both $\dot{\mathbf{q}}$-distributions, large change in the heat-transfer gradient is found for the present (ZONA) solution at about one radius distance from the nose. The Blunt-Wedge (Case B) Case is well understood in that the large gradient point corresponds to the tangent point θ_1, where the pressure also suffers from a high gradient change.

However, for the Blunt-Cone Case (Case A), the cause of such a high gradient in $\dot{\mathbf{q}}$ is not clear which requires further investigation.

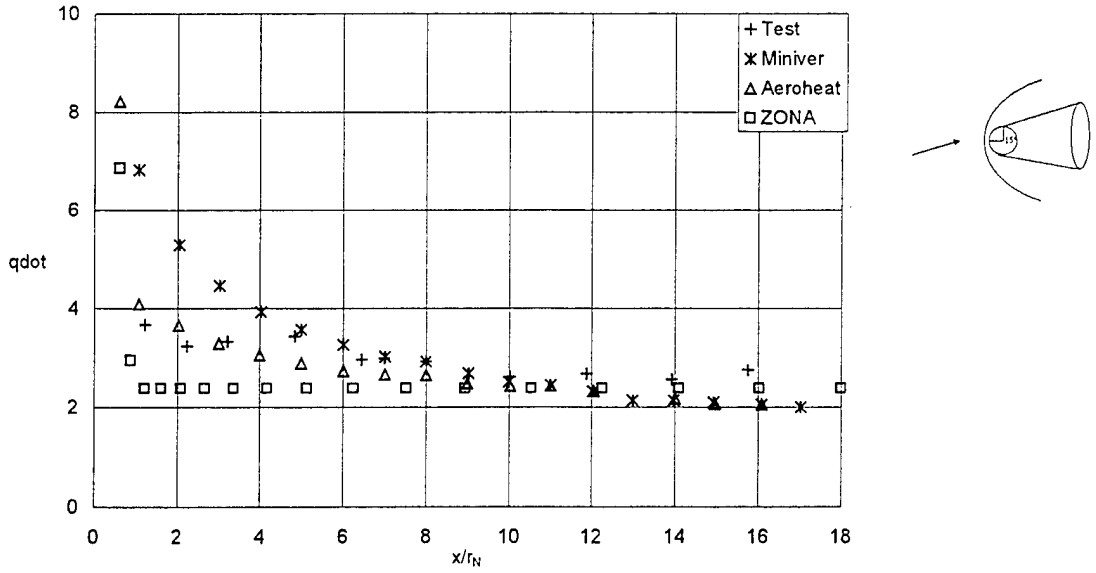

Fig. 3.10 $\dot{q}$ for 1.1-in. Nose Radius 15° Half-Angle Cone at M_∞=10.6, α= 10°, φ= 180°

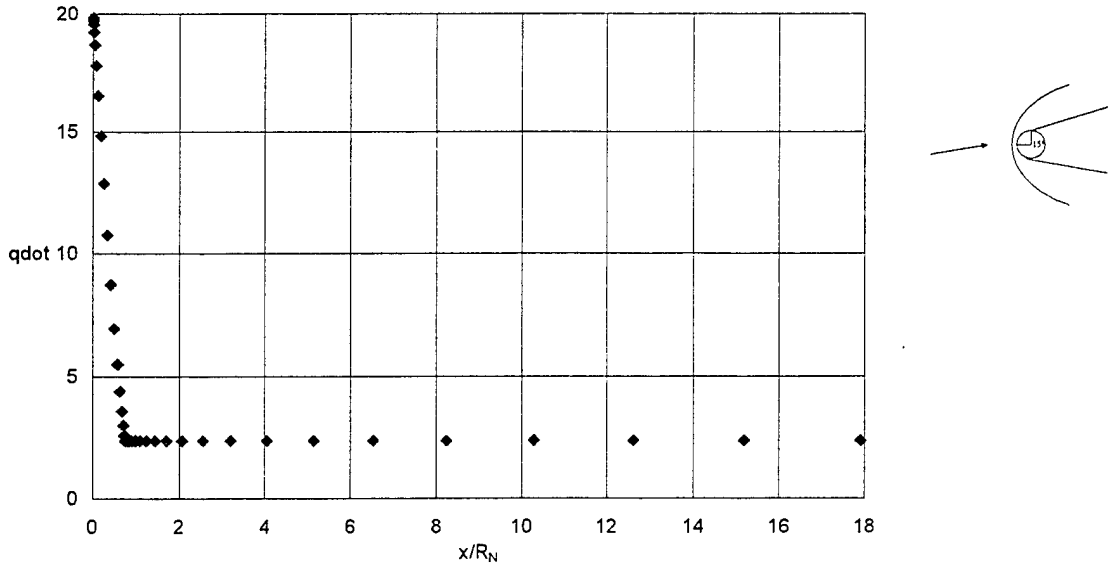

Fig. 3.11 $\dot{q}$ for 1.1-in. Nose Radius 15° Half-Angle Wedge at M_∞=10.6, α= 10°, φ= 180°

SECTION 4

Application of ZONA Hypersonic Aerothermodynamic Method to X-34

Summary

- *The developed ZONA Hypersonic aerothermodynamic method consists of coupled software of ZONA7U + ZSTREAM + SHABP. To demonstrate the developed methodology, we apply the software to X-34 for solution validation with that of CFD aerothermodynamic method (For example, CFL3D+LATCH) in terms of pressure distributions and temperature distributions on the front/lee/wind-side surfaces of X-34, at two selected flow conditions.*
- *Streamlines of X-34 at these conditions are displayed. Note that the X-34 wing-body adopted for demonstration is defined as the partial configuration (Fig 4.1(b)) by NASA-LaRC (Ref 13, AIAA98-0880)*

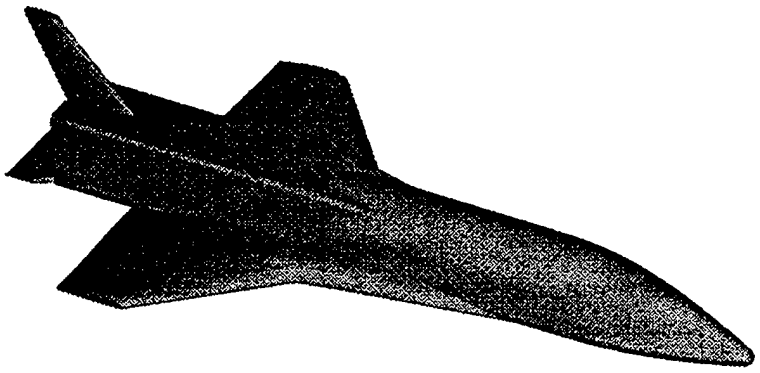

a) Full configuration used for viscous solutions.

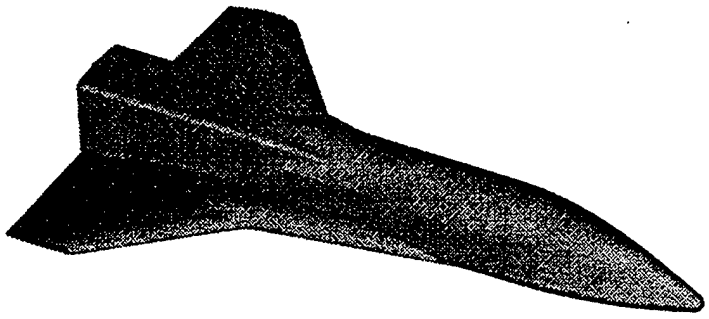

b) Partial configuration used for inviscid solutions.

Figure 4.1 X-34 Configurations Taken From AIAA 98-0880 (Ref 13)

4.1 Pressure Coefficients of X-34 Wing-Body Configuration at M = 6.0, α = 9° and 15.22°

The X-34 wing-body configuration consists of a body with a round nose of 7.0" radius, a strake, and a swept wing. The inviscid surface C_p distributions computed by ZONA7U and CFL3D Euler solver on the wind-side and lee-side of X-34 are shown in Fig 4.2 for the M = 6.0, α = 9° case and Fig 4.3 for the M = 6.0, α = 15.22° case. In general, ZONA7U results on the wind-side correlate well with the CFL3D results but those on the lee-side present discrepancies. This is caused by the flow separation on the lee side at high angle of attack (α = 9° and 15.22°) that cannot be handled well by the ZONA7U attached-flow assumption. Nevertheless, in the high pressure regions such as at the round nose of the body, and along the leading edge of the wing, ZONA7U results give good agreement with those of the CFL3D. Note that those high-pressure regions represent the high temperature area on the configuration, and therefore, are critical for the TPS design.

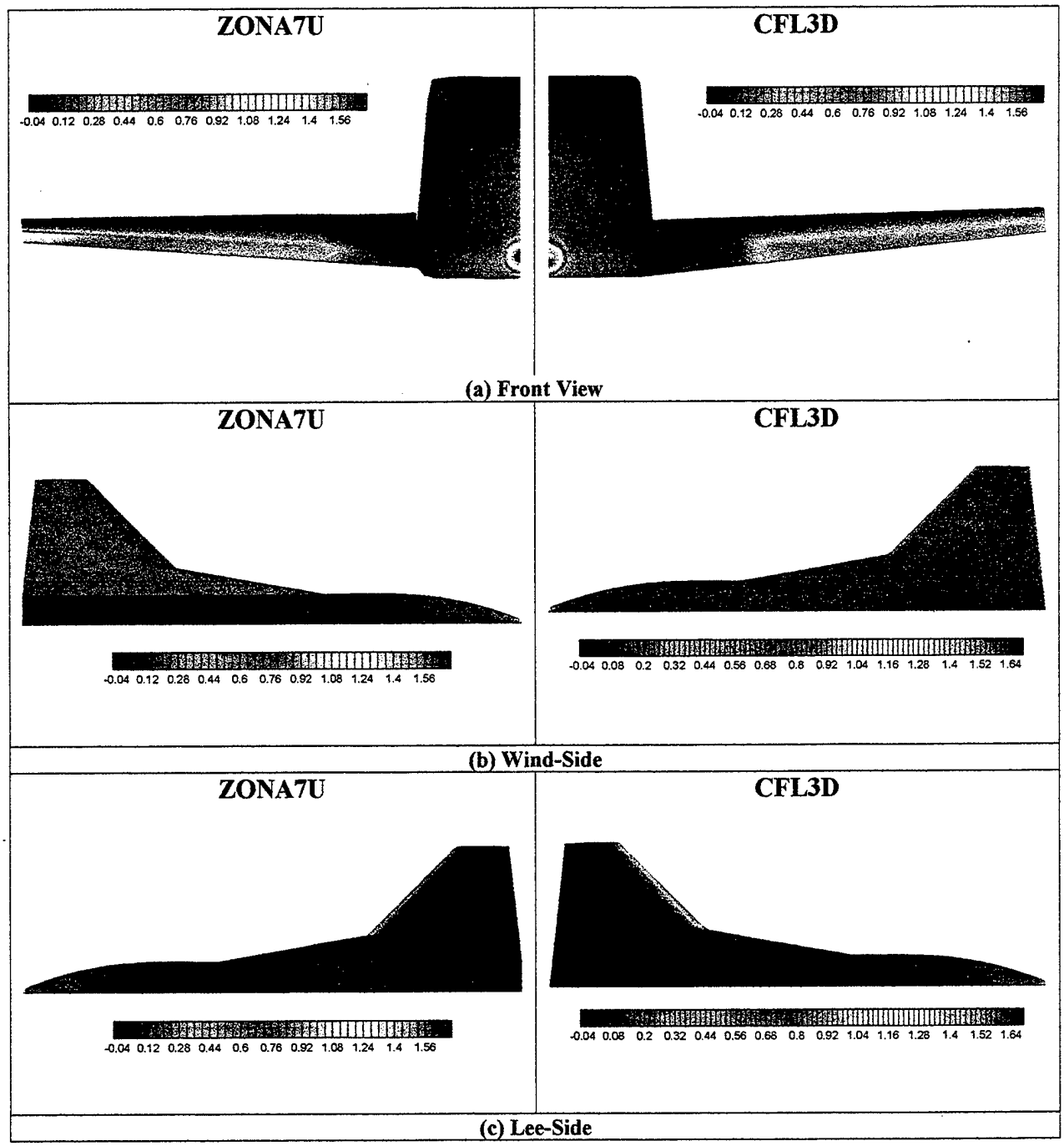

Figure 4.2 Inviscid Surface Pressure Distributions on the X-34 at M_∞=6, α=9°; (a) Front View, (b) Wind-Side, and (c) Lee-Side.

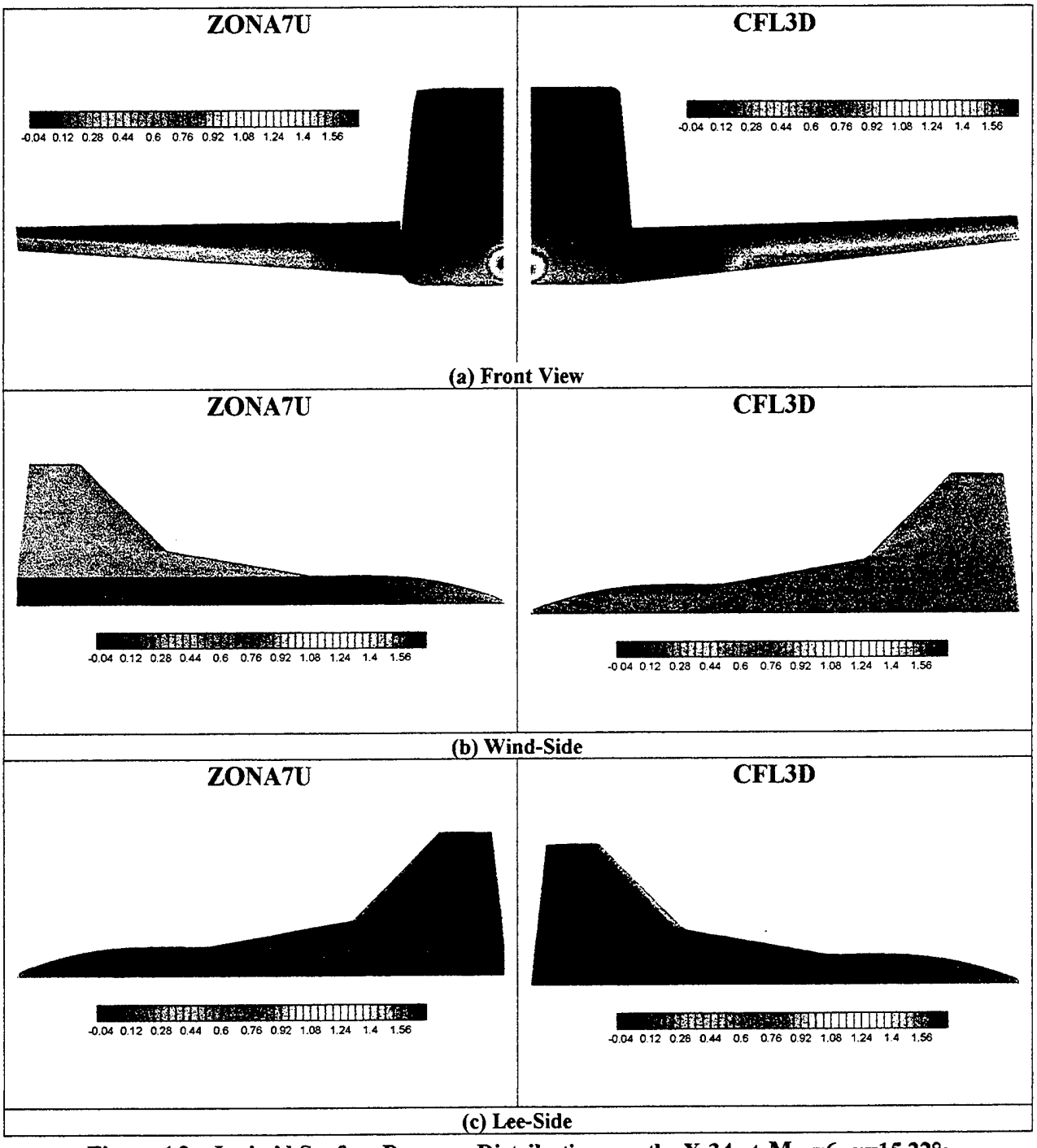

Figure 4.3 Inviscid Surface Pressure Distributions on the X-34 at M_∞=6, α=15.22°; (a) Front View, (b) Wind-Side, and (c) Lee-Side.

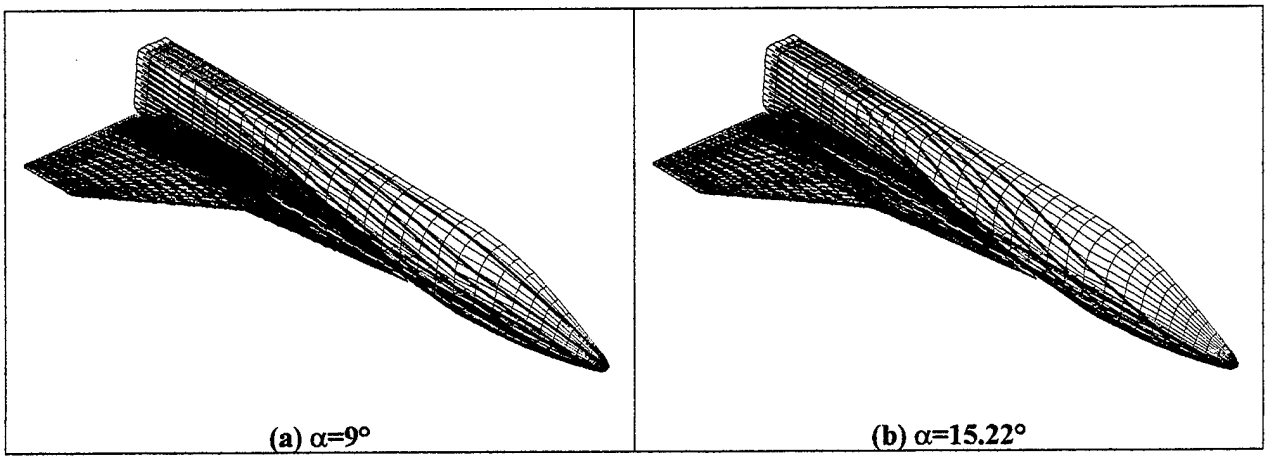

(a) α=9° (b) α=15.22°

Figure 4.4 Streamlines Computed by ZSTREAM on the X-34 at M_∞=6; (a) α=9°, (b) α=15.22°.

4.2 Streamlines and Temperature Distributions on X-34 Wind Body: M=6.0, α=9° and 15.22°

Fig 4.4 depicts the streamlines computed by ZSTREAM for α = 9° and 15.22° cases. The aeroheating analysis is performed using the radiative equilibrium temperature wall boundary condition (the "hot wall" condition) with emissivity of 0.8. The temperature distributions computed by ZONA7U + SHABP and CFL3D + LATCH on the wind-side and lee-side of X-34 at M = 6.0, are presented in Fig 4.5 for the α = 9° and the altitude = 183 Kft. condition and in Fig 4.6 for the α = 15.22° and altitude = 112 Kft condition. In both cases, the temperature distributions computed by ZONA7U + SHABP on the wind-side of X-34 correlate well with CFL3D + LATCH whereas some discrepancies are shown on the lee-side of X-34.

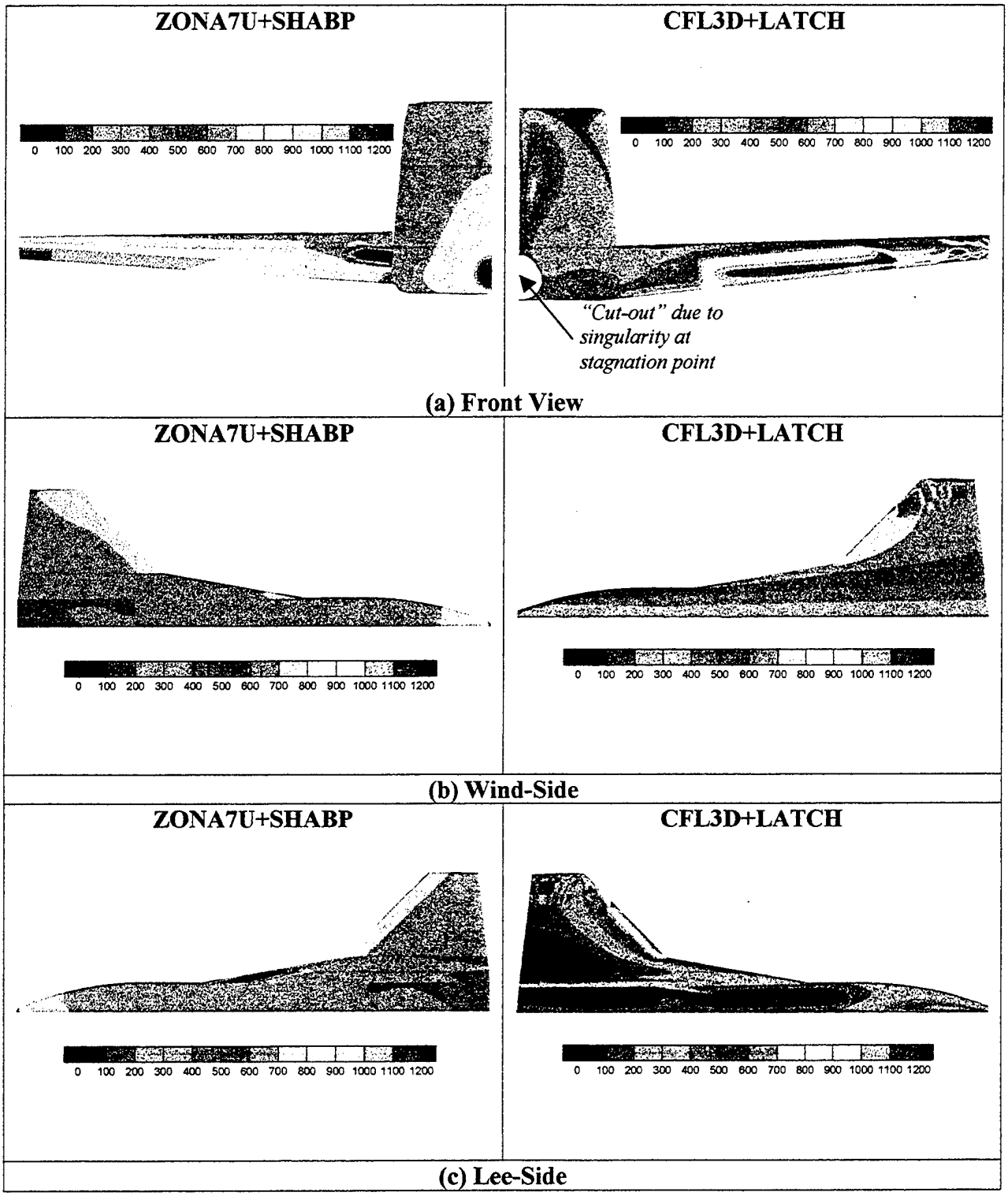

Figure 4.5 Turbulent Surface Temperatures (°F) on the X-34 at M_∞=6, α=9°, Alt.=183 Kft; (a) Front View, (b) Wind-Side, and (c) Lee-Side.

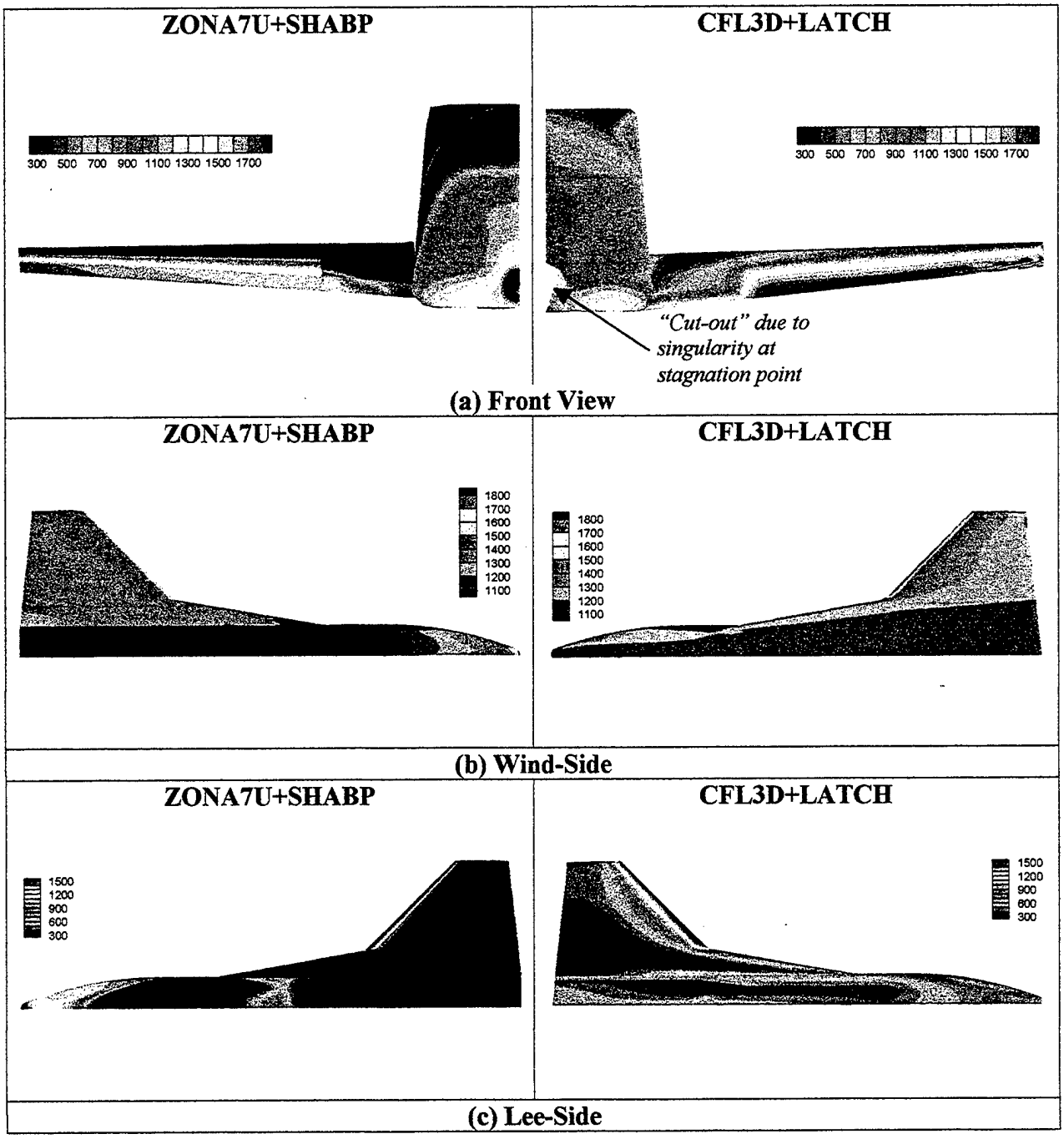

Figure 4.6 Turbulent Surface Temperatures (°F) on the X-34 at M_∞=6, α=15.22°, Alt.=112 Kft; (a) Front View, (b) Wind-Side, and (c) Lee-Side.

SECTION 5

TRAJECTORY ANALYSIS

Summary

ZONA7U + SHABP is used to compute the heat rate at the stagnation point of the X-34, according to two assigned trajectories S_g, namely X1004601 and X1004701. Here ZONA7U + SHABP only requires the trajectory to be submitted once, then it outputs the pressure C_p and the heat rate $\dot{q}$ throughout the complete trajectory. For 14 time steps with a stretch of 800 seconds, it requires 10 minutes of computing time. By contrast, MINIVER requires manual input for each point of interest, i.e. each output $\dot{q}$ solution requires approximately 5 to 10 minutes.

5.1 Descriptions and Functionality of Blocks 5: Trajectory Analysis (Block 5)

Description:

- Two trajectory analysis codes used within industry (OTIS and POST/OTIS) have often been adopted by the Air Force Research Laboratory (AFRL). The trajectory code POST will be adopted in the program integration.
- POST (Program to Optimize Simulated Trajectories, Version II) is a generalized point mass, three and six-degree-of-freedom (3-6 DOF) trajectory program. The 3-DOF-trajectory simulation can be used to compute loads, propellant requirements, propulsion and aerodynamic trim interactions for ascent trajectories.
- POST II has a discrete parameter targeting an optimization capability that can be used to guide the user to the optimum trajectory (dynamic pressure profile) and fuel and oxidizer settings to minimize propellant requirements for a given mission.
- POST II can model multiple powered and unpowered vehicles including SSTO, TSTO, VTHL, HTHL, re-entry problems, as well as exo-atmospheric orbital transfer problems.

Functionality:

- The main function of the trajectory analysis is to obtain an optimal trajectory that minimizes the fuel while satisfying other constraints such as Mach number needed for specific engine usage, final velocities, altitudes, launch angle, etc. (Ref 36).
- Inputs include forces, moments of TRIM aerodynamics and mass from ASTROS*. Other inputs based on the requirements from propulsion, mission and TPS performance considerations.
- Provide trajectory/flight condition history as inputs to TPS for heat rate estimate (see cases studied)

5.2 Phase I Achievements in Trajectory Analysis/Case Demonstration Trajectory Analysis Example (Block 4)

Here, ZONA7U + SHABP is used to compute for the heat rate at the stagnation point of the X-34 according to two assigned trajectories (X1004601 and X1004701). Good correlation is found between the present ZONA7U + SHABP method and MINIVER (Fig 5.1). Clearly, the advantage of the ZONA7U + SHABP method over MINIVER is two fold:

1. Automated generation of heat rate solutions once the trajectory history is given as input
2. Formulation of the aerodynamic (C_p) and aerothermodynamic ($\dot{q}$) is based on a rigorous panel methodology which accounts globally for the aerodynamics/aerothermodynamics of the complete X-34 configuration.

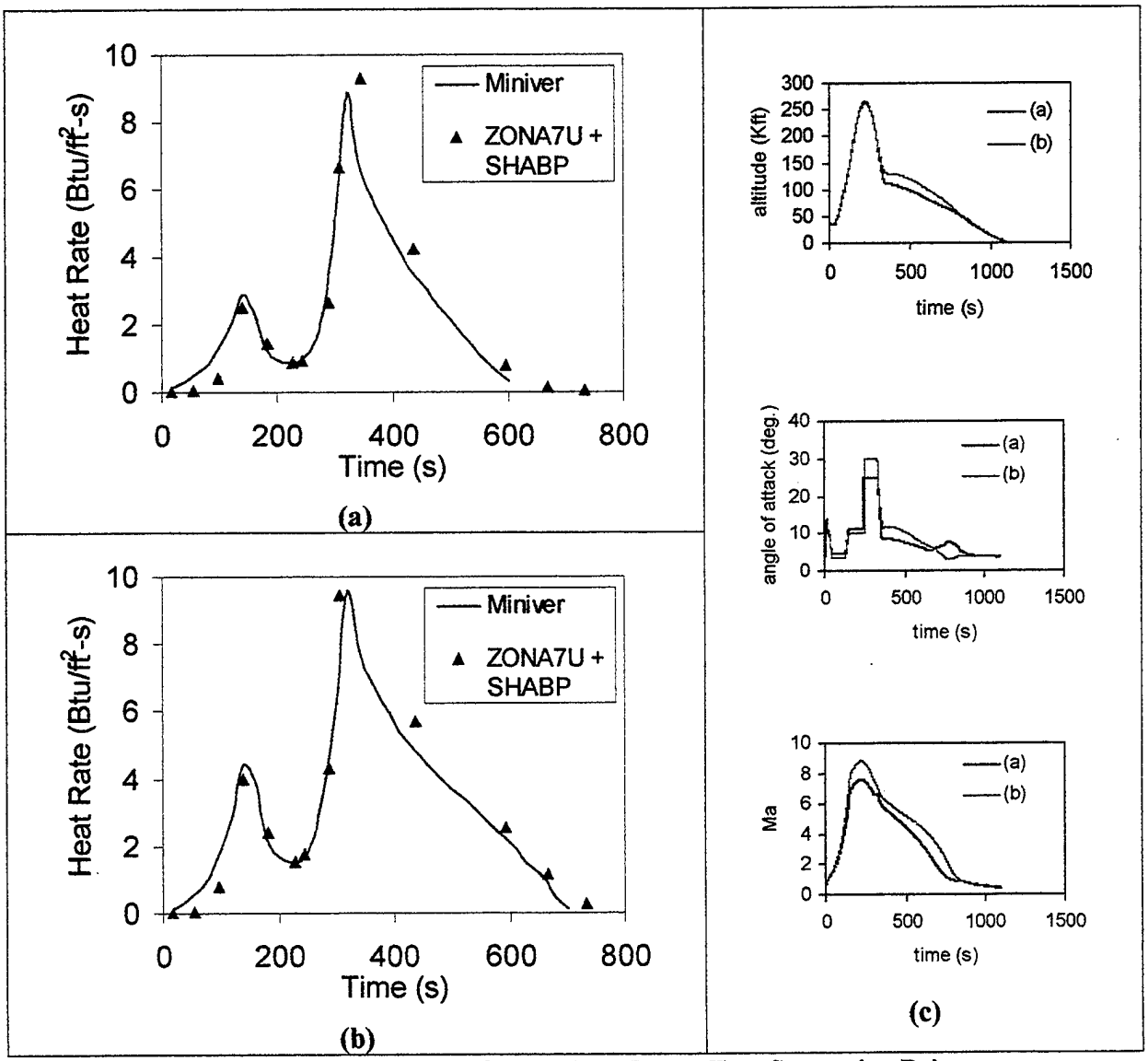

Figure 5.1 Heat Rate Comparison (hot wall) at Stagnation Point
(a) X1004601, (b) X1004701, (c) Trajectory and flight condition history.

5.3 Case Study (D): Trajectory Analysis/Case Demonstration

The example case demonstrates the heat rate computation methodology in the presence of two given trajectory profiles. The trajectory cases X1004601 and X1007401 were selected from a previous NASA study (Ref 36) upon the recommendation of OSC (Orbital Sciences Corporation).

The following is noted in the present cases studied:

1. Trajectory X1004601 has a peak Mach number of 7.4 and a maximum AoA at 25°, trajectory X1004701 has a peak Mach number of 8.6 and a maximum AoA at 30°.
2. Similar to the previous NASA study, we simply computed the heat-rate at the stagnation point of X-34, only to demonstrate the capability of the present methodology.
3. We employ MINIVER and ZONA7U + SHABP for heat-rate computation. Hot-wall condition is imposed, where the emissivity is given as $\varepsilon = 0.8$.
4. ZONA7U + SHABP only requires the trajectory inputs to be submitted once, then it outputs the pressure (C_p, not shown) and the heat-rate ($\dot{q}$) solutions. For 14 time steps along a stretch of 800 seconds, it requires less than 10 minutes of computing time. By contrast, MINIVER requires manual input for each point of interest; i.e., each output $\dot{q}$ solution requires approximately five to ten minutes.

SECTION 6

TPS SIZING

Summary

- *The TPS sizing objective is to develop a procedure to minimize the TPS weight while satisfying the thermal protection requirement and the load-carrying requirement of the combined TAV/TPS structure. An elementary TPS sizing procedure can be established by constructing a prototypical TPS/AFRSI model.*
- *With this model, the objective becomes one to minimize the weight of the middle insulation layer (3). The inequality constraints are the operating temperatures of each layer including that of the skin layer. The TPS element is selected on the windward centerline of X-34. The model input is the heat rate, which is provided by ZONA7U+SHABP from trajectory aerothermodynamic prediction. Based on a hot-wall consideration, maximum temperatures in outer/interior skin layers and minimum TPS weight are resulting outputs obtained by applying an iterative procedure using MINIVER/EXITS. A formal TPS optimization method using Complex-Variables Differentiation Sensitivity with MINIVER/EXIT is proposed in Section 9.*

6.1 Description and Functionality of TPS Sizing (Block 4)

Description:

- Factors that influence the design of TPS include TPS weight, heat transfer property, mechanical property, manufacturability, and price.
- In the present design concept, there should be at least two disciplines involved in the TPS design: the heat transfer analysis for TPS size and the stress analysis for TPS strength.
- MINIVER/EXITS is used for heat transfer analysis and ASTROS* is used for stress analysis.
- TPS debonding from the main structure is of concern. Shear stress applied on the TPS and aeroelastic behavior of the vehicle should be accurately predicted form the ASTROS* computation outputs in order to prevent the TPS from a debonding design under load.
- TPS is non-sizable with respect to the ASTROS* main structure design cycle. It will be sized independently; while from a structural standpoint, it will be considered jointly with the entire structure.

Functionality:

- Objective is to minimize the TPS weight while satisfying the thermal protection requirement and the load-carrying requirement of the combined TAV/TPS structure.
- Provide feedback to ASTROS* for the load carrying design: TPS mass, stiffness, material degradation, temperature mapping to the main structure.
- Shock/Shear loads input from ASTROS* for TPS heat/stress analyses.
- Heat rate input from trajectory analysis (Block 5)

6.2 Phase I Achievements in TPS Sizing Case Demonstration: TPS Sizing Example (Block 4)

1. In order to facilitate the case studied, ZONA has integrated the EXITS module of MINIVER with ZONA7U+SHABP. In so doing, this automated procedure allows the heat rate solutions of the latter to be directly input into EXITS for heat transfer analysis.
2. The following TPS sizing example (case studied) demonstrates that a TPS sizing procedure has been developed and tested out successfully on a typical case (TPS element) previously adopted by NASA (Ref 37). This case yielded a minimum weight insulated layer, among the three such layers selected, resulting in realistic thermal solution in the structure layer (skin). A flow chart is attached showing such a optimization concept utilizing EXITS for TPS/AFRSI sizing (see Fig 6.1)
3. The case studied suggests that present procedure can be generalized into the following
   - it poses no restriction on the number of selected insulated layers to be considered
   - the thickness of the other layers of the TPS can be adjusted at will
   - it should also include shear-stress consideration
   - it can be developed into an automated optimization scheme for TPS minimum weight objective with required thermal/mechanical constraints.

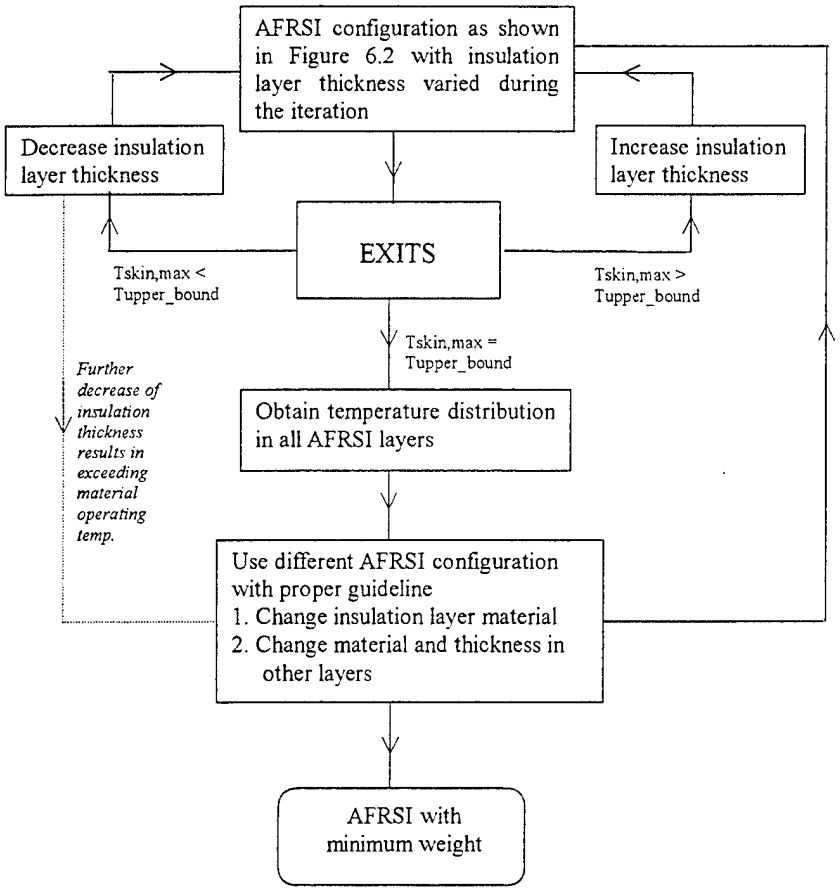

Figure 6.1 Trial-and-Error Procedure to Obtain an Optimized AFRSI.

6.3 Case Study (C): TPS Sizing Case Demonstration

Example Case: TPS of X-34

Case example of a TPS unit is selected from Ref 37 (pg 7 NASA TM 2000-210289). The AFRSI concept modeled in the example is composed of an outer fabric with C-9 coating, 6 lb/ft^3 Q-fiber felt insulation, and an inner fabric layer, and it is attached to the structure with RTV adhesive (Fig 6.2).

This TPS unit is placed at the windward bottom surface of the X-34 centerline at 50 in. from the nose (see Fig 6.3, Pt. A). The X-34 is subject to a trajectory with heat rate limiting at point A.

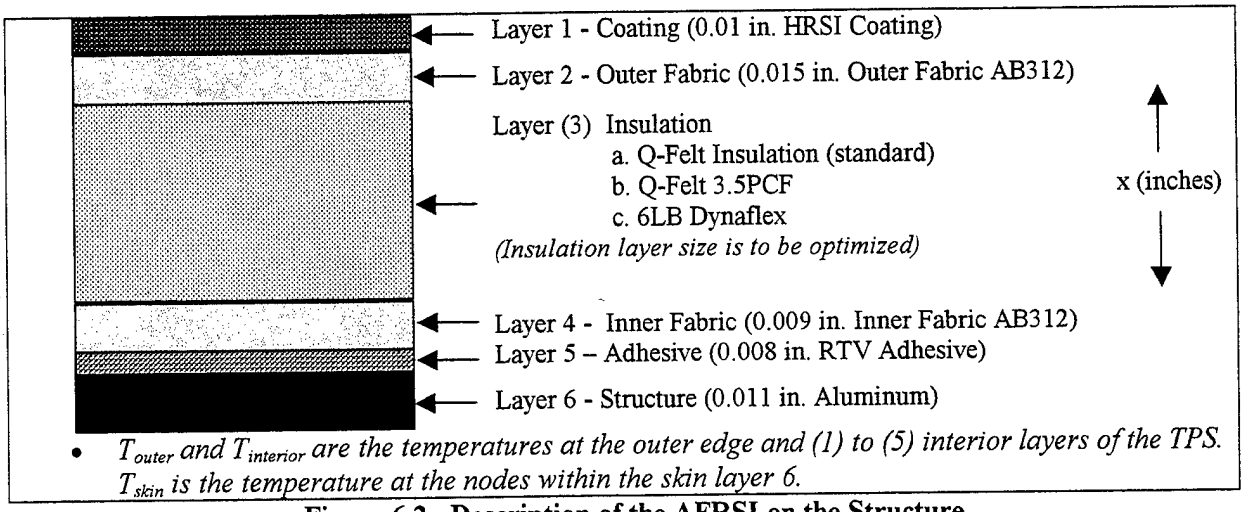

Figure 6.2 Description of the AFRSI on the Structure.

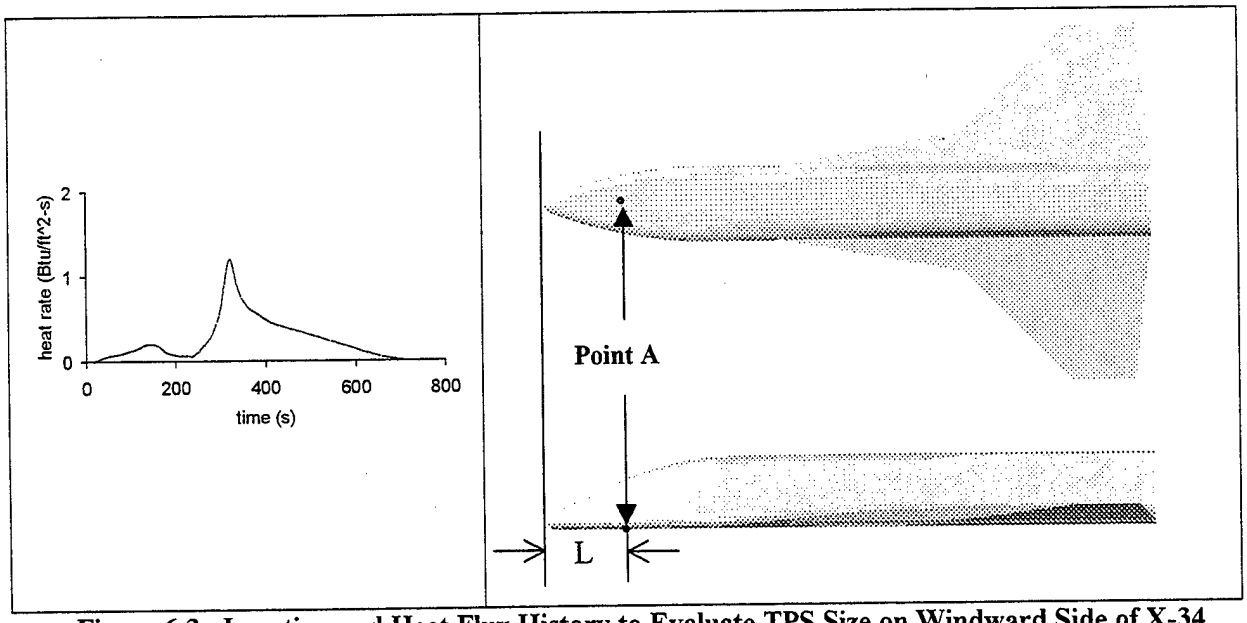

Figure 6.3 Location and Heat Flux History to Evaluate TPS Size on Windward Side of X-34 Centerline (bottom view and side view, L=50 in.)

The TPS/AFRSI Model

According to the above, a TPS/AFRSI model is constructed in Fig 6.2. The modeled AFRSI consists of six layers with layer three being the insulation layer subjected to adjustment and layer six being the structure (or the skin) layer, within which a temperature is set ($T_{upper\text{-}bound}$ = 300° F) as a constraint.

The Iteration Process

In the present case, we fix all other layers; the objective then becomes the minimum weight of layer three, the insulation layer. The inequality constraints are the operating temperatures of each layer including the skin layer (T_{skin} = 300° F). Each layer has a $T_{upper\text{-}bound}$ specific to the material composition.

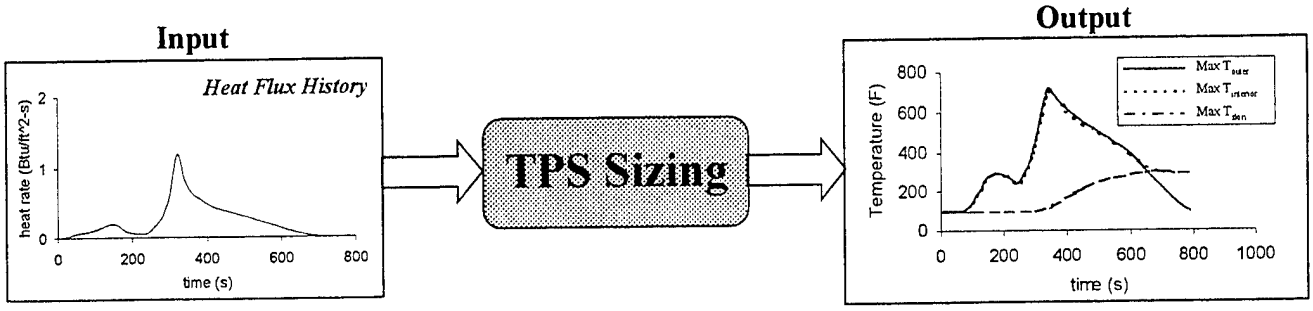

Figure 6.4 Input/Output of TPS Sizing

Discussion of Results

In Table 6.1, the thickness of insulation materials used as layer 3 is adjusted to have maximum of T_{skin} within 0.1% of 300° F (the constraint of the skin material, Aluminum) throughout the entire trajectory. The initial temperature is set as 100° F and the inner edge is assumed insulated.

Table 6.1 Thickness and Weight Comparison Between Insulation Materials used in AFRSI.

Layer 3 material	Thickness	Normalized weight, TPS	Normalized weight, layer 3	Max T_{outer}	Max $T_{interior}$	Max T_{skin}
Q-Felt insulation	0.456 in	1.000	1.000	708.7° F	696.4° F	300.3° F
Q-Felt 3.5PCF	0.638 in	0.694	0.408	713.6° F	702.0° F	300.2° F
6LB Dynaflex	0.560 in	1.118	1.228	696.9° F	681.6° F	300.2° F

(T_{outer} and $T_{interior}$ are the temperatures at the outer edge and interior of TPS. T_{skin} is the temperature at the nodes within the skin. "Maximum temperature" is determined by scanning all temperatures obtained throughout the trajectory history.)

Computation results indicate that T_{outer} and $T_{interior}$ reach maximum at t = 340 sec, which is right after the peak heating condition of the X1004601 trajectory at t = 330 sec. (ZONA7U + SHABP result has been verified at t = 340 sec.)

Because of AFRSI, the T_{skin} reaches its maximum at t = 680 sec. The temperature drop from the outer edge of AFRSI to skin is about 400 °F.

Table 6.1 shows that an iteration process can be used to find a AFRSI design (using Q-Felt 35PCF as insulation layer) which outperforms current AFRSI design (using Q-Felt) with 69% of original weight from the heat transfer analysis. This is a trial-and-error procedure and is a time consuming process. In Phase II, we will develop an optimization driver for MINIVER/EXITS that can automatically achieve a minimum weight design of the TPS system.

SECTION 7

TRIM ANALYSIS

Summary
To demonstrate one of the multifunctional capabilities of ASTROS, we used its Trim Module to perform trim analysis of a modeled X-34, at a selected flight condition (M=6.0, AoA=9°, h=183K ft) With X34/FEM model provided by OSC/NASA-Langley, ASTROS*/TRIM results in a trim condition requiring trailing edge flap angle δ=2.05°, load factor N=0.97g, and total weight of vehicle W=16,000 lbs. The aerodynamic loads at the trim condition is then mapped to the FEM grid by means of ASTROS*/3D Spline Module, thus allowing a subsequent analysis of the X-34 structures. Accordingly, the resulting stress distribution of the X-34 at time is obtained.*

7.1 Descriptions and Functionality of Blocks 3:ASTROS* Structural Optimization

Description:

- As shown in Fig 7.1 below, ASTROS* consists of at least 8 comprehensive modules; these include the Structural FEM module, the ZAERO Aerodynamic module, the Aeroelastic Stability module, the ASE module, the Optimization module, the Trim module, the Smart structures module, and the Sensitivity module.
- The outcome of the proposed ASTROS* optimization is a minimum-weight structural design.
- It uses the Aerodynamic Influence Coefficient (AIC) matrices from ZONA7U/AIC to obtain steady/unsteady airloads and it performs Trim analysis to yield flight loads.
- It performs aeroelastic analysis to yield Flutter/Divergence constraints.
- It will receive the shock impingement location from a high fidelity Unified hypersonic aerodynamics.

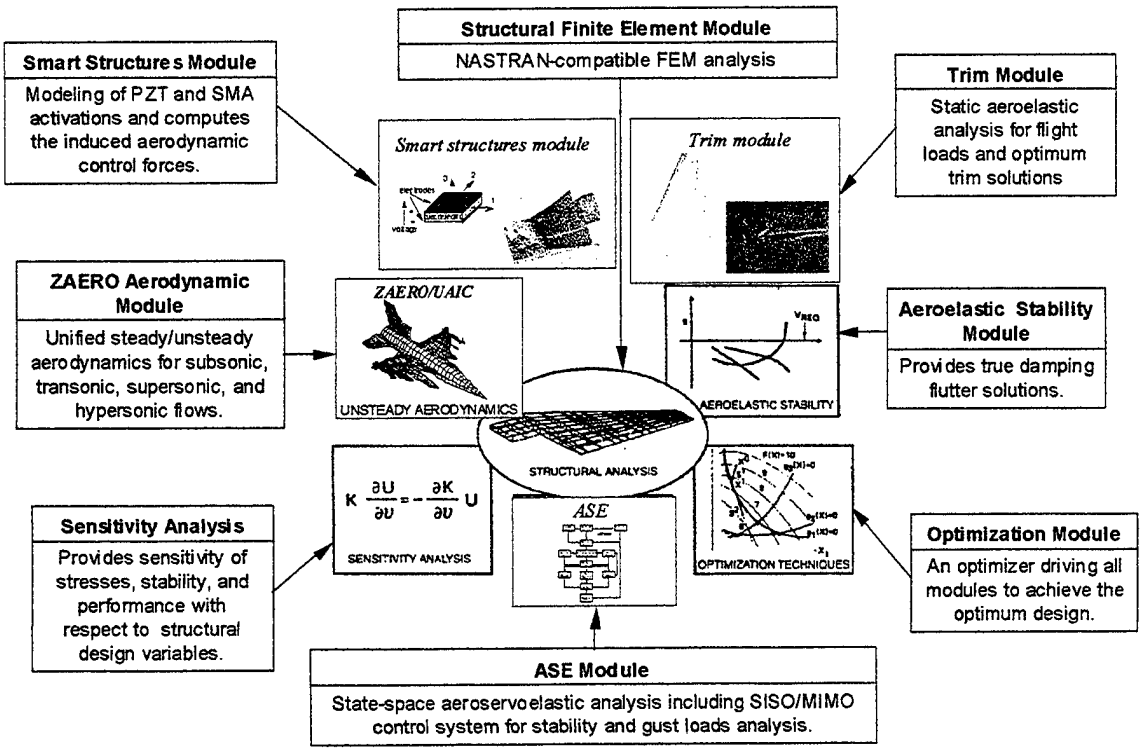

Figure 7.1 ASTROS* Engineering Modules.

Functionality:

- The flight conditions for defining the aeroelastic constraints are provided by the results of the trajectory analysis.
- For TAV/TPS design, the effects of the TPS mass and the material property degradations and the temperature on the load-carrying structure due to aero-heating must be included in the FEM model.
- The objective function of the ASTROS* structural optimization is the minimum weight, which is a feedback information to the trajectory analysis.
- With the aerodynamics input from Block 1, the flight loads including the shear loads and shock loads computed by the trim module of ASTROS* is another feedback information to the stress analysis of the TPS design.
- The total mass of this design is the feedback information to the trajectory analysis for the next design iteration. Other important ASTROS* results are the loads and structural deformation computed by the ASTROS*/Trim module for the TPS stress analysis.
- Several trim solutions computed by the trajectory analysis will be selected as the flight conditions for defining the aeroelastic constraints. These constraints include the flutter and divergence at various Mach number and the strength constraints of each designed structural element at various angles of attack and Mach numbers.

7.2 Phase I Achievements in X-34 TRIM Analysis using ASTROS*/FEM: Block 3

The objective of this study is to demonstrate the trim analysis capability of ASTROS* for the flexible X-34 in hypersonic flow. The outcomes of the trim analysis are the control surface deflection angles, load factors, etc. as well as the stress distribution in the structures. Fig 7.2 depicts an ASTROS* finite element model of the X-34 that was converted from a MSC/NASTRAN X-34 model originally provided by the Orbital Sciences Corporation. Using the aerodynamic influence coefficient (AIC) matrix computed by ZONA7U in conjunction with the stiffness matrix of the FEM model, the ASTROS* trim analysis shows that in order to trim the X-34 at M = 6.0, $\alpha = 9°$ and altitude = 183 Kft, the required trailing edge flap angle is 2.05° degrees and a load factor of 0.97-g for a total weight of 16,000 lbs. At this condition, the aerodynamic loads computed at the ZONA7U panels are then mapped to the FEM grid using the 3D spline module; allowing a subsequent stress analysis of the structures. Such a stress distribution is shown in Fig 7.3.

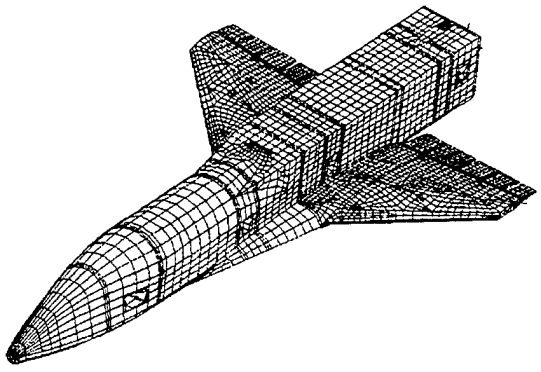

Figure 7.2 X-34 Finite Element Model.

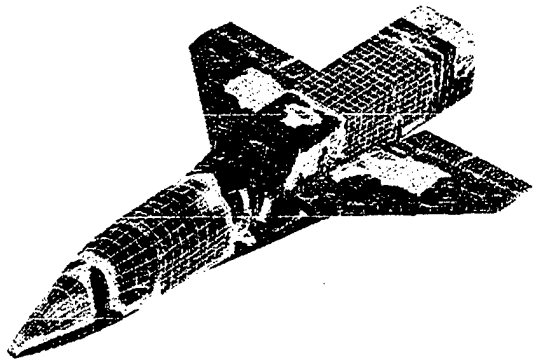

Figure 7.3 X-34 Stress Distribution at M=6.0, α=9°, Alt=183 Kft.

SECTION 8

CONCLUDING REMARKS AND RECOMMENDATION FOR PHASE II WORK

1. *Central Methodologies (Blocks 1-5)* required for aerothermodynamic optimization were individually developed and validated.

2. Hypersonic Aerodynamics and Aerothermodynamic methodology for Blocks1/2 are aimed at replacing the high-level method CFL3D+LATCH and the low-level method MINIVER by a *mid-level method ZONA7U+ SHABP* which has been developed in Phase I.

3. For ZONA7U+SHABP to generate one set of X-34 aerodynamic/heat rates typically requires *10 minutes on a 550 MHZ PC*, whereas for CFL3D+LATCH it requires 30 hours.

4. *ZSTREAM* was developed in Phase I to replace the QUADSTREAM streamline generator of SHABP in that the latter, derived from the Newtonian flow consideration, has a stagnation-point singularity in its streamline solution and it does not depend on freestream Mach number.

5. Validation/verification of ZONA's aerothermodynamic method ZONA7U+SHABP suggests that further improvement is needed in the following: ZONA7U requires *higher-fidelity upgrade* in order to cope with the high AoA and the lee-side aerodynamics of SHABP needs to be replaced by the *AEROHEAT methodology* (Ref 34) in order to further improve the local heat rate estimates.

6. The TPS weight sizing example shows that the designed TPS weight can be further reduced if *an automated optimized scheme* can be developed. A *database of TPS material* in terms of their thermal and mechanical properties must be fully established in order to enhance the capability of the optimized scheme.

7. *The trim solution of the X-34* in terms of the flight loads, input to the structural FEM within ASTROS*, will yield shear loads and shock loads which will result in strength constraint in the ASTROS* optimization procedure.

8. Given trajectory inputs, ZONA7U+SHABP aeroheating solution at the nose of X-34 was verified with previous solutions obtained by NASA (Ref 36). *Total optimization loop including ASTROS** will be tested next using an X-34 example as a demonstration case.

SECTION 9

PHASE II PLAN

Summary
In Phase I, the ZONA unified hypersonic/supersonic aerodynamic method ZONA7U in the aerothermoelastic software development for TPS/TAV design/analysis, was proven a successful tool through feasibility cases studied in the CKEM body, blunt cones and X-34 wing-body. Further upgrade of ZONA7U to a high-fidelity panel method ZONAIR is proposed in order to enhance the universality of the aerodynamic capability with: 1) unified AIC for hypersonic/supersonic/subsonic Mach numbers; 2) exact paneling to model OML surface; 3) high AoA flow; 4) corrected location/strength of impinged shocks; 5) two-body interference aerodynamics. Other proposed improvements of the aerothermoelastic software include: i) incorporation of AEROHEAT to replace SHABP with ZONAIR and ZSTREAM; ii) optimized TPS sizing procedure using Complex Variable Differentiation Sensitivity with MINIVER/EXIT; iii) applying temperature mapping onto structural FEM. The structural optimizer ASTROS is used throughout for sizing TAV/TPS while maintaining the TPS design as a part of the load-carry structure. The TPS design adopts POST/OTIS for trajectory optimization in the outmost design cycle, thereby leading to a final minimized fuel and weight objective. Meanwhile, ZONAIR and ASTORS* FEM will be driven by the automated parametric grid-panel mesh generation of AML, developed by Technosoft. By means of AML, an integrated software framework with a feature-based environment can be established to support an underlying object-oriented architecture that will harness and link all software modules in configuration geometry, aerothermoelastic analysis, TPS design, etc. RMLS and HyperX are proposed as the test-bed vehicles for software demonstration in Phase II.*

9.1 Phase II Technical Objectives

Main Goal:

The ZONA team proposes to continue the phase I development in a unified hypersonic/supersonic aerothermoelastic methodology, to enhance its geometry high-fidelity and to integrate it with a TAV/TPS structural design/optimization procedure for TAV/TSP weight minimization throughout TAV's re-entry/maneuver flight phases.

Further, the above development will be integrated in a feature-based design environment with parametric control of models and data exchange using the Adaptive Modeling Language (AML).

Specific Objectives:

1. Development of an expedient conceptual/preliminary design tool that allows varying of parametric geometry for rapid assessment of design concepts.

2. The TPS sizing is to meet the thermal protection requirements of the main structures while being included with the main structures and treated together as a part of the load–carrying structure.

3. The developed software can be utilized by a design engineer as an outer loop design procedure for trajectory optimization, which in turn will lead to a minimum fuel and weight TAV design.

9.2 Phase II Work Plan

The ZONA team proposes a two-year effort with eight tasks for Phase II. A block diagram showing a work plan for performing these eight tasks is depicted in Fig 9.1.

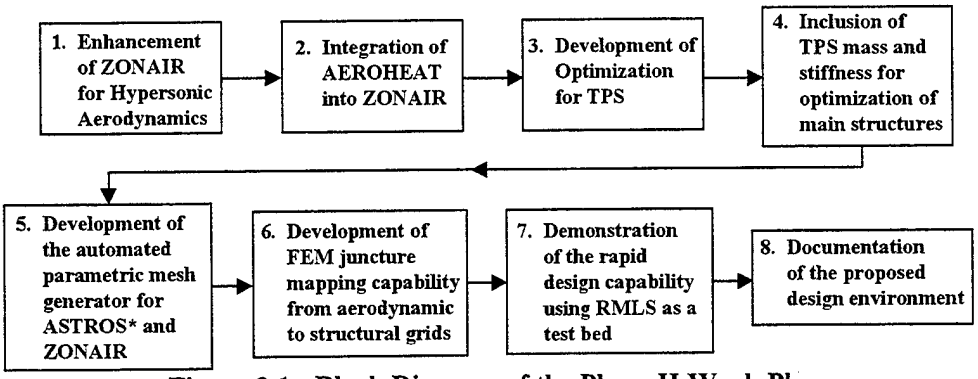

Figure 9.1 Block Diagram of the Phase II Work Plan.

- *AML*

In Phase II, a framework with a feature-based design environment will be developed supporting an underlying object-oriented architecture that will link various aspects of vehicle configuration, geometry, analysis, and sizing using the Adaptive Modeling Language (AML) developed by TechnoSoft, Inc.

The design environment will support the parametric design of the vehicle outer mold line and primary internal structure geometry. Fully automated parametric grid-panel-based mesh generation for aerodynamic analysis and structured meshes for structure analysis will be integrated.

- *TPS Sizing*

The environment will provide links to various analysis applications through a common computational model. These links will support the automated exchange of information among the analyses, geometry and grids. Links to different analysis tools will be provided including: aerodynamic, aeroheating, trajectory, thermal protection system (TPS) sizing, and structural sizing (all included in the Block diagrams of Fig 1.1 and Fig 9.1). A closure model supporting the direct link among the analysis tools and iteration control will be incorporated for vehicle sizing.

Based on an initial design configuration, aerodynamic loads are computed and fed into a trajectory analysis. The results of the trajectory analysis are used as input for TPS analysis and sizing algorithms. The TPS configuration will be computed at selected points on the vehicle outer mold line (OML).

While considered jointly with the TPS as a load-carrying structure, the main structure will be optimized subjected to strength requirements based on a set of critical load conditions. After the TPS and main structure are determined, an updated vehicle weight is created. Based on this new weight model, a new trajectory analysis is initiated. This automated loop iterates until the TPS design converges.

- *ZONAIR, ZSTREAM, and AEROHEAT*

The aerothermodynamic analysis is performed using the ZONAIR code, a high-fidelity, high-order, unified subsonic/supersonic panel method. In Phase II, we will enhance ZONAIR to include hypersonic aerodynamics by incorporating the hypersonic methodology of ZONA7U into ZONAIR. This enhancement is discussed in section 4.1. The enhanced ZONAIR will be integrated with ZSTREAM to provide inviscid surface pressure distribution and streamlines to the AEROHEAT code, a more accurate aeroheating tool than SHABP. The background of AEROHEAT is discussed in section 4.2. The integrated ZONAIR + ZSTREAM + AEROHEAT code will be used to generate an aerodynamic and temperature database for trajectory analysis performed either by POST or OTIS. The resulting time history of the aeroheating data computed by POST/OTIS will be the input of the MINIVER/EXITS code for TPS sizing at various vehicle locations. In Phase II, we will develop an optimization driver of MINIVER/EXITS to automate the TPS sizing procedure using an innovative complex-variable differentiation sensitivity. The formulation of the complex-variable differentiation scheme will be presented in section 4.3

After the design is completed, the TPS stiffness and mass effects will be included in the FEM model using the approach discussed in section 4.4. This FEM model is generated using the automated parametric grid-panel-based mesh generator of AML discussed in section 4.5. Meanwhile, the temperature distribution resulting from the TPS design will be mapped onto the surface elements of the FEM model. This mapping procedure is fully automated using a procedure presented in section 4.6.

- *ASTROS**

ASTROS* will be used to perform the structural optimization of the main structures. However, prior to this optimization computation, an ASTROS*/trim analysis will first be performed at various conditions along the vehicle trajectory to obtain the critical load conditions. Strength constraints at these critical load conditions along with the other aeroelastic instability constraints will be imposed to achieve an optimum structural design. The results of the structural design and TPS sizing will allow for the creation of an updated weight model. The analysis closure loop is then re-initiated with this new weight model and the process iterates until convergence is reached.

- *Test Beds*

To validate the proposed design environment and demonstrate its rapid design capability, we propose to apply the developed software on two configurations, namely, the RMLS and the Hyper-X as test beds. Section 9.8 presents twelve subtasks outlining a step-by-step design procedure to conduct this task. The outcome of this task will be a preliminary RMLS design.

9.3 High Fidelity, High-Order Panel Method for Hypersonic/Supersonic Aerodynamics

As shown in the Phase I study of the 15° blunt cone and X-34 cases, ZONA7U loses its accuracy at high angles-of-attack due to the attached-flow formulation. With continuous R&D in panel method development since 1995, ZONA has developed a unique software product called ZONAIR, a high fidelity unified subsonic/supersonic panel code. ZONAIR has the following capabilities.

- *Unstructured Grids for Modeling Complex Air Vehicles such as Conventional Aircraft Blended Wing-Body and TAV Configuration*

ZONAIR's paneling scheme is based on the so-called "unstructured" grids as opposed to the "structured" grids adopted by other high-fidelity panel codes such as PANAIR. Fig 9.2 presents the comparison between ZONAIR's unstructured paneling scheme and PANAIR's paneling scheme where the advantages of adopting the unstructured grids are described.

ZONAIR *Unstructured Grids*	**PANAIR** *Structured Grids*
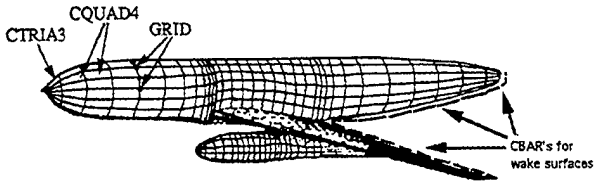	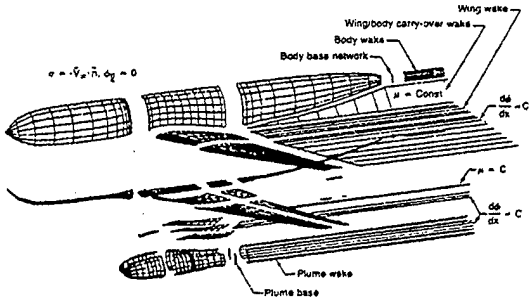
• Similar to structural FEM (MSC/NASTRAN), the entire configuration is defined by "grids". CTRIA3's and CQUAD4's define the connectivity between the grids. • Only the starting lines of the wake need to be defined (via CBAR elements). There are no input requirements for the surface wake. • PATRAN, FEMAP, etc., can be employed directly for pre- and post-processing. ZONAIR outputs PLOAD4 bulk data cards for pressures, local Mach numbers, and velocities on each aerodynamic panel.	• The entire configuration is first divided into several "networks". Each network is further divided by m x n set of grids. • The location of the wake surfaces must be explicitly defined. • No commercially available software can be used directly for pre- and post processing.

Figure 9.2 · Comparison of ZONAIR and PANAIR Paneling Schemes.

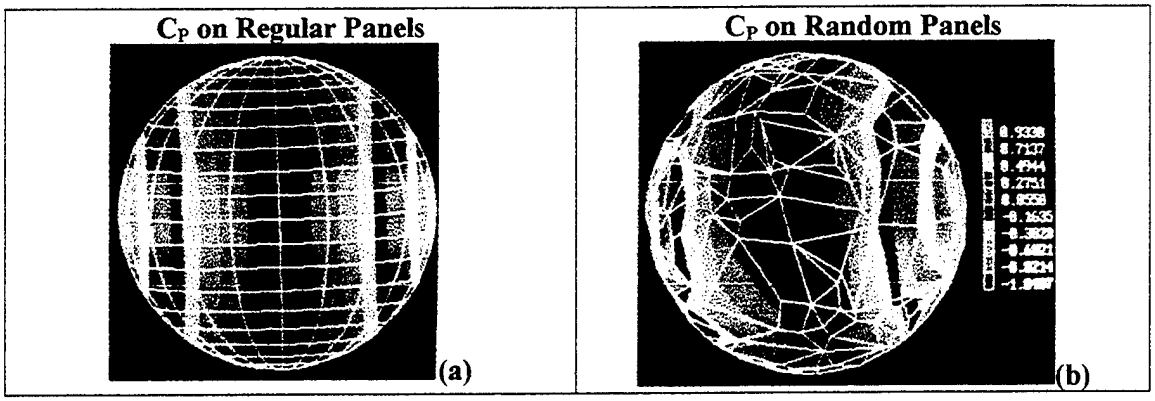

Figure 9.3 Regular and Random Paneling of a Sphere at M=0.0 and α=0.0 deg.

Another advantage in using unstructured grids is that it allows arbitrary grid point selection for a given configuration. In order to demonstrate this feature, a sphere is modeled by using regularly spaced/shaped panels (called Regular Panels) and randomly spaced/shaped panels (called Random Panels) whose pressure distribution results are shown in Figs 9.3(a) and 9.3(b), respectively. Clearly, this arbitrary grid point selection capability of the unstructured grids can greatly reduce the user burden in the grid generation process.

- *Vortex Roll-Up for High Angles-of-Attack Aerodynamics*

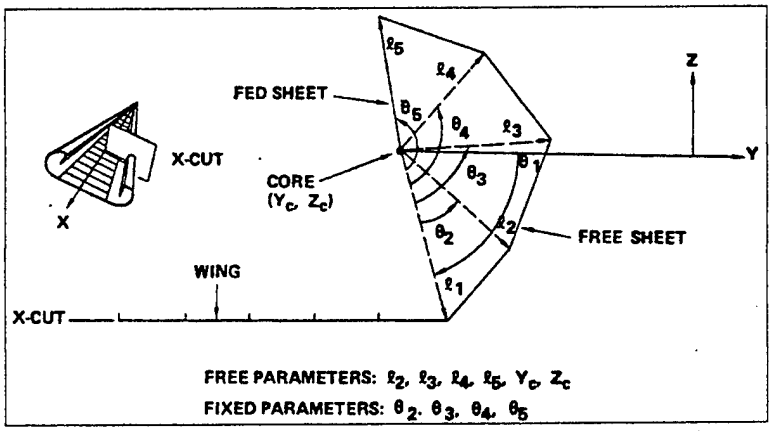

9.4 Free/Fed Vortex Sheet Kinematics for Vortex Roll-up.

Fig 9.4 shows the essential elements in ZONAIR for vortex roll-up modeling; the vortex sheet emerging from the wing leading edge and tip (free vortex sheet) and the rolled-up core or spiral region (fed vortex sheet) fed by the leading-edge and tip-vortex sheets. The following boundary conditions are imposed on these elements:

- The configuration surface must be impermeable.
- The free sheet and wake cannot support a pressure difference and must be impermeable as well.
- The fed sheet is an extension of the free sheet and feeds vorticity to the vortex core (modeled as a simple line vortex). The boundary condition governing the fed sheet size and core

orientation is that the total force induced on the fed sheet and core by the rest of the configuration be parallel to the core.

- Kutta conditions are imposed along the appropriate leading, side, and trailing edges of the wing in the presence of free sheets emanating from these edges.

Using the above vortex roll-up model, the induced drag, lift, and pitch moment versus angles-of-attack of a generic advanced fighter (GAF) at M = 1.8 is shown in Fig 4.1.4. It can be seen that ZONAIR's prediction correlates very well with the wind tunnel data up to $\alpha = 20°$.

- *Unified Hypersonic/Supersonic ZONAIR*

Currently ZONAIR is based on the potential flow equation, which is valid only in the supersonic Mach number range. In Phase II, we will incorporate the hypersonic methodology of ZONA7U into ZONAIR, that is:

- Equivalent Mach number transformation to circumvent the superinclined panel problem.
- Local pulsating body analogy to include the flow rotationality effects.

Additionally, ZONAIR will be further improved on its hypersonic capability in two aspects by using a Perturbed-Euler formulation (Ref 21).

- Correct the impinged shock strength and location (e.g., nose shock of the X-34 impinging on the wing).
- Account for the cross-flow near-normal shock effect on the lee-side due to high AOA flow (in addition to the vortex roll-up effect).

Shown in Fig 9.5 are two such PEF shock solutions versus that of CFL3D. Without other secondary shock interaction, the PEF could correct the nose shock on the wing to provide more accurate shock load.

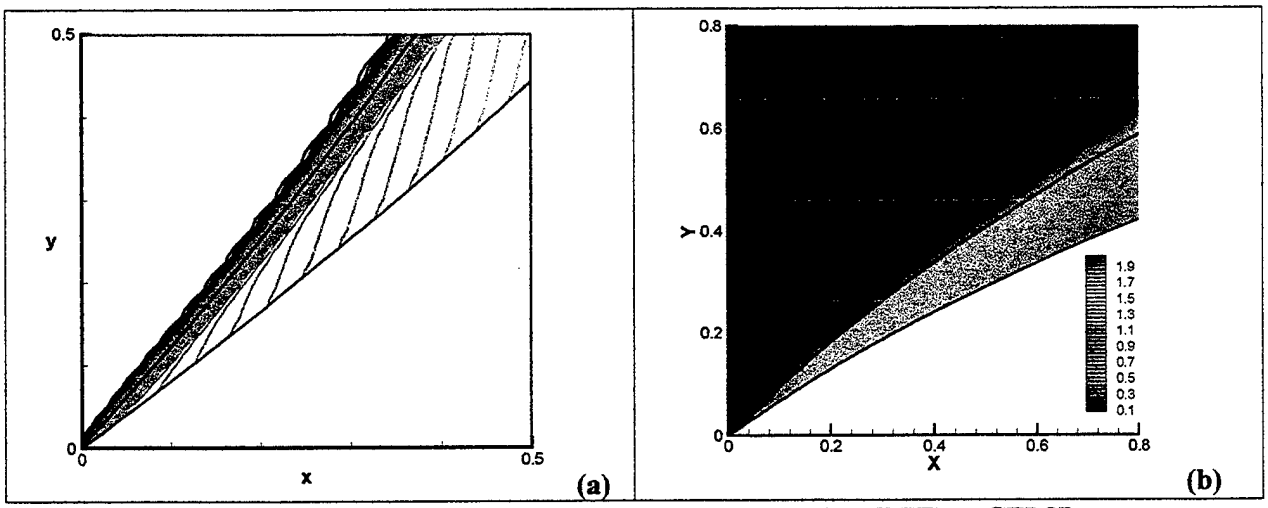

Figure 9.5 Solutions of Perturbed Euler Formulation (PEF) vs CFL3D, (a) Concave Body at M=50, γ=1.4, θ=38°, and (b) Convex Body at M=15, γ=1.4, θ=35°.

Once the above hypersonic methodology is incorporated into ZONAIR, the three test cases shown in section 2.0, namely the CKEM body, the 15° blunt cone, and the X-34 wing-body

configuration will be employed to validate ZONAIR at high angles-of-attack and for the correction of impinged shock location.

The enhanced ZONAIR, once developed, can serve as a universal aerodynamic tool for aerodynamic force/moment generation, streamline generation for aeroheating analysis, AIC generation for aeroelastic analysis, and trim solutions for critical loads. Its high-fidelity paneling scheme is compatible with FEM mesh generation, whereas its computing time is two-orders less than that of CFD codes. Table 9.1 shows the comparison of functionality between ZONAIR and other aerodynamic codes where by comparison ZONAIR's universality and superiority is clearly seen.

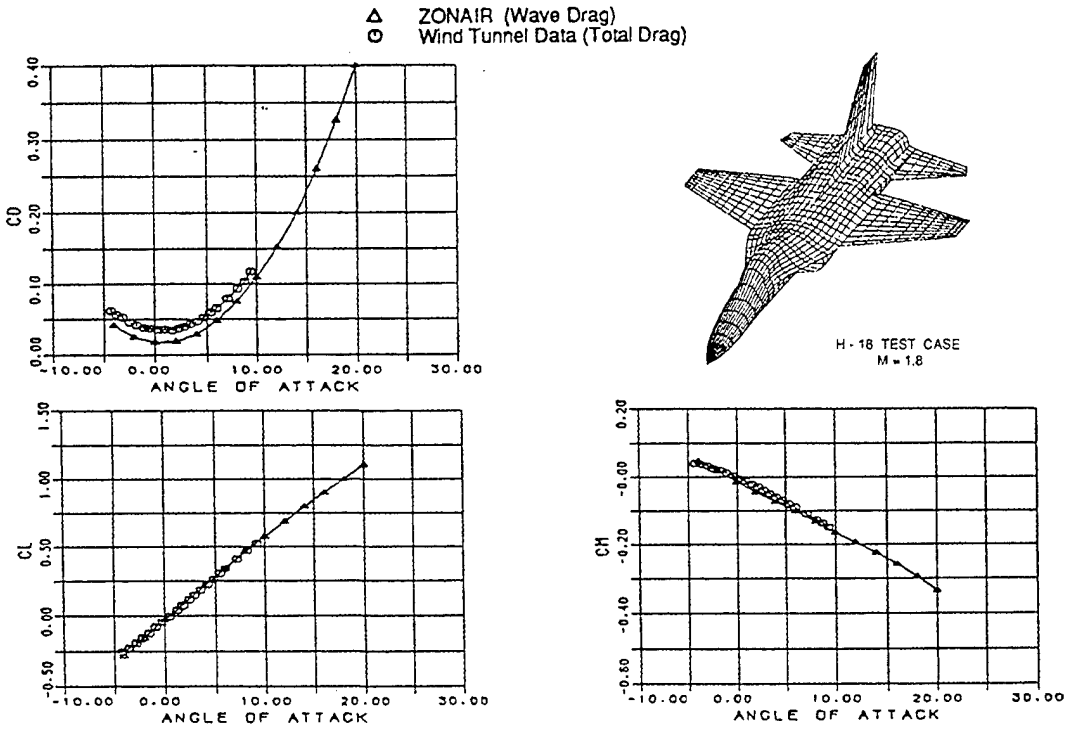

Figure 9.6 Force and Moment Coefficients of GAF vs Angle-of-Attack at M = 1.8

Table 9.1 Comparison between ZONAIR and Other Aerodynamic Codes.

Code	Method	Compu-tational Efficiency	Streamline Solution For Aeroheating	Hypersonic/ *Supersonic/* Subsonic Mach No.	AIC for Structural FEM	Geometry High Fidelity	High AOA	2 Body Aero Inter-ference
CFL3D	Euler/N-S	30 hrs/ X-34	Yes	All	No	Yes	Yes	Yes
PANAIR	Potential	20 min/ X-34	No	Supersonic/ Subsonic	No	Yes	No	Yes
ZONAIR	Potential + PEF	20 min/ X-34	Yes	All	Yes	Linear-Order Panel	Yes	Yes
ZONA7U	Potential + PEF	10 min/ X-34	Yes	All	Yes	Constant-Order Panel	No	Yes
APAS	Potential + Empirical	< 10 min	Newtonian S.L.	Empirical for hypersonics	No	Low-Order Panel	No	Yes

MINIVER	Analytical/ Empirical	<< 10 min	No	No subsonics	No	No	No	No
DATCOM	Analytical/ Empirical	<< 10 min	No	All	No	No	Yes	No
AP98	Analytical/ Empirical	<< 10 min	No	All	No	No	Yes	No

9.4 Adopting the AEROHEAT Code for Accurate Aerothermodynamic Analysis

SHABP's empirical equations for aeroheating analysis are based on two simple hypersonic similarity solutions; one for stagnation point and one for flat plates. As shown in our Phase I study on the CKEM body and 15° blunt cone, these similarity solutions are not accurate particularly near the stagnation point.

In Phase II, we will replace SHABP by a more accurate aeroheating code called AEROHEAT. AEROHEAT solves the convective-heating equations using an axisymmetric analogy that allows any axisymmetric boundary layer method to be applied along an inviscid surface streamline. These convective-heating equations consist of a set of approximate convective-heating equations developed by Zobyl (Ref 38) that provides accurate surface heating rates with a minimal amount of computational effort. Laminar and turbulent heating rates are calculated by relating the surface skin friction to the momentum thickness Reynolds number. Note that the 3D effects of the AEROHEAT methodology is included through the streamline metric coefficients, which can be accurately provided by the ZSTREAM code. The inviscid aerodynamic solutions required by AEROHEAT will be computed using ZONAIR. The integrated ZONAIR + ZSTREAM + AEROHEAT solutions will be validated with the CFL3D + LATCH results and test data for CKEM body, 15° blunt cone and the X-34 wing-body configuration.

9.5 Optimization Procedure for TPS Sizing

In Phase I we conducted a TPS sizing study on the X-34 using the EXITS module of MINIVER (as described in section 6). Based on the temperature constraint of 300° F on the skin layer, we have shown that a minimum weight TPS can be achieved by a trial-and-error procedure. However, performing such a trial-and-error procedure for minimum weight TPS design over the whole vehicle is a very time consuming process. In Phase II, we will develop an automated TPS design procedure using the feasible direction method as an optimization driver of MINIVER/EXITS to achieve the optimum design.

Fig 9.7 depicts a typical TPS sizing problem that consists of n layers with thickness h_1, $h_2 \ldots h_n$, respectively. For a given heat flux $\dot{q}$ applied on the outer boundary, the objective is to minimize the total weight of the TPS system while keeping the temperature at each layer (T_i) below their respective maximum operational temperature, T_{oi}. The corresponding optimization formulation is shown as follows:

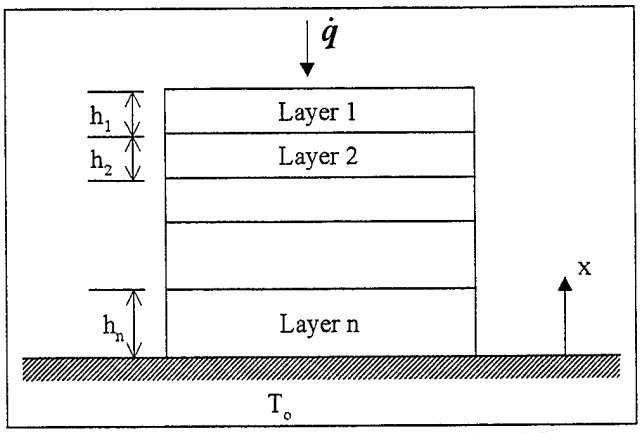

Figure 9.7 Typical TPS Sizing Problem.

Minimize: $W = \sum_{i=1}^{n} \rho_i h_i$ where ρ_i is the density of the i^{th} layer

Subjected to: $T_i < T_{oi} \qquad i = 1, 2...n.$

Design variables: $h_i > 0 \qquad i = 1, 2...n.$

This optimization problem can be effectively solved by the feasible direction method if the sensitivity of the constraint function can be evaluated accurately and efficiently. The MINIVER/EXITS module can be used to compute the temperature distribution at each layer, but it can not provide the sensitivity of the temperature distribution with respect to the design variables h_i.

To obtain this sensitivity information, we will apply the complex-variable differentiation approach on the MINIVER/EXITS module. The complex-variable differentiation technique, first proposed by Lyness and Moler (Ref 39) and extended to BEM solution recently by ZONA (Ref 40), is a powerful mathematical technique that can provide the "numerically exact" derivatives of a complicated function. In this complex variable approach, the variable h of a real function $T(h)$ is replaced by a complex one, $h + i\Delta h$. For a small Δh, $T(h+\Delta h)$ can be expanded into a Taylor's series as follows:

$$T(h+i\Delta h) = T(h) + i\Delta h \frac{\partial T}{\partial h} + \ldots$$

The first derivative of the above function can be expressed as:

$$\frac{\partial T}{\partial h} = \frac{Im(T(h+i\Delta h))}{\Delta h} + 0(\Delta h^2)$$

It can be seen that the derivative using the complex variable approach only requires function evaluation whereas the conventional finite differencing technique involves the differencing of two functions. Therefore, the complex variable approach does not suffer from the cancellation errors, hence, becomes step-size independent in the small asymptotic limit. In fact, the step size can be as small as machine zero (10^{-35}) and still retain accuracy (Ref 40).

To incorporate the complex variable technique into the MINIVER/EXITS module for sensitivity analysis is straightforward simply by declaring all variables in the MINIVER/EXITS module as complex variables. The imaginary part of the thickness input of MINIVER/EXITS represents a small incremental thickness whereas the sensitivity is the imaginary part of the temperature output divided by the incremental thickness.

9.6 Inclusion of TPS Mass and Stiffness Effects in FEM for Optimization of Main Structures

As discussed earlier, the TPS design is primarily based on the thermo-protection constraints, not the structural constraints. Detailed structural design/analysis of the TPS system can be performed only if the load paths from the main structures to the TPS are known. Therefore, such

a structural design/analysis of TPS should be performed in the detailed design stage. On the other hand, because the TPS is placed on the vehicle outer mold line that gives significant area moment of inertia, excluding the TPS stiffness from the FEM model can lead to a over-designed main load-carry structure.

To overcome the above issue, in Phase II we will develop a procedure that can automatically convert the overall stiffness and mass of TPS into equivalent composite laminate properties. Those laminates will be included as the top layer of the vehicle composite skin or in terms of ASTROS* input bulk data cards, the top layer in the PCOMP bilk data cards of the skin elements. While the thickness of each layer in the skin elements can be defined as design variables of the ASTROS* structural optimization, these top layers remain non-sizable. In doing so, the TPS structures are not part of the ASTROS* optimization but their load-carry capability can influence the size of the main load-carry structures.

After the ASTROS* optimization is completed, the load paths from the TPS including the interlaminar shear stresses (from ASTROS* stress recovery calculations) and the shock loads (from the ZONAIR pressure distributions according to corrected shock location) will be output for the subsequent detailed design of the TPS structures.

9.7 Automated Parametric Mesh Generation for ASTROS* and ZONAIR

Automated parametric mesh generation for MSC/NASTRAN models is an existing capability in the Supersonic Hypersonic Vehicle Design (SHVD) system developed by LMCO/TechnoSoft. Because of the similarity between the MSC/NASTRAN and ASTROS* bulk data cards, a mesh generator for ASTROS* FEM models can be developed with minor modification to the SHVD system. The mesh generator of ASTROS* can also directly be employed for the ZONAIR aerodynamic model generation because of the unstructured paneling scheme of ZONAIR.

In addition to the mesh generation, the ASTROS* optimization requires the selection of design variables and the definition of constraint functions. The development of an automated procedure to establish such an optimization input will be a major effort of this task. In order to monitor the progress of the ASTROS* optimization computation, we will develop a real-time graphical capability to display the design variables on the FEM model along with the active constraints at each optimization iteration. If an optimum solution can not be achieved, the graphical capability will help the user to quickly identify the source of the problem and consequently modify the optimization problem statement until an optimum solution is obtained.

9.8 Temperature and Aeroloads Mapping from Aerodynamic to Structural Grids

For the present aerothermoelastic analysis, two types of data mapping between the aerodynamic grid (the aerodynamic panels) and the structural finite element (FEM) grid are required. The first type is the mapping of the aerodynamic forces from the aerodynamic grid to the structural grid as well as the displacement from the FEM grid back to the aerodynamic grid. This type of data mapping procedure has been fully developed in the ASTROS* code that contains four spline methods, namely the infinite plate spline method (Ref 41), the thin plate spline method (Ref 42), the beam spline method and the rigid body attachment method that jointly generate a spline matrix for displacement mapping from FEM grid to aerodynamic grid. Based on the principle of

virtual work, the transposed spline matrix can be employed for the force mapping from the aerodynamic grid to the FEM grid.

The second type mapping requirement is the temperature mapping from the aerodynamic grid to the FEM surface grid. In Phase II, we will develop a finite-element-based mapping procedure as shown in Fig 9.8. This procedure assumes a bilinear temperature distribution over the aerodynamic quadrilateral panel and temperature are defined at the corners of the panel. Fig 9.8 indicates the equations used in the temperature projection process. These corner temperatures to the individual aerodynamic panels are then mapped to the surface of the FEM model that is comprised of plate or membrane elements.

The output of this temperature mapping procedure will be a set of TEMP and TEMPD NASTRAN or ASTROS* bulk data cards to define the temperature at FEM grid points for determination of thermal loading, temperature-dependent material properties, or stress recovery.

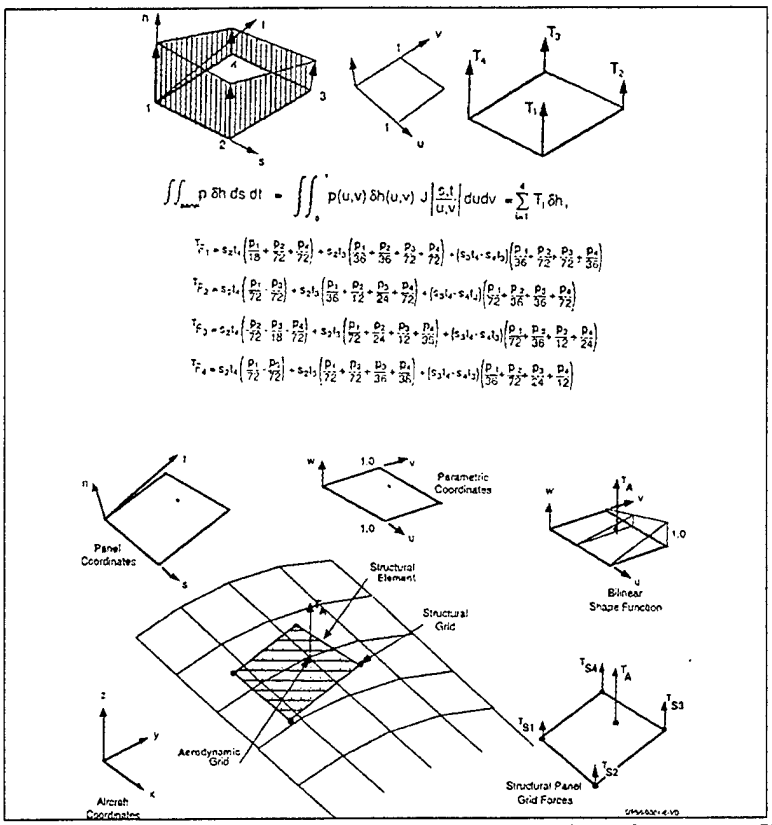

Figure 9.8 Temperature Mapping from Aerodynamic to Structure Grids.

9.9 Test Beds of the Proposed Design Environment

The proposed design environment, once developed, will be validated and tested on two TAV configurations, a Reusable Military Launch System (RMLS) shown in Fig 9.9 and the Hyper-X shown in Fig 9.10. The Hyper-X is an existing TAV design whose aerodynamic and structural models are shown in Fig 9.11. Since the models exist, no mesh generation effort will be required. In addition to the X-34, the selection of Hyper-X is primarily for the validation of

ZONAIR+ZSTREAM+AEROHEAT with CFL3D+LATCH results. One such a CFDL3D pressure distribution on the Hyper-X is shown in Fig 9.12.

The RMLS system is a two-stage reusable launch vehicle concept whose exact outer mold line is presently undetermined and is subject to the design of several geometric controlling parameters such as fuselage fineness ratio, nose fineness ratio, wing span, wing chord, etc. In particular, ZONAIR is the only successful software that has a proven capability in 2-body separation by its store separation option in validation with wind tunnel and drop test data at subsonic and supersonic speeds. Here, this project provides an ideal test bed of the proposed design environment to demonstrate its rapid design capability for an optimum and converged solution.

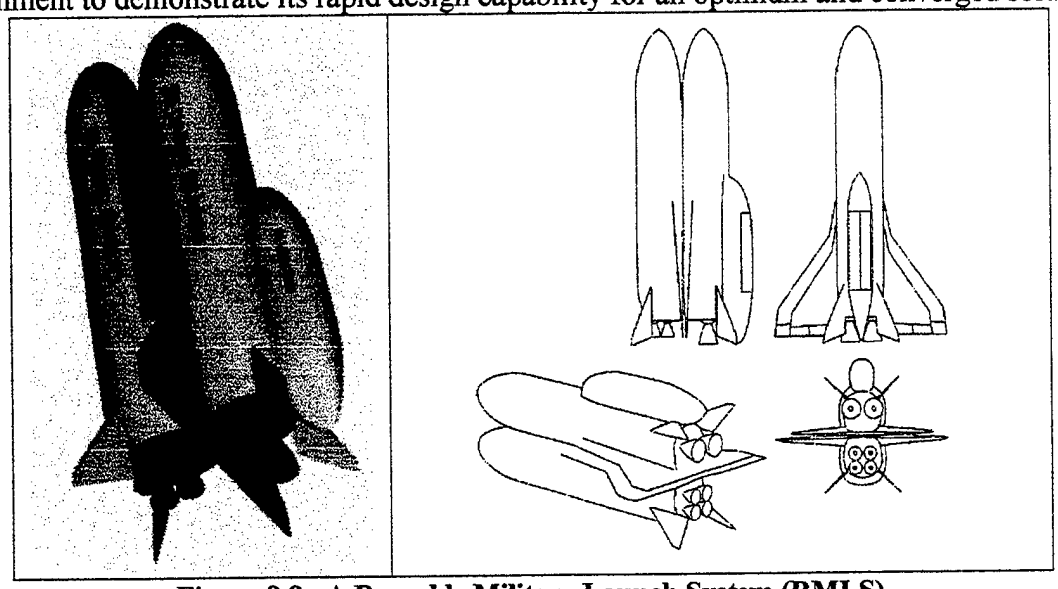

Figure 9.9 A Reusable Military Launch System (RMLS).

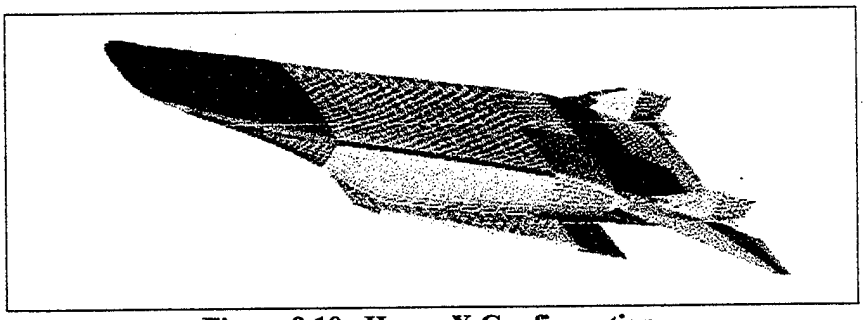

Figure 9.10 Hyper-X Configuration.

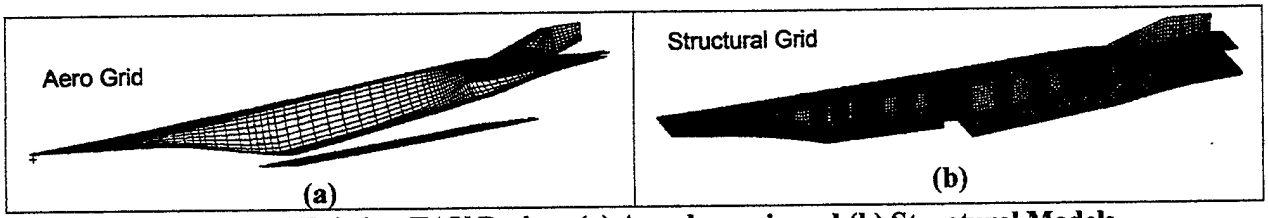

Figure 9.11 Hyper-X Existing TAV Design; (a) Aerodynamic and (b) Structural Models.

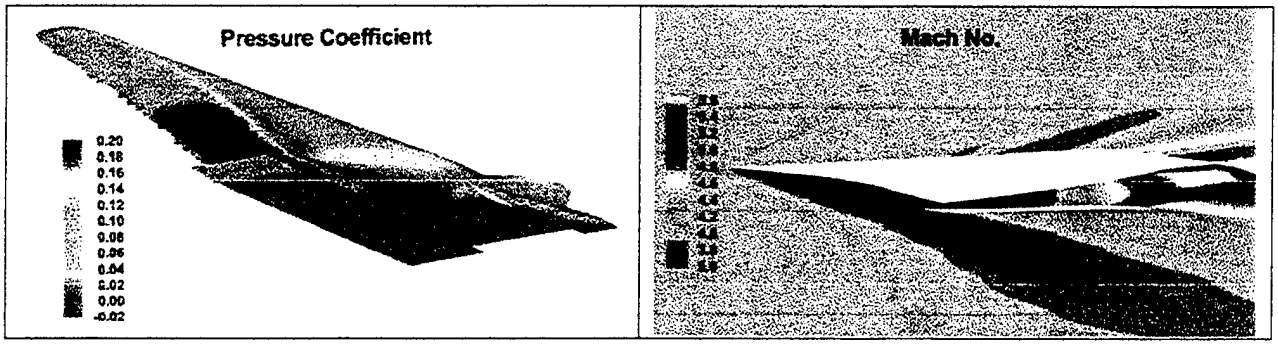

Figure 9.12 CFDL3D pressure distribution on the Hyper-X.

First, based on a set of initially guessed values of the geometric controlling parameters, a ZONAIR model and an ASTROS* FEM model are generated using the automated parametric mesh generator. Consequently, an initial vehicle weight is calculated using the weight model. Meanwhile, an aerodynamic and aeroheating database is generated by performing the ZONAIR+ZSTREAM+AEROHEAT computations at a set of Mach numbers and angles of attack. This provides the input database of the POST/OTIS code to acquire a trajectory for the initial design. The output of POST/OTIS will be the heat rate time histories that are used for the TPS sizing over the entire vehicle. The stiffness and mass effects of the TPS system will be included in the ASTROS* main structure optimization. An updated weight is then obtained from the ASTROS* optimization result and a new trajectory analysis is initiated. This process is repeated until a converged solution is achieved.

Next, a second set of geometry controlling parameters will be defined, leading to a second converged solution by following the same procedure described above. The comparison of weight and performance between the first and the second converged solutions will be conducted. This will provide the sensitivity of the RMLS performance with respect to the geometry controlling parameters and provide guidelines regarding changes of the geometry controlling parameters to yield the final optimum solution.

Finally, all intermediate solutions during the iteration phase of the two converged solutions will be graphically documented. Based on experience gained during the RMLS design, operational guidelines of the proposed design environment will be established and final adjustments of the software system will be made.

9.10 Phase II Statement of Work

The tasks to be performed in Phase II are defined below. A schedule of the tasks is shown in section 9.11, which also shows the timing for related program deliverables, meetings, and presentations.

Task 1: Enhancement of ZONAIR for Hypersonic Aerodynamics

- Incorporate the hypersonic methodology of ZONA7U into ZONAIR.
- Validate the enhanced ZONAIR with the CFL3D results of the X-34 and Hyper-X configurations.

Task 2: Integration of AEROHEAT into ZONAIR

- Modify the AEROHEAT code to accept streamlines and inviscid pressures computed by ZSTREAM and ZONAIR, respectively.
- Validate the ZONAIR+ZSTREAM+AEROHEAT results with CFL3D+LATCH aeroheating results of the CKEM body, 15° blunt cone, X-34, and Hyper-X.

Task 3: Development of Optimization for TPS Sizing

- Incorporate the complex-variable differentiation sensitivity into the MINIVER/EXITS module.
- Develop an optimization driver using the feasible direction method for TPS optimization.

Task 4: Inclusion of TPS Mass and Stiffness Effects for Optimization of Main Structures

- Develop an automated procedure to convert the TPS overall stiffness and mass into equivalent composite laminate properties.
- Extract the inter-laminar shear stresses and shock loads from ASTROS* for detailed design of TPS structures.

Task 5: Development of the Automated Parametric Mesh Generator for ASTROS and ZONAIR*

- Modify the SHVD system for ASTROS* and ZONAIR mesh generations.
- Establish an automated procedure for defining the design variables and constraint functions.
- Develop a real-time graphical capability to display the progress of the ASTROS* optimization computations.

Task 6: Development of Temperature Mapping Capability from Aerodynamic to Structural Grids

- Establish a projection process to map the temperature distribution from the aerodynamic to structural grids.
- Output the mapping results in terms of NASTRAN or ASTROS* TEMP and TEMPD bulk data cards.

Tasks 7: Demonstration of the Rapid Design Capability of the Proposed Design Environment Using the Reusable Military Launch System (RMLS) as a Test Bed

- Generate an ASTROS* and ZONAIR model based on a set of initially guessed values of the geometric controlling parameters.

- Perform a ZONAIR+ZSTREAM+AEROHEAT analysis to establish the aerodynamic and aeroheating database.
- Obtain a trajectory of the initial design using POST/OTIS.
- Conduct a TPS sizing over the entire vehicle based on the heat rate time histories computed by POST/OTIS.
- Perform an ASTROS* optimization computation for an optimum structural design.
- Establish an updated weight of the vehicle and initiate a new trajectory analysis.
- Repeat the above process until a converged solution is achieved.
- Obtain a converged solution by defining a second set of geometric controlling parameters.
- Compare the weight and performance of the two solutions for the sensitivity of the RMLS performance with respect to the geometric controlling parameters.
- Graphically document all intermediate solutions during the iteration phase of the above two converged solutions.
- Establish operational guidelines of the proposed design environment.
- Conduct a final adjustment of the software system based on the experience gained during the RMLS design.

Task 8: Documentation of the Proposed Design Environment

- Four manuals will be generated. The User's Manual will include the input instructions, modeling guidelines, etc. The complete theoretical formulation will be presented in the Theoretical Manual. Sample test cases for demonstrations of problem set-up will be documented in the Applications Manual. The Programmer's Manual will present the total program architecture, the contents of database data entities, and the functionality of each submodule.

9.11 Planned Program Schedule

Tasks	Yr 1 Quarter 1	2	3	4	Yr 2 Quarter 1	2	3	4	Performed by
1. Enhancement of ZONAIR for Hypersonic Aerodynamics									
• Incorporate the hypersonic methodology into ZONAIR									Z
• Validate the enhanced ZONAIR with the CFL3D results									Z
2. Integration of AEROHEAT into ZONAIR									
• Modify the AEROHEAT code to accept streamlines and inviscid pressures computed by ZSTREAM and ZONAIR									Z/D
• Validate the ZONAIR+ZSTREAM+AEROHEAT results with CFL3D+LATCH aeroheating results									Z
3. Development of Optimization for TPS Sizing									
• Incorporate the complex-variable differentiation sensitivity									Z
• Develop an optimization driver for TPS optimization									Z
4. Inclusion of TPS Mass and Stiffness Effects for Optimization of Main Structures									
• Develop an automated procedure to convert TPS stiffness/mass into equivalent composite laminate properties									Z
• Extract the inter-laminar shear stresses and shock loads from ASTROS* for detailed design of TPS structures									Z
5. Development of the Automated Parametric Mesh Generator for ASTROS* and ZONAIR									
• Modify the SHVD system for ASTROS*/ZONAIR meshes									T/Z
• Establish an automated procedure for defining the design variables and constraint functions.									Z/T
• Develop a real-time graphical capability to display the progress of the ASTROS* optimization computations.									Z
6. Development of Temperature Mapping Capability from Aerodynamic to Structural Grids									
• Establish a projection process to map the temperature distribution from the aerodynamic to structural grids									Z
• Output the mapping results in terms of NASTRAN or ASTROS* TEMP and TEMPD bulk data cards									Z
7. **Demonstration of the Rapid Design Capability Using the RMLS as a Test Bed**									
• Generate ASTROS*/ZONAIR model of the initial design									T/Z
• Perform a ZONAIR+ZSTREAM+AEROHEAT analysis									Z
• Obtain a trajectory of the initial design using POST/OTIS									Z
• Conduct a TPS sizing over the entire vehicle									Z
• Perform an ASTROS* optimization computation									Z
• Establish an updated weight of the vehicle									Z
• Repeat the above process for a converged solution									Z
• Obtain a converged solution by defining a second set of geometric controlling parameters									Z
• Compare the weight and performance of the two solutions for the sensitivity of the RMLS performance									Z
• Graphically document all intermediate solutions									Z/T
• Establish operational guidelines									Z
• Conduct a final adjustment of the software system									Z/T
8. Documentation of the Proposed Design Environment									Z/T
Kick-Off Meeting	▲								
Final Oral Presentation								▲	

Z = ZONA Technology; T = TechnoSoft; D = Dr. DeJarnette

9.12 Phase II Endorsement

For assessment of ZONA's unified hypersonic/supersonic unsteady aerodynamics, ZONA7U capability the reader is recommended to contact the following users:

- Warren Smith / Lockheed Martin/LMMFC
  (972) 603-7726, smith@vs.lmco.com
- Rudy Yurkovich / Boeing Company
  (314) 233-2563, rudolph.yurkovich@mw.boeing.com
- Bart Fowler / NASA-Marshall
  (256) 544-2691, bart.fowler@msfc.nasa.gov

Endorsement letter from Dr. Zarda of LMCO/LMMFC and from Dr. Henri Fuhrmann of Orbital (OSC) for the proposed effort are attached below.

Lockheed Martin Endorsement Letter

LOCKHEED MARTIN
Missiles and Fire Control – Orlando

Mr. Adel Chemaly
TechnoSoft, Inc.
4434 Carver Woods Drive
Cincinnati, Ohio 45242

To whom it may concern:

Lockheed Martin Missiles and Fire Control fully supports the proposal effort of TechnoSoft, Inc., submitted to the United States Airforce, in response to the Small Business Innovation Research USAF Topic AF01-252, Aerothermoelastic Optimization Methods for Reusable Launch Vehicles.

As manager of the Engineering Methods Group at Lockheed Martin Missiles and Fire Control (LMM&FC), I lead a team of engineering design experts. These experts develop and utilize sophisticated engineering tools to solve complex problems related to designing and manufacturing missiles, gimbals, rockets, and space systems in general. Current Space Access and Future Strike Vehicles (SA-FSV) analysis indicates that substantial aeroheating is present. Aerothermoelastic analysis and Thermal Protection System (TPS) sizing of this phenomenon collaboratively contribute to vehicle configuration and structural layout. Additionally, consideration of the various stage flight conditions along the vehicle's trajectory should be included. Fundamental to this improvement in design methods are the methods that enable the capture of design interactions with optimizations within the integrated Adaptive Modeling Language (AML) framework. We regard built-in, Multi-Disciplinary Optimization (MDO) technology as a next generation capability for improving air vehicle design and manufacturing technology. The potential impact of the proposed work represents a paradigm shift in the design and corresponding manufacturing processes, enabling greatly improved design optimization.

Over the last four years, LMM&FC has collaborated with TechnoSoft, Inc. on several developmental efforts centered on TechnoSoft's AML Web-based Design Environment (WDE). Our relationship has resulted in revolutionary innovations within our domain of missile design. Our past experience, coupled with their sophisticated technology and innovative organizations of experts, has us convinced that the Phase I SBIR proposal effort submitted by TechnoSoft, Inc. will be ensured success. This success will give rise to a Phase II SBIR effort, which, if awarded, will receive our complete support. Our organization within Lockheed Martin anxiously anticipates participation within the development and implementation of the resulting SA-FSV integrated framework architecture.

Sincerely,

Dr. Richard Zarda
Manager, Engineering Methods Group
Lockheed Martin Missiles and Fire Control, Orlando

Some Excerpts...

Lockheed Martin Missiles and Fire Control supports the proposal effort ... AF01-252, Aerothermoelastic Optimization Methods for Reusable Launch Vehicles.

We regard built-in, Multi-Disciplinary Optimization (MD) technology as a next generation capability for improving air vehicle design and manufacturing technology.

The potential impact of the proposed work represents a paradigm shift in the design and corresponding manufacturing processes, enabling greatly improved design optimization.

This success will give rise to a Phase II SBIR effort, which, if awarded, will receive our complete support. Our organization within Lockheed Martin anxiously anticipates participation within the development and implementation of the resulting SA-FSV integrated framework architecture.

Orbital Sciences Corporation Endorsement Letter

Orbital

November 2, 2001

Dr. Danny D. Liu
ZONA Technology
7430 E Stetsm Drive
Scottsdale, AZ 85251-3540

SUBJECT: Orbital Support of ZONA Phase II Proposal entitled "Integrated Hypersonic Aerothermoelastic Methodology for TAV/TPS structural Design and Optimization."

Dear Dr. Liu:

Orbital Sciences Corporation is please to extend our support for ZONA's AFRL/SBIR phase II proposal entitled, "Integrated Hypersonic Aerothermoelastic Methodology for TAV/TPS structural Design and Optimization." Your work in this area is serving to bridge the gap between analytical methods and more labor-intensive computational approaches for hypersonic vehicle design. Specifically, your product will have relevancy beyond the AFRL need and will address a requirement in the launch community especially within NASA's Space Launch Initiative.

We are pleased that you have been able to use data generated for the X-34 program in the development of your methodology. ATA successfully applied ZONA developed methods to the X-34 program during aeroelastic analysis of the airframe and your support of a troublesome speed brake "buzz" prediction was appreciated. Though the X-34 has yet to become the national hypersonic testbed that it was intended for, much useful experimental and computational data exists for just such efforts.

Thank you for allowing us the opportunity to view and comment on your work. I hope the TPS links we provided have been helpful. Please consider us as a resource for Reusable Launch Vehicle and aerothermal information.

Sincerely

Henri D. Fuhrmann
Flight Dynamics Manager
Advanced Programs Group

Some Excerpts...

Orbital Sciences Corp. is pleased to extend our support for ZONA'' AFRL/SBIR phase II proposal ...

Your work in this area is serving to bridge the gap between analytical methods and more labor-intensive computational approaches for hypersonic vehicle design.

Specifically, your product will have relevancy beyond the AFRL need and will address a requirement in the launch community especially within NASA's Space Launch Initiative.

ATA successfully applied ZONA developed methods to the X-34 program during aeroelastic analysis of the airframe and your support of a troublesome speed brake "buzz" prediction was appreciated.

For further information of ZONA Technology software, please visit www.zonatech.com.

REFERENCES

1. "The Adaptive Modeling Language," TECHNOSOFT, Inc., Copyright 1993-1999, *www.technosoft.com*
2. Krasnov, N.F. "Aerodynamics of Bodies of Revolution," Edited and Annotated by Morris, D.N., American Elsevier Publishing Company, Inc., New York 1970, pp. 603-607.
3. Lees, L., "Hypersonic Flow," Proceedings of the Fifth International Aeronautical Conference, Los Angeles, Institute of the Aeronautical Sciences, 1955, pp. 241-275.
4. Chen, P. C., and Liu, D. D., "Unified Hypersonic/Supersonic Panel Method for Aeroelastic Applications to Arbitrary Bodies," International Forum of Aeroelasticity and Structural Dynamics, Madrid, Spain, June 5-7, 2000.
5. Burns, K.A., Deters, K.J., Haley, CP, and Kihlken, T.A., "Viscous Effects on Complex Configurations," AFRL Final Report WL-TR-95-3059, August 1995.
6. Engel, C. D., and Schmitz, C. P., "MINIVER Upgrade for the AVID System", Vol. 3: "EXITS User's and Input Guide," NASA CR-172214, Aug. 1983.
7. Kleb, W. L., Wood, W. A., Gnoffo, P. A., and Alter, S. J., "Computational Aeroheating Predictins for X-34," Journal of Spacecraft and Rockets, Vol. 36, No. 2, 1999, pp. 179-188.
8. Palmer, G., and Polsky, S., "Heating Analysis of the Nosecap and Leading Edges of the X-34 Vehicle," Journal of Spacecraft and Rockets, Vol. 36, No. 2, 1999, pp. 199-205.
9. Berry, S. A., Horvath, T. J., DiFulvio, M., Glass, C., and Merski, N. R., "X-34 Experimental Aeroheating at Mach 6 and 10," AIAA 98-0881.
10. Brauckmann, G. J., "X-34 Vehicle Aerodynamic Characteristics," AIAA 98-2531.
11. Wood, W. A., "Aerothermodynamic Calculations on X-34 at Mach 6 Wind Tunnel Conditions," NASA TM-1999-208998.
12. Pamadi, B. N., and Brauckmann, G. J., "Aerodynamic Characteristics and Development of the Aerodynamic Database of the X-34 Reusable Launch Vehicle," International Symposium on Atmospheric Reentry Vehicles and Systems, Arcachon, France, March 16-18, 1999.
13. Riley, C. J., Kleb, W. L., and Alter, S. J., "Aeroheating Predictions for X-34 Using an Inviscid-Bouncary Layer Method," AIAA Paper 98-0880.
14. Murry, A. L., "Further Enhancements of the BLIMP Computer Code and User's Guide," Air Force Wright Aeronautical Labs., AFWAL-TR-88-3010, June 1988.
15. Bonner, E., Clever, W., and Dunn, K., "Aerodynamic Preliminary Analysis System II Part I – Theory," NASA CR 182076, Apr. 1991.
16. Hoak, D. E., and Finck, R. D., "USAF Stability and Control Datcom," Vol. 1-4, Air Force Wright Aeronautical Labs., Apr. 1978.
17. Moore, F. G., Mcinville, R. M., and Hymer, T., "The 1998 Version of the NSWC Aeroprediction Code: Part I – Summary of New Theoretical Methodology," NSWCDD/TR-98/1, Apr. 1998.
18. *Supersonic/Hypersonic Vehicle Design (SHVD) Simulation System*, Dual Use Science & Technology (DUS&T) Program FY-2001, Lockheed Martin Missiles and Fire Control
19. Liu, D.D., Yao, Z.X., Sarhaddi, D. and Chavez, F.R., "From Piston Theory to a Unified Unsteady Hypersonic-Supersonic Lifting Surface Method," Journal of Aircraft, Vol. 34, No. 3, May-June 1997.

20. Liu, D.D., Chen, P.C., Yao, Z.X. and Sarhaddi, D., "Recent Advances in Lifting-Surface Methods," the Aeronautical Journal of the Royal Aeronautical Society, Vol. 100, No. 998, October, 1996, pp. 327-339.
21. Chavez, F.R. and Liu, D.D., "Unsteady Unified Hypersonic/Supersonic Method for Aeroelastic Applications Including Wave/Shock Interaction," AIAA Journal, Vol. 33, No. 6, June, 1995, pp. 1090-1097.
22. Krist, S.L., Biedron, R.T. and Rumsey, D.L., "CFL3D User's Manual Version 5.0," NASA Langley Research Center, Hampton, VA, Sep. 1997.
23. Sims, J.L., "Tables for Supersonic Flow Around Right Circular Cones at Small Angle of Attack," NASA SP-3001, 1964.
24. Brong, E.A., "The Flow Field about a Right Circular Cone in Unsteady Flight," AIAA Paper 65-398, San Francisco, CA, Jul. 1965
25. Dorodnitsyn, A.A., "The Method of Integral Relations for the Numerical Solution of Partial Differential Equations," (in Russian), in *Trudy instituta mekhaniki I vychislitelnoi tekhnik,* AN SSSR, 1958. Also in *Aerodynamics of Bodies of Revolution,* by N.F. Krasnov, edited and annotated by D.N. Morris, American Elsevier Publishing Company, Inc., New York, 1970.
26. Liu, D.D. and Chen, P.C. "Aerodynamic Predictions Using ZONA Technology's ZONAIR/ZAERO Code for Bent Nose," Contract No. DAAH 01-96-C-R194, August 25, 2000.
27. Johnson, E.H. and Venkaya, V.B., "Automated Structural Optimization System (ASTROS), Theoretical Manual," AFWAL-TR-88-3028, Vol. 1, Dec. 1988.
28. Neill, D.J. and Herendeen, D.L., "ASTROS Enhancements, Volume I/II/III – ASTROS User's/Programmer's/Theoretical Manuals," WL-TR-96-3004/3005/3006, May 1995.
29. Chen, P.C., Liu, D.D., Sarhaddi, D., Striz, A.G., Neill, D.J. and Karpel, M., "Enhancement of the Aeroservoelastic Capability in ASTROS," STTR Phase I Final Report, WL-TR-96-3119, Sep. 1996.
30. Chen, P.C., Sarhaddi, D. and Liu, D.D., "Development of the Aerodynamic/ Aeroservoelastic Modules in ASTROS," ZAERO User's/Programmer's/Applications/ Theroretical Manuals, AFRL-VA-WP-TR-1999-3049/3050/3051/3052, Feb. 1999.
31. Petley, D. and Yarrinton, P., "Design and Analysis of the Thermal Protection System for a Mach 10 Cruise Vehicle," JANNAF Meetings, Albuquerque, New Mexico, Dec. 9-13, 1996.
32. Moore, F.G., "Engineering Codes for Aeroprediction: State-of-the-Art and New Methods," AGARD Report, AGARD-R-804, presented at an *AGARD Special Course on Missile Aerodynamics,* Jun. 1994, pp 2.1-2.82.
33. Hender, D.R., "A Miniature Version of the JA70 Aerodynamic Heating Computer Program, H800(MINIVER)," McDonnel-Douglas Astronautics Co., Rep. MDC G0462, June 1970.
34. Riley, C.J. and Dejarnette, F.R., "Engineering Aerodynamic Heating Method for Hypersonic Flow," *Journal of Spacecraft and Rockets,* Vol. 29, No. 3, May-June 1992.
35. Cleary, J.W., "Effects of Angle of Attack and Bluntness on Laminar Heating Rate Distribution of a 15° Cone at a Mach Number of 10.6," NASA TND-5450, 1969.
36. Wurster, K. E., Riley, C. J. and Zoby, E. V., "Engineering Aerothermal Analysis for X-34 Thermal Protection System Design," Journal of Spacecraft and rockets, Vol. 36, No. 2, 1999, pp. 216-228.

37. Myers, D. E., Martin, C. J. and Blosser, M. L., "Parametric Weight Comparison of Advanced Metallic, Ceramic Tile, and Ceramic Blanket Thermal Protection Systems," NASA TM 2000-210289.
38. Zobyl, E.V., Moss, J.N., and Sutton, K., "Approximate Convective-Heating Equations for Hypersonic Flow," Journal of Spacecraft and Rockets, Vol. 18, pp. 64-70, Jan-Feb 1981.
39. Lyness, J.N. and Moler, C.B., "Numerical Differentiation of Analytic Functions," SIAM J. Num. Anal. 4: 202-210, 1967.
40. Gao, X.W., Liu, D.D., and Chen, P.C., "Internal stresses in Inelastic BEM Using Complex Variable Differentiation," Computational Mechanics, 28, 2001.
41. Harder, R.L. and Desmarais, R.N., ".Interpolation Using Surface Splines," AIAA Journal, Vol. 9, No. 2, 1972, pp. 189-191.
42. Duchon, J., "Splines Minimizing Rotation-Invariant Semi-Norms in Sobolev Spaces," Constructive Theory of Functions of Several Variables, edited by W. Schempp and K. Zeller, Springer, Oberwolfach, Germany, 1976, pp. 85-100.

APPENDIX A

PRELIMINARY STUDY ON THE AML SYSTEM INTEGRATION OF THE ZONA AEROTHERMOELASTIC SOFTWARE FOR TPS/TAV DESGIN

ZONA Prime Contract No:	F33615-01-M-3131
Subcontract No:	ZTTSI010801
ZONA Project No:	010801

Subcontractor Name:

TECHNOSOFT INC.
4434. Carver Woods Drive
Cincinnati, OH 45242-5545
Phone: (513) 985-9877
Fax: (513) 985-0522

A.1 Introduction

The design of Trans Atmospheric vehicles is a complex multidisciplinary problem. The process is collaborative and often requires interaction between numerous engineers to refine a design from the conceptual to the preliminary stage. It is a highly iterative and interactive process, often involving many proprietary engineering applications. This process involves geometric modeling, aerodynamics, propulsion, thermal analysis, trajectory analysis, structural analysis, subsystem layout, and internal and external interface specifications. Historically, these analyses and simulations have not been integrated and the overall design process has been inefficient and poorly defined. TechnoSoft is working with ZONA Technology on developing an environment that will mitigate these drawbacks by possessing the following attributes:

- Integrated geometry, meshing, aerodynamics, aerothermal, thermal protection system design, weight modules, trajectory simulation, closure, and design exploration and optimization
- Multiple (arbitrary body) aerodynamic and aerothermal codes that range from subsonic to hypersonic regimes
- Rocket and air-breathing propulsion
- Common (arbitrary) geometry models for all analysis tools
- A proven integration approach for geometry and analysis tools
- Built-in design exploration methods that allow the user to conduct HAV trade studies and multidisciplinary optimizations
- An object-oriented architecture that allows for the efficient capture of knowledge and processes
- An open architecture that allows for efficient integration of legacy application codes
- Platform independence
- A web-enabled distributed architecture
- A design methodology architecture that can simultaneously support conceptual, preliminary, and detailed designs and simulations within the same environment
- An integrated, feature-based design environment with a parametric link to Pro/E that will allow geometry and packaging parameters to be integrated efficiently with performance and cost studies

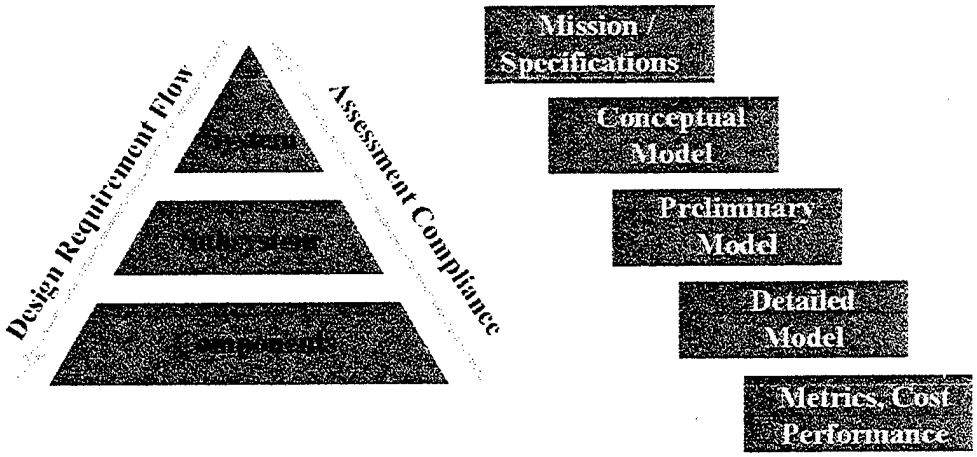

Vehicle Design Process

An architecture and functional specification were developed for a collaborative environment based on an underlying object-oriented, web-enabled, multidisciplinary, distributed framework supporting the design and analysis of Trans Atmospheric Vehicles (TAV). The developed architecture and the prototype system are tied to ZONA's hypersonic program.

The developed framework seamlessly integrates several domain-specific analyses and general-purpose modules into one coherent environment that is linked to ZONA's analysis codes. The common computational model will allow users to utilize the full capabilities of ZONA's analysis codes from a user-friendly, web-enabled, collaborative environment.

The environment provides a customizable graphical user interface supporting a feature-based design environment integrating ZONA's analysis codes, and geometry enabling the rapid prototyping of TAVs. It supports a unified geometric part model, providing various levels of modeling fidelity to capture conceptual and preliminary design processes. The environment links multiple users in a collaborative process, automating and managing data transfer and interactions among users, designs, analyses, and tools. It provides multidisciplinary optimization capabilities to enhance vehicle analysis, reducing engineering time and cost while expanding the design space explored. A common computational model seamlessly integrates geometry and ZONA's analysis codes to support closure of the process through iterative control.

The prototype environment that was developed in Phase I highlighted the exchange of model information among various modules.

The prototype that was developed includes a module for automating the generation of panel meshes (quad panels). Meshes can be generated from native AML geometries or imported geometries. Standard queries and data structure interfaces have been developed which allow the generation of geometric input data for ZONA's analysis codes.

Detailed studies and reports can be fully automated. All data exchange between the various modules (in different disciplines) is fully automated and tracked through the CCM. User

interaction with the system is facilitated through a GUI that allows for the exploration of design specifications and the investigation and visualization of results.

A.2 Functional Specification Overview

To achieve the technical objectives of Phase I, TechnoSoft Inc. has divided the tasks into five focus areas.

1. Underlying framework development
The overall functional specifications of the underlying framework was reviewed and developed. The prototype framework was developed using the Adaptive Modeling Language (AML) from TechnoSoft and inherited the various aspects of its object-oriented environment. The event-driven nature and dependency tracking of AML is used to control and management of the various resources of and the data flow among the application modules and the CCM.

2. General-purpose modules development
The prototype environment employed a modular architecture developed around a kernel implemented in AML to create an underlying framework with resource management and dependency tracking. Various modules, both general-purpose and domain-specific, were developed as an extension to the core system. While the domain-specific modules in the framework focused on one engineering discipline, the general-purpose modules provide functionality that is independent of any specific engineering domain knowledge.

a. The core provides functionality inherent within the AML environment including: 1) a visual class and part model builder, 2) a fully-portable graphical user interface builder supporting a 3D interactive visualizer, 3) a powerful model-querying engine, 4) a model manager incorporating various utilities for managing a distributed model and multiple users, 5) a model browser and inspector, and 6) an object-oriented, fully-parametric, rule-based geometric modeler with full access and querying of geometric topology. In addition, the geometric modeler is fully compliant to various modeling standards, including IGES and proprietary formats such as SHAPES, ACIS, and ParaSolid.
b. Feature-based grid generation module. This prototype module provides the capability to automate the generation of panel-based mesh models. Controls for panel size and distribution, enabled through various mechanisms, allows for panel size and curvature refinements with a parametric link to the geometry. Changes in part geometry will automatically trigger the system to re-compute the panel model if required. The grid automation supports the automated mesh generation of the outer body and substructure meshes required for structural analysis. The prototype module developed has limited, case-specific functionality.
c. External application linking. This module provides a general-purpose environment supporting the linking, input and output data management, and execution control of standalone external applications.
d. Criteria management and design exploration and optimization (CMDEO) module. This module supports the exploration and evaluation of the design using various MDO methods, design of experiments, and enumeration methods. Visualization methods are employed to view the resulting trade studies and correlations as well as optimum design configurations.

3. Domain specific analysis modules development
These modules focus on the various design disciplines, integrating the tools and applications used in the disciplines and capturing the algorithms, processes, and methods used. These modules include ZONA's aerodynamics analysis, aerothermal, structural thermal analysis, thermal protection system design and configuration, structural analysis, engine sizing and configuration, weight and closure, and trajectory analysis.

4. Common computational model development
The functional specifications of the environment were reviewed and the CCM was developed to support the control and exchange of data between the geometry, mesh, and analysis modules. The CMDEO module will provide direct control of the CCM data for design exploration and optimization. Geometric parameters, meshing details, and application input and output are fully controlled through the dependency management and tracking mechanism employed by the framework to enable the support of automated studies and distributed analyses required for the assessment of design criteria for the computation of objectives.

5. Environment integration and testing
The prototype environment modules were tested and integrated and a limited set of models was tested.
TechnoSoft has developed a prototype, case-specific environment that illustrates the great value of developing a fully functional TAV design, analysis, and evaluation integration environment.

A.3 Results

A prototype, case-specific environment was developed to demonstrate the feasibility of the architecture. The environment allows users to generate geometry decks that can be used to run ZONA's analysis codes.
The prototype environment includes a number of modules:

1. Fuselage modeling
2. Wing modeling
3. TAV modeling
4. Import Geometry
5. Mesh generation
6. ZONA's geometry deck generation

Fuselage Modeling

This portion of the environment allows users to rapidly model a TAV fuselage. This conceptual level model allows users of the system to rapidly evaluate the viability of a fuselage design in an efficient manor.

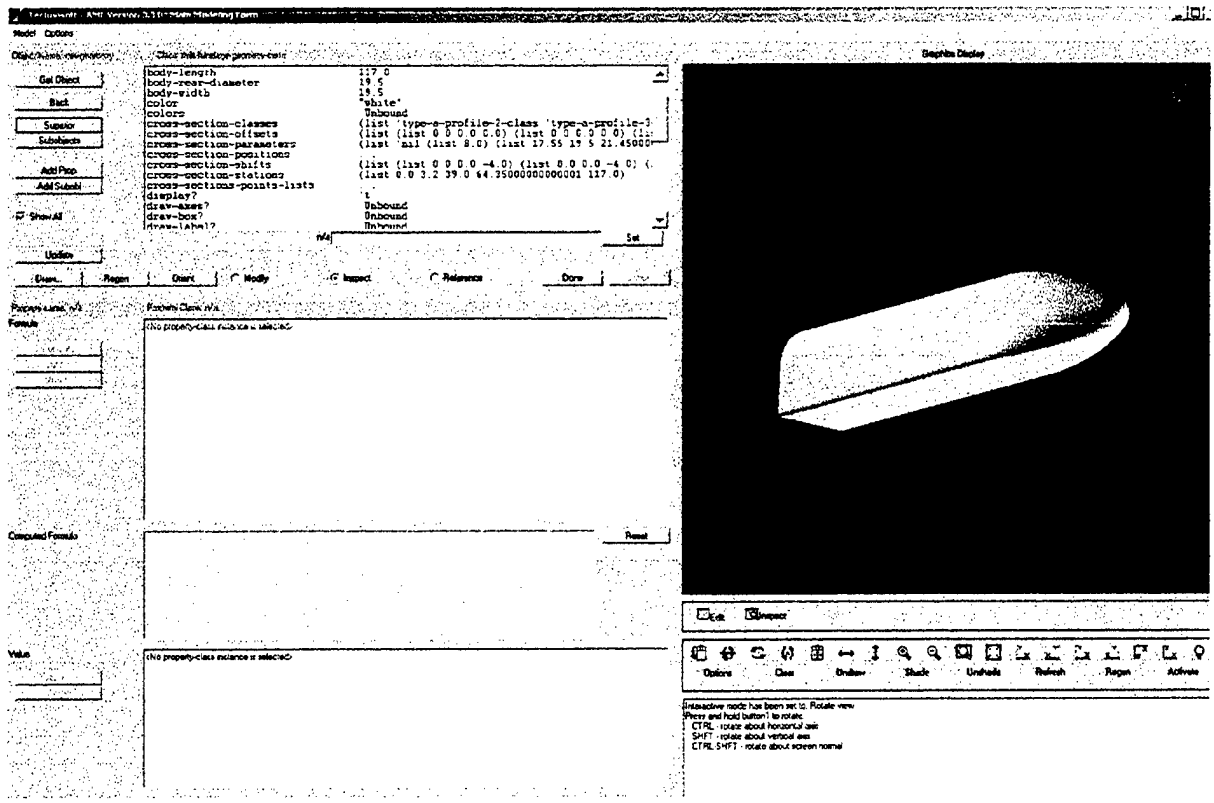

Figure A.1 Fuselage Modeling

Figure A.1 is a sample fuselage that was defined in the environment. Users of the environment have full control over the shape of the fuselage, and can drastically change the shape of a fuselage by varying the control parameters.

Wing Modeling

Similar to the fuselage modeling concept described previously, users of the system can describe a wing geometry that can be used for analysis.

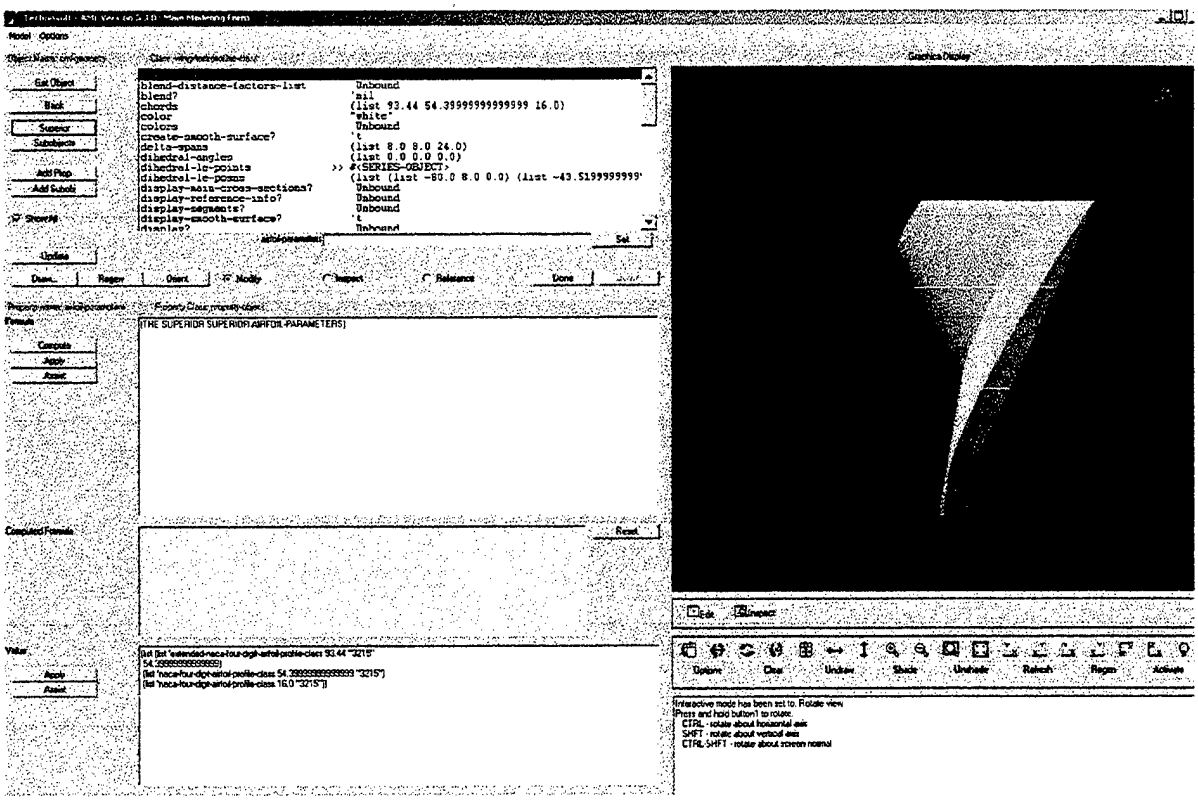

Figure A.2 Wing geometry

TAV modeling

This allows the user to define a TAV geometry where the position of the wing and tail are driven by the fuselage shape and size. The AML TAV model allows users to explore "what if" scenarios in an efficient manor.

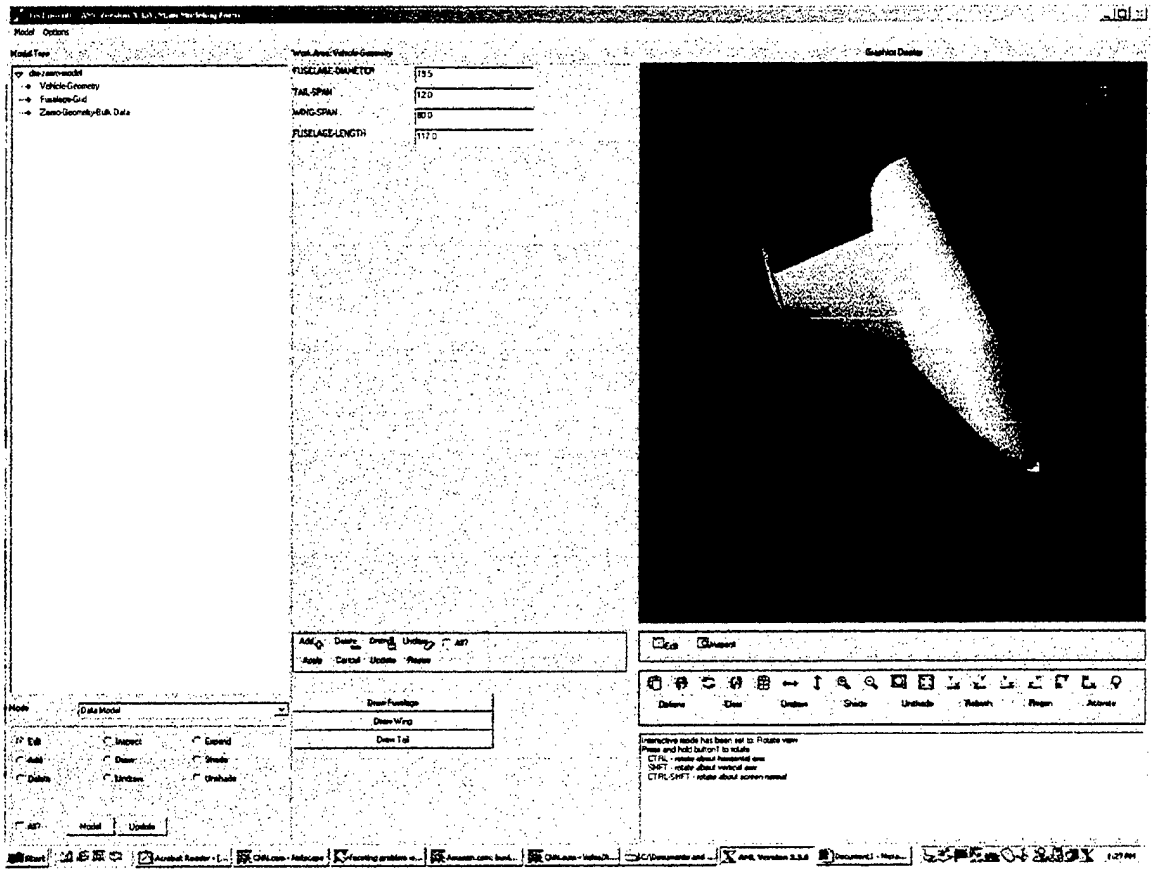

Figure A.3 TAV design module

Import Geometry

The developed environment allows users to import IGES, and STEP geometries. The user can then group the imported geometries, and mesh the grouped geometry. The mesh can then be used to generate geometry decks for ZONA's analysis codes.

Mesh Generation

The mesh generation process is one of the most labor-intensive and time-consuming components of the aerodynamic design, analysis, and optimization process. Great benefits can be achieved by building an environment that allows users to parametrically link the mesh to geometry and to save meshing strategies for future use.

TechnoSoft Inc. is developing a novel approach that will allow users to parametrically link the TAV geometry to the mesh.

The focus will be on three areas of research:

- parametric meshing
- cleanup of imported geometries
- attribute propagation

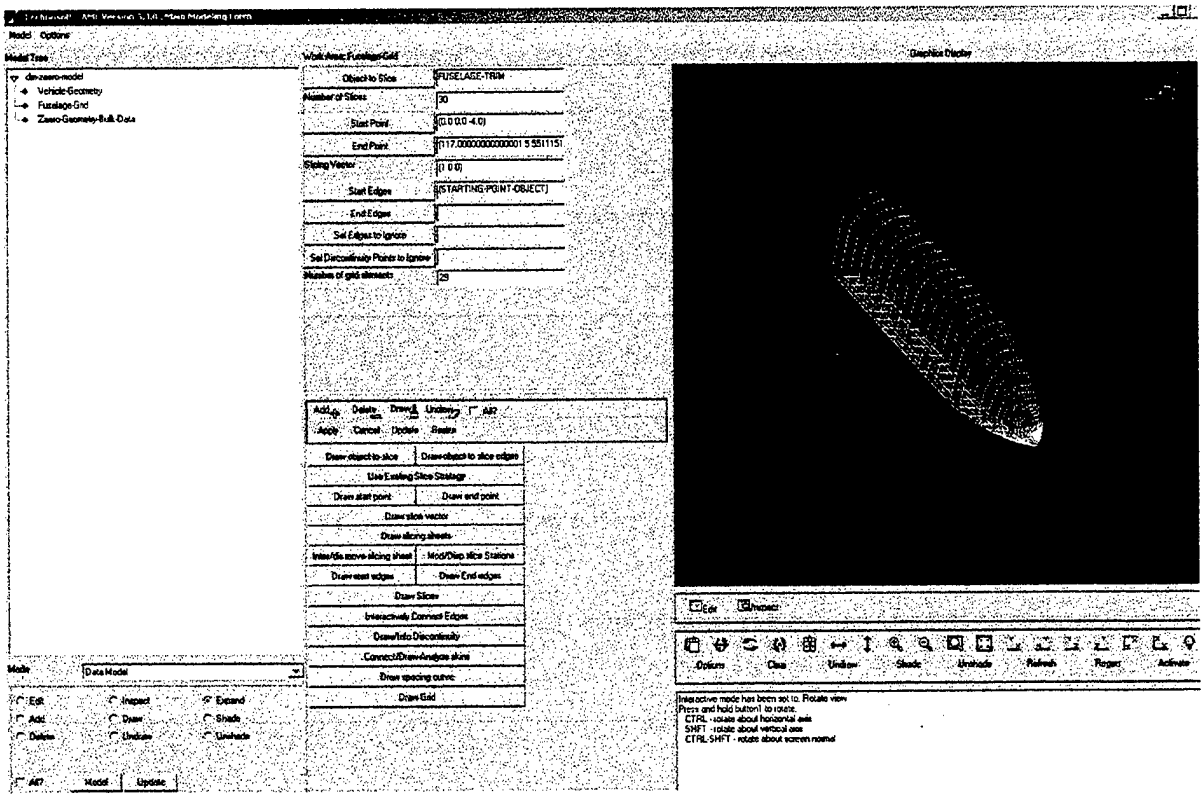

Figure A.4 Parametric panel based mesh

The prototype environment developed has a limited case-specific parametric-automatic meshing functionality. A set of methods has been implemented that will allow user to automatically mesh imported geometries that need "cleanup".

ZONA's geometry deck generation

TAV geometry and a fuselage grid are used to generate geometry decks that can are used to run ZONA's analysis codes.

A set of classes that will allow users to generate complete ZONA analysis code decks is under development. The functionality these classes will provide is critical to closing the design, analysis, and evaluation loop.

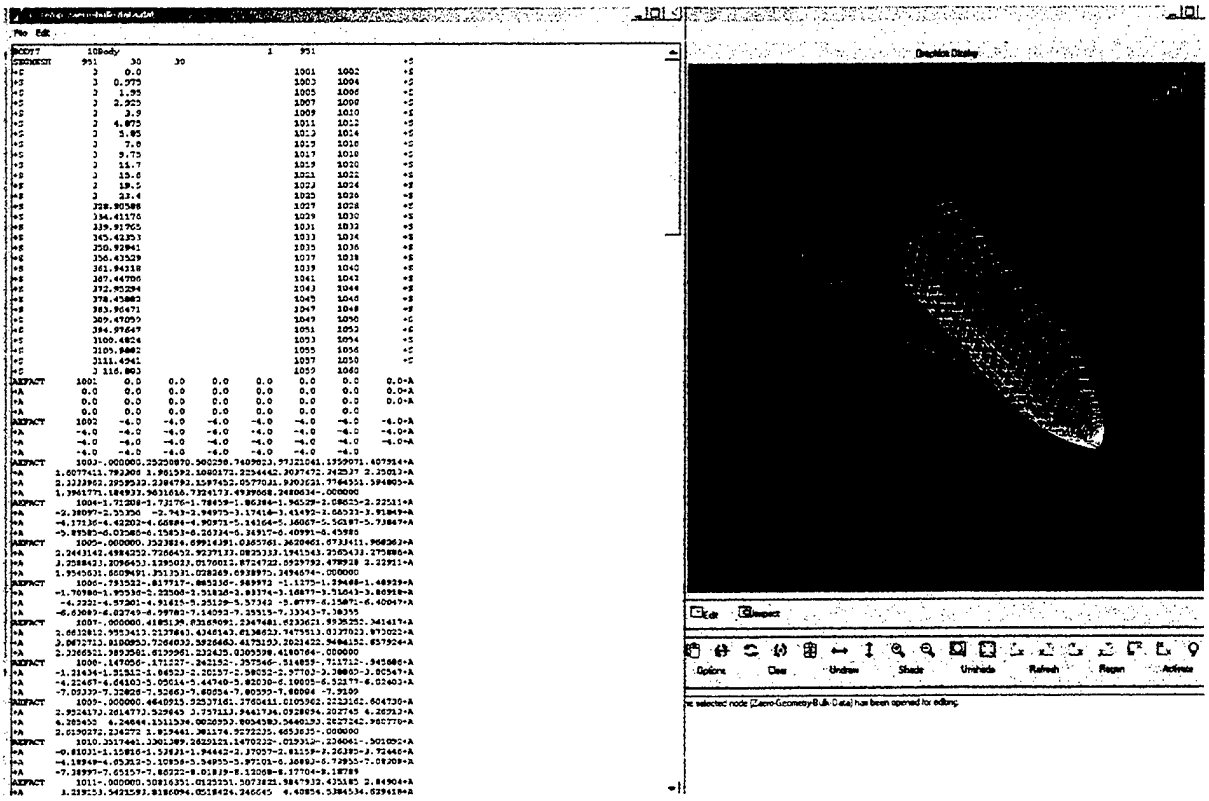

Figure A.5 ZONA's geometry deck

A.4 Conclusion

TechnoSoft and ZONA Technology have a rare and valuable opportunity to develop a TAV design, analysis, and evaluation environment that will allow users to explore "what if" scenarios in an efficient manor, and that will facilitate the sharing of data between the different disciplines. The prototype environment is a proof of concept that illustrates both the value and need for such an environment.

APPENDIX B

HYPERSONIC/SUPERSONIC INVISCID SOLUTION FOR BLUNTED CONES

Blunted Cones in hypersonic flow require delicate aerodynamic treatment. Unlike sharp-cone hypersonic aerodynamics, conical flow does not hold for a blunted-cone whereby its flowfield is non-uniform. Nevertheless, there exist various approaches to the blunted cone problem due to its practical importance in aerospace applications. Most approaches in the past were phenomenological in formulation, notably the Lees modified Newtonian formula (Ref B1)

$$C_p = C_{p_0} \sin^2 \theta_b \qquad (B.1)$$

where C_{p_0} takes up the normal shock solution θ_b is the local surface inclination with respect to the freestream.

Further generalizations of (B.1) is the so-called modified Newtonian theory (MNT,B1) for blunt-nose bodies under angles-of-attack, α, reads

$$C_p = C_{p_0} \sin^2 \delta_{eq} \qquad (B.2)$$

Note that θ_b of (B.1) is replaced by δ_{eq} where

$$\delta_{eq} = \sin^{-1}\{\sin\phi\cos\alpha - \cos\phi\cos\theta\sin\alpha\}$$

is the local inclination angle between the body slope to the freestream; ϕ is the azimuthal angle and θ is the angle measured from the local tangent vector to the x-axis (Figure B.1), i.e.

$$\theta = \frac{dr}{dx} \quad \text{where } r^2 = y^2 + z^2$$

Although equations (B.1) and (B.2) serve as accurate and convenient formulas, the validity of these equations are confined to the blunt-nose region.

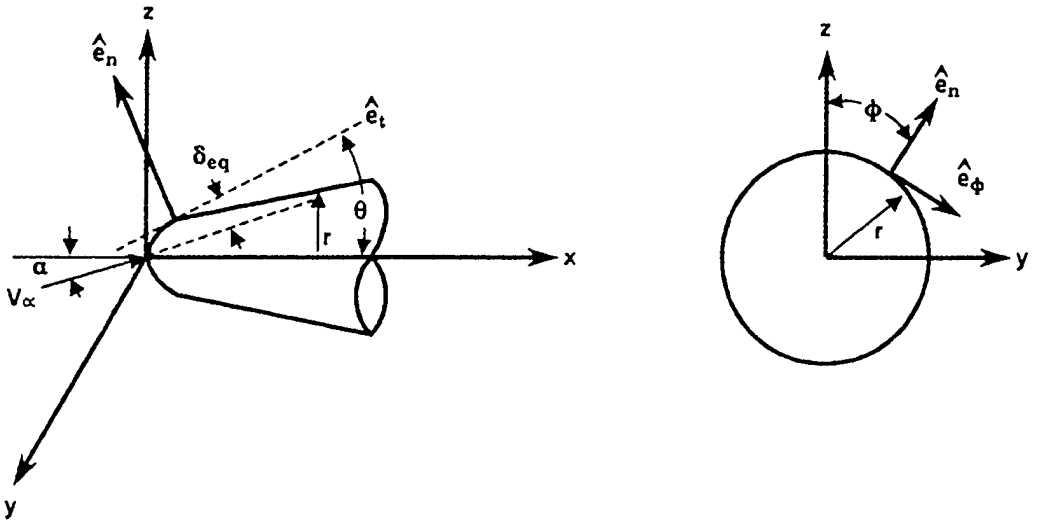

Figure B.1 Nomenclature Used For Determination Of Angle δ_{eq}

B.1 The Blunted Cone Flow Regions

The blunt-cone problem that we intend to solve is not confined to the nose region, however. With TAV/RLV type configurations in mind, the blunt-cone model is of further extent in its conical section. From test data and previous CFD solutions (Fig B.2), it can be seen that such a pressure solution has typically three distinctive regions. Shown in Fig B.2, region I is the nose section, where Equations (B.1), (B.2), and (B.3) would be valid. Region III is the "conical section" in which the surface pressure returns to that of the conical flow and maintains at a constant pressure thereupon according to that of the corresponding sharp cone value.

Region II is the transition zone, where the highly compressed flow in Region I is gradually recovered toward the conical flow solution of Region III. There are two demarcations that feature this flow region: the point of minimum pressure and that reaching the conical pressure.

To solve for the surface pressure distribution starting from the tangential point (between the nose cylinder and the cone) toward the conical-section surface going through the demarcation points, is not a trivial matter. For slender blunted-cones, there exist analytical blast-wave solutions due to Cheng et al (Ref B2) and Chernyi (Ref B3). For general blunted-cones, there exists several CFD solution methods, including that of Cleary (Refs B4 & B5) and Hamilton et al (Ref B6), among others. The outstanding work of Dejarnette and his associates (Refs B7 and B8) has provided a surface streamline method with a flow solution method for Region II. Although the resulting pressure in AEROHEAT (Ref B8) is well correlated with various CFD results, it is nevertheless a curved-fitted (by Chebyshev Polynomials) correlation with the known CFD/MOC solutions (Ref B9, B10)

B.2 Pressure Solutions of the Transition Zone

The blast-wave solution of Cheng and Chernyi for slender cones could be expressed in terms of a similarity solution format, i.e.

$$\frac{C_p}{\delta_c^2} = P\left(x^*, K, \gamma\right) \qquad \text{(B.3)}$$

where $\delta_c = tan\,\theta_c$

K is Tsiems Hypersonic Parameter, $K = M_\infty \delta_c$

γ is the specific heat ratio of the gas

x^* is the nondimensional distance, $x^* = \frac{1}{M_\infty^2 \sqrt{C_{D_N}}}\left(\frac{x}{D_N}\right)$

D_N is the nose diameter.

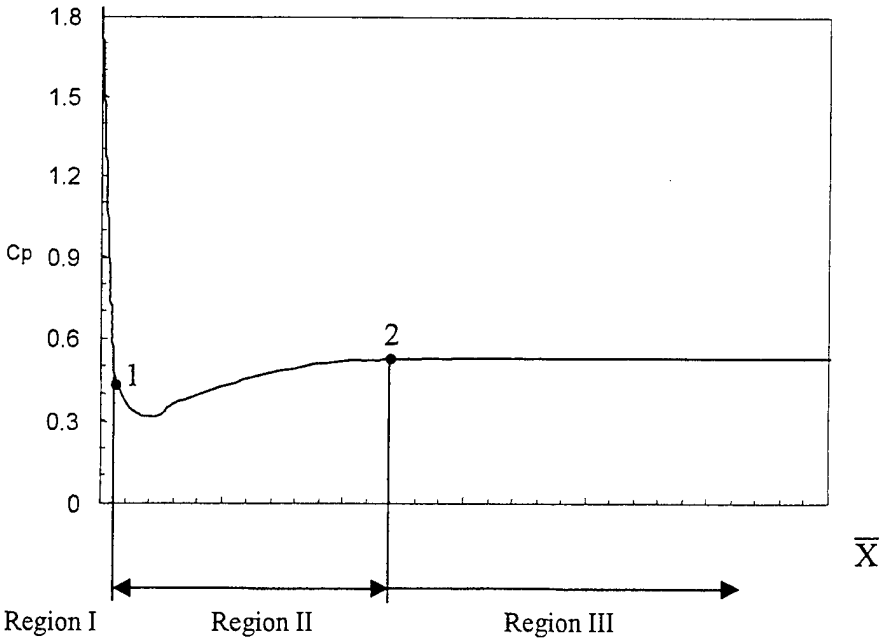

Figure B.2 Three Regions of a Blunted-Cone in Hypersonic/Supersonic Flow

After substantial correlation effort with test data, Krasnov (Ref B11) has arrived at a modified formula after Cheng/Chernyi's similarity format, i.e.

$$\frac{C_p}{\delta_c^{\sigma}} = K^{\nu} P(\bar{x})$$

where $\bar{x} = K^{\mu} x^*$, $\sigma = 1.8$, $\nu = -0.2$ and $\mu = 1.5$ (B.4)

Equation (B.4), under nominal conditions, does not take the γ-effect into account and is named universal-curve formula by Krasnov. It is this formula we have adopted for the pressure solutions in region II.

B.3 Blunted Cone at Yaw (AoA)

For blunted cones at angle of attack, we adopted an "equivalent local cone" concept. That is, we evaluate the pressure C_p according to a local cone angle, which is based on the expression:

$$\theta_c(\alpha, \phi) = \theta_c(0, 0) + \sum_{n=1}^{N} -1^n \alpha^n \cos n\phi \qquad \text{(B.5)}$$

For simplicity, we merely pick N=1 for all cases of AoA. Improvement in the pressure solutions is expected for N=2.

Next, substituting θ_c from (B.5) into equation (B.3) yields the pressure coefficients, C_p, for all cases of AoA.

B.4 Total C_p Solution

The C_p solution covering regions I, II, and III is constructed by a 4th-order polynomial fit within these regions. Shown in Figure B.2 is a $C_p \sim \overline{X}$ plot, whereby point 1 ($\overline{X}_1$) is the tangent point of the cone surface and the semisphere nose and point 2 ($\overline{X}_2$) is selected at $\overline{X}_2 = 1.0$.

To connect the C_p solution of Region I (due to Equations (B.1, B.2)) with that of Region III (where $C_{p\ III} = C_{p\ sharp\ cone}$), we impose the following connectivities for C_p expressions of Equations (B.4, B.5), i.e.,

1) Specifying $C_p(\overline{X}_1)$ and $\frac{dC_p}{dx}(\overline{X}_1)$ at $\overline{X} = \overline{X}_1$,
to connect Region I solution with Region II solution

and

2) Specifying $C_p(\overline{X}_2) = C_{p\ sharp\ cone}$ and letting $\frac{dC_p}{dx}(\overline{X}_2) = \frac{d^2C_p}{dx}(\overline{X}_2) = 0$, where $\overline{X}_2 = 1.0$
to connect Region II with Region III solution.

REFERENCES FOR APPENDIX B

B1. Lees, L. "Hypersonic Flow," *Proceedings of the Fifth International Aeronautical Conference*, Los Angeles, Institute of the Aeronautical Sciences, 1955, pp 241-275.

B2. Cheng, H.K., Hall, J.G., Golian, T.C., Hertzberg, A. (1960) "Boundary layer displacement and leading edge bluntness effects in high temperature hypersonic flow." Cornell Aero. Lab. Report No. AD-1052-A-9 also *J. Aero/Space Sci.* 28, 353-381, 410 (1961).

B3. Chernyi, G.G., *Introduction to Hypersonic Flow*, R.F. Probstein (trans. and ed.), Academic Press, New York, 1961.

B4. Cleary, J.W. "An Experimental and Theoretical Investigation of the Pressure Distribution and Flow Fields of Blunted Cones at Hypersonic Mach Numbers," TN D-2969, Aug. 1965, NASA.

B5. Cleary, J.W. *Effects of Angle of Attack and Bluntness on Laminar Heating Rate Distribution of a 15° Cone at a Mach Number of 10.6, NASA TN D-5450, 1969.*

B6. Hamilton, H.H., II, DeJarnette, F.R. and Weilmuenster, K.J. "Application of Axisymmetric Analog for Caluculating Heating in Three-Dimensional Flows," *Journal of Spacecraft and Rockets*, Vol. 24, July-Aug. 1987, pp 296-302

B7. DeJarnette, F.R. and Hamilton, H.H., "Inviscid Surface Streamlines and Heat Transfer on Shuttle-Type Configurations," *Journal of Spacecraft and Rockets*, Vol. 10, May 1973, pp. 314-321.

B8. Riley, C.J., DeJarnette, F.R. and Zoby, E.V. "Surface Pressure and Streamline Effects on Laminar Heating Calculations", J.Spacecraft, Vol. 27, No. 1, Jan.-Feb. 1990, pp. 9-14.

B9. Morrison, A.M., Solomon, J.M., Ciment, M. and Ferguson, R.E. "Handbook of Inviscid Sphere-Cone Flowfields and Pressure Distributions: Volume I," Navale Surface Weapons Center, White Oak, MD, NSWC/WOL/TR 75-45, Dec. 1975.

B10. Blick, E.F. and Francis, J.E., "Spherically Blunted Cone Pressure Distributions," *AIAA Journal*, Vol. 4, March 1966, pp. 547-549

B11. Krasnov, N.F. "Aerodynamics of Bodies of Revolution," Edited and Annotated by Morris, D.N., American Elsevier Publishing Company, Inc., New York 1970, pp. 603-607.

APPENDIX C

PHASE I FINAL REPORT PRESENTATION AT AFRL/WPAFB on NOVEMBER 14, 2001

Presented by Danny Liu (P.I.) and P.C. Chen

Integrated Hypersonic Aerothermoelastic Methodology for TAV/TPS Structural Design and Optimization

Proposal for AF/SBIR/Phase II: F33615-01-M-3131/AF01-252

ZONA Technology, Inc. *
Danny Liu
P.C. Chen

Technosoft
Adel Chemaly

AFRL
Lt. Mark Stevenson
David Adamczak
Jeffery Zweber
Maxwell Blair
Amarshi Bhungalia

Presented at Wright Patterson AFB, Dayton, OH, November 14, 2001.

* 7430 E. Stetson Drive, Suite 205, Scottsdale, AZ 85251-3540, Tel (480) 945-9988, Fax (480) 945-6588, E-mail: pc@zonatech.com

Overview

- Project Objective
- Phase I Work
- Phase II Proposal
- Discussion

Total Hypersonic Aerothermoelastic Program Architecture

- TAV/TPS Design Strategy

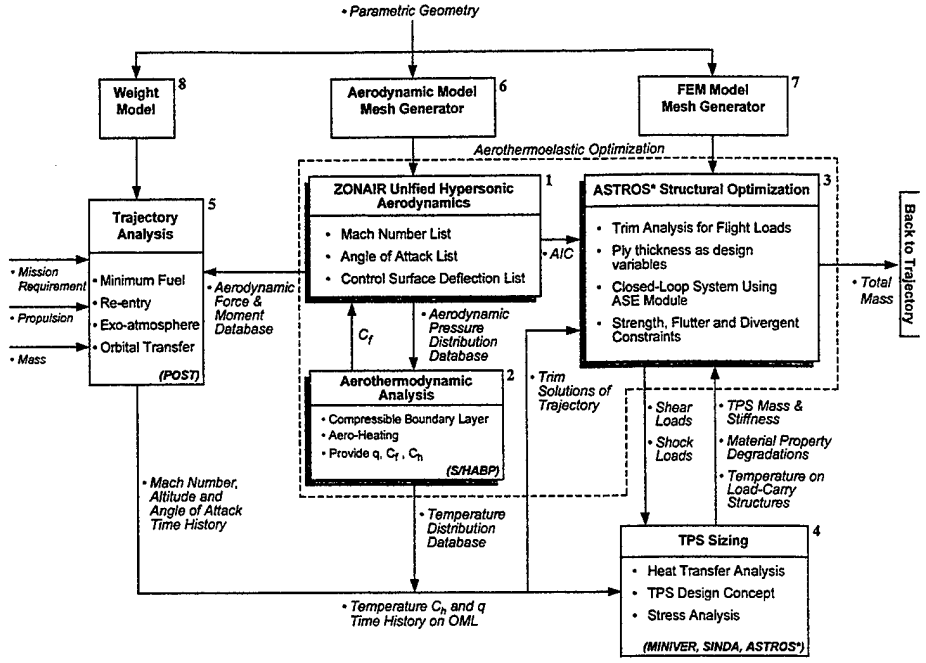

ZONA TECHNOLOGY

Phase II Technical Objectives

Goal:

The ZONA team proposes to continue the phase I development in a unified hypersonic/supersonic aerothermoelastic methodology, to enhance its geometry high-fidelity and to integrate it with a TAV/TPS structural design/optimization procedure for TAV/TSP weight minimization throughout TAV's re-entry/maneuver flight phases.

Further, the above development will be integrated in a feature-based design environment with parametric control of models and data exchange using the Adaptive Modeling Language (AML).

Objectives:

1. Development of an expedient conceptual/preliminary design tool that allows varying of parametric geometry for rapid assessment of design concepts.
2. The TPS sizing is to meet the thermal protection requirements of the main structures while being included with the main structures and treated together as a part of the load–carrying structure.
3. The developed software can be utilized by a design engineer as an outer loop design procedure for trajectory optimization, which in turn will lead to a minimum fuel and weight TAV design.

ZONA TECHNOLOGY

Phase I Achievement

- Developed ZSTREAM for streamline solutions
- Integrated ZONA7U+ZSTREAM+SHABP for hypersonic aeroheating analysis and validation
- Validation cases include:

  -CKEM Body

  -Blunt Cones

  -X-34 Wing-Body

- Nose Heat-rate validation with MINIVER through two trajectories
- Demonstrated protypical TPS sizing procedure
- X-34 aeroelastic trim analysis using ASTROS*

ZSTREAM for Stream Line Solution

- Aeroheating analysis requires inviscid flow streamlines
- QUADSTREAM in SHABP is Mach number independent
- ZSTREAM is finite-element-based derived from ZONA7U surface velocities

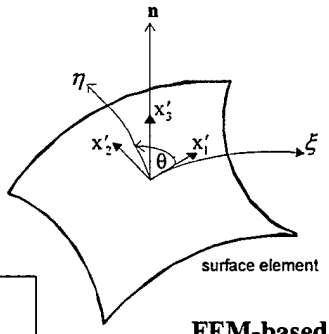

FEM-based

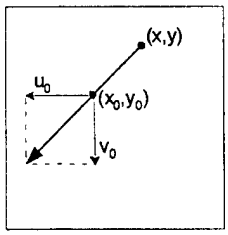

Marching from position (x_0, y_0) to (x, y)

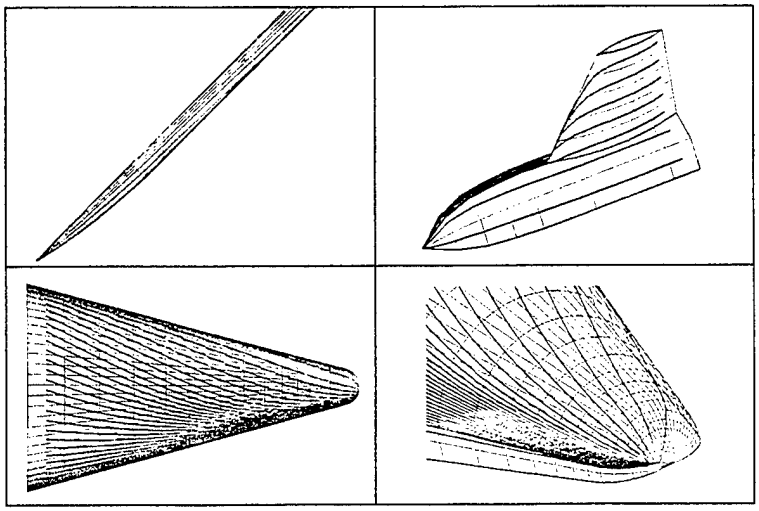

Validation: Cases Studied

- CKEM Body: $M = 6.0, \alpha = 2°$
- 15° Blunt Cone: $M = 10.6, \alpha = 0°, 5°, 10°$
- X-34 Wing-Body: $M = 6.0, \alpha = 9°, 15.22°$
- Inviscid Aerodynamics are validated with CFL3D
- Aerothermodynamics/Heat rates are validated with CFL3D + LATCH
- Some solutions are validated with test data
  - 15° Blunt Cone: Aerodynamics / NASA TND-2969
    Aeroheating / NASA TND-5450
  - X-34 Wing-Body: Aeroheating / AIAA 98-0881

Pointed-Nose CKEM Body: Aerodynamics

$M_\infty = 6.0, \alpha = 2°$

Inviscid Surface Pressure Distribution

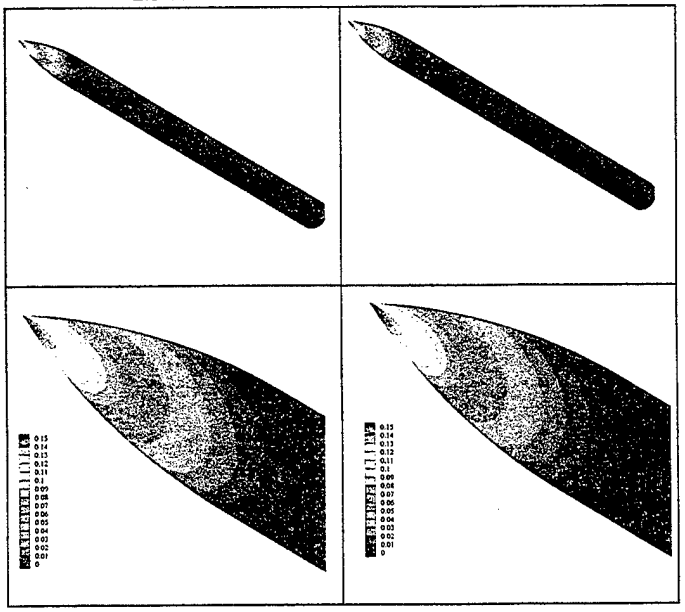

ZONA7U **CFL3D/Euler**

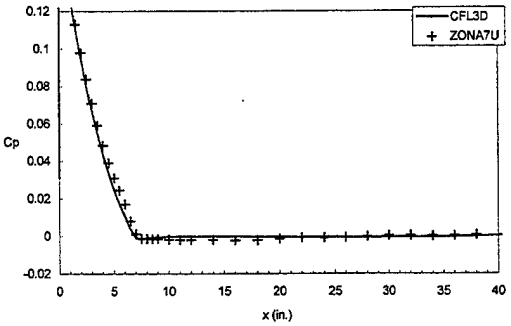

Wind-Side Inviscid Surface Pressure Distribution ($\phi = 180$)

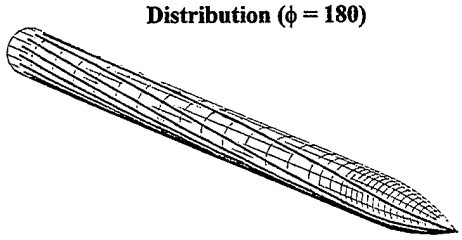

Streamlines Computed by ZONA7U/ZSTREAM, M = 6.0

Pointed-Nose CKEM Body: Aerodynamics

$M_\infty = 6.0$, $\alpha = 2°$, $P_\infty = 2.66$ psf, $T_\infty = 89.9°R$, $T_W = 540°R$

Laminar Heat Transfer Rate (Btu/ft²s)

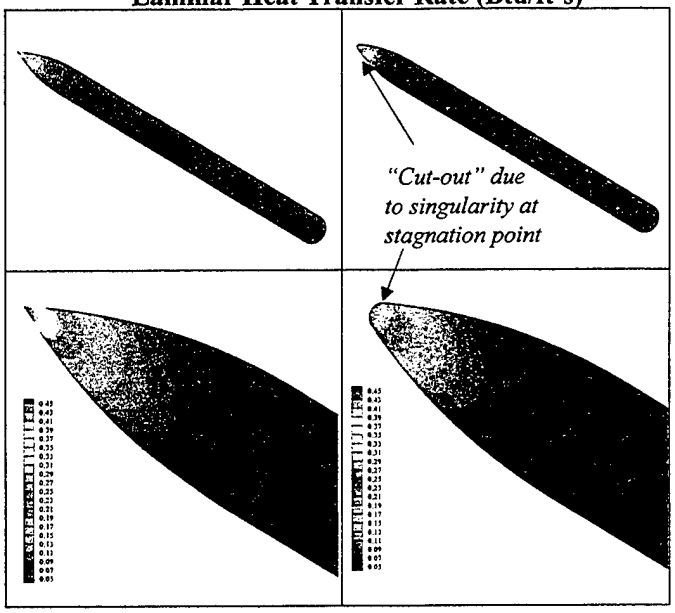

ZONA7U **CFL3D/Euler**

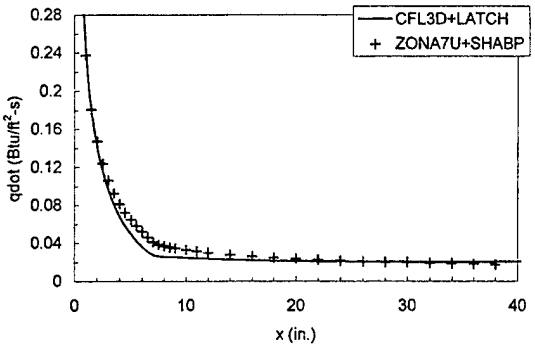

Wind-Side Laminar Heat Transfer Rates ($\phi = 180°$)

15° Blunt Cone: Aerodynamics

$M = 10.6$, $\alpha = 0°$

ZONA7U **CFL3D/Euler**

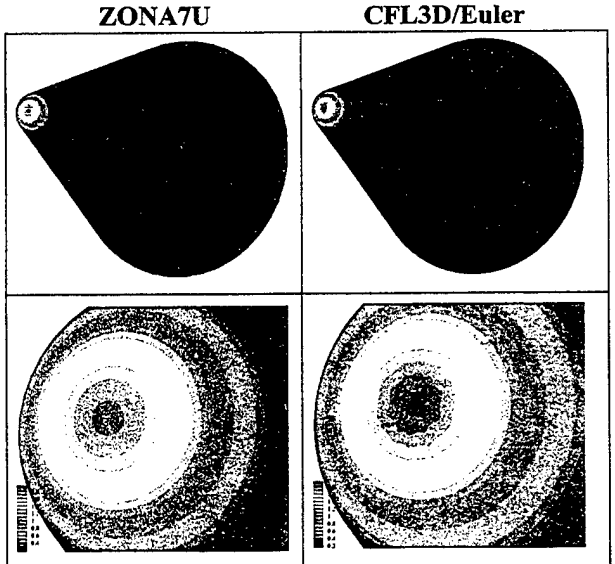

Inviscid Surface Pressure Distribution

Inviscid Surface Pressure Distribution

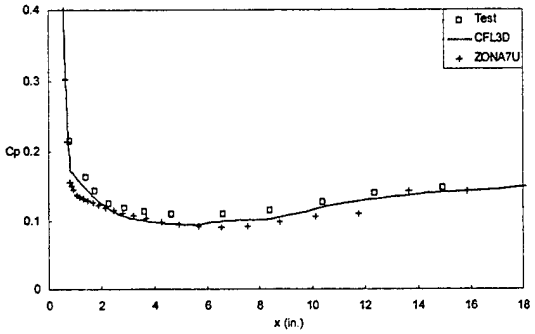

15° Blunt Cone: Aerodynamics

M = 10.6, α = 5°

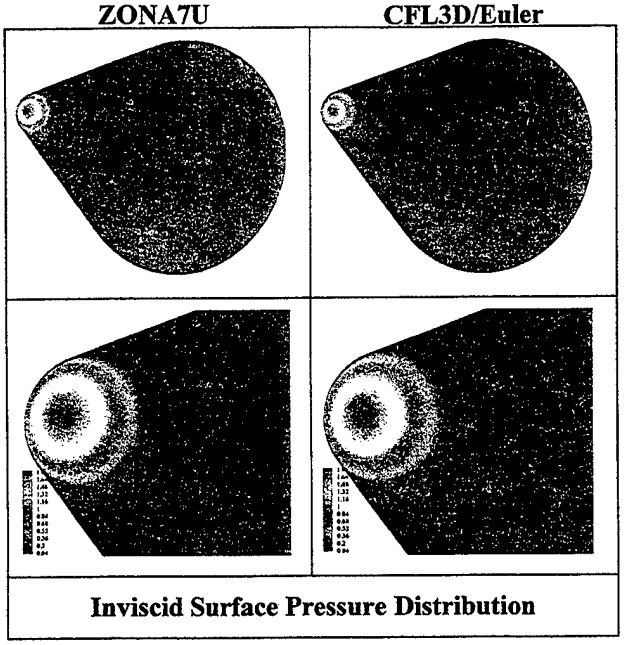

Inviscid Surface Pressure Distribution

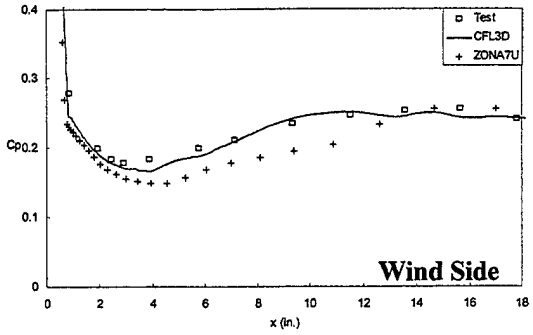

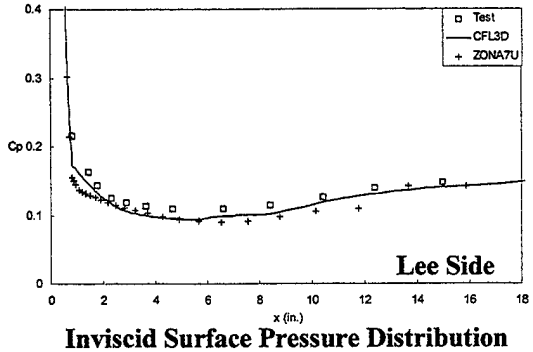

Inviscid Surface Pressure Distribution

ZONA TECHNOLOGY

15° Blunt Cone: Aerodynamics

M = 10.6, α = 10°

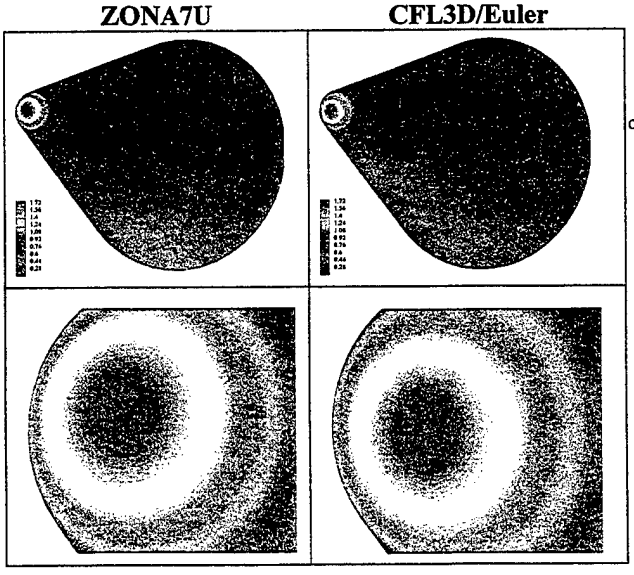

Inviscid Surface Pressure Distribution
(ϕ = 180°)

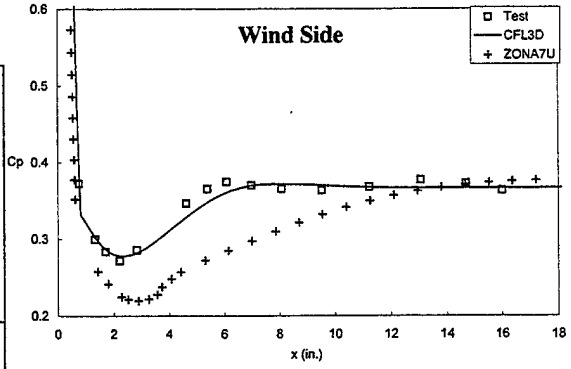

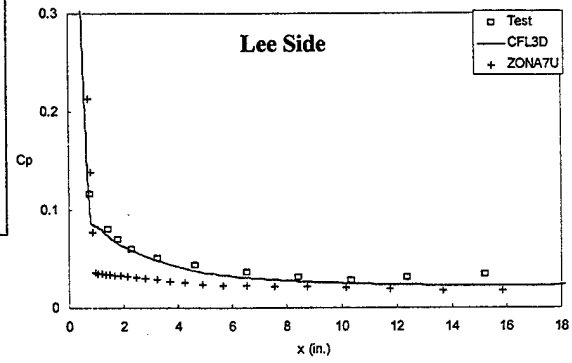

ZONA TECHNOLOGY

Laminar Heat Rate: 15° Blunt Cone

$M_\infty = 10.6$, $\alpha = 0°$, $P_\infty = 2.66$ lb/ft^2, $T_\infty = 89.971°R$, $T_W = 540°R$

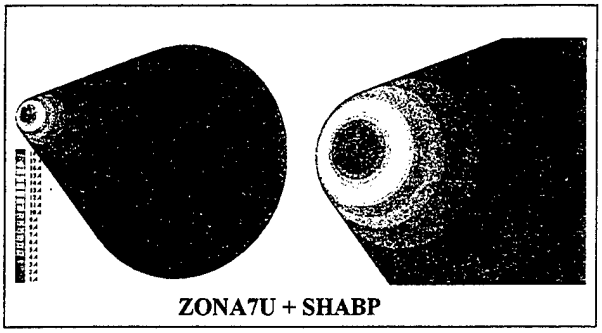

ZONA7U + SHABP

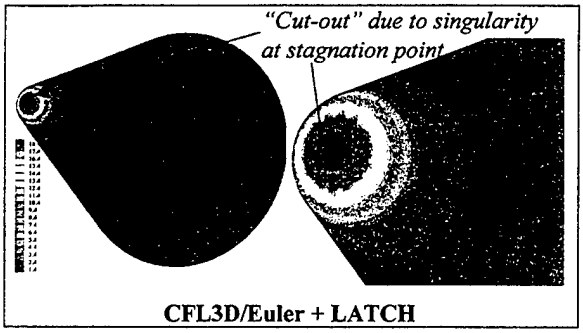

CFL3D/Euler + LATCH

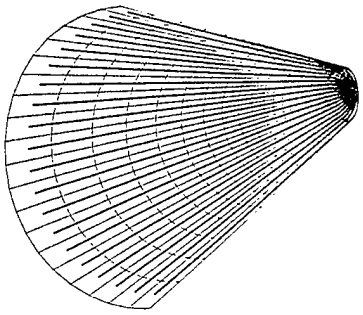

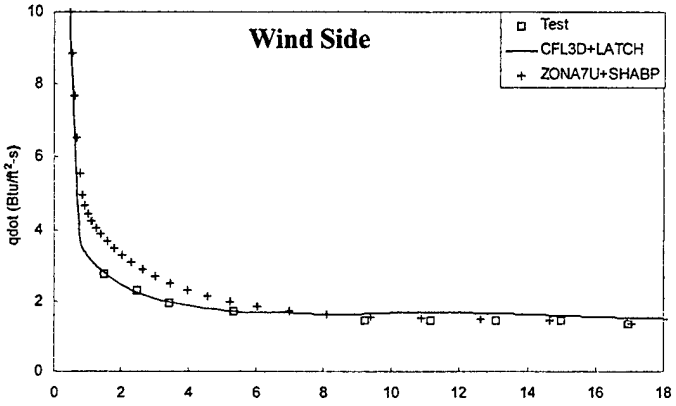

ZONA TECHNOLOGY

Laminar Heat Rate: 15° Blunt Cone

$M_\infty = 10.6$, $\alpha = 5°$, $P_\infty = 2.66$ lb/ft^2, $T_\infty = 89.971°R$, $T_W = 540°R$

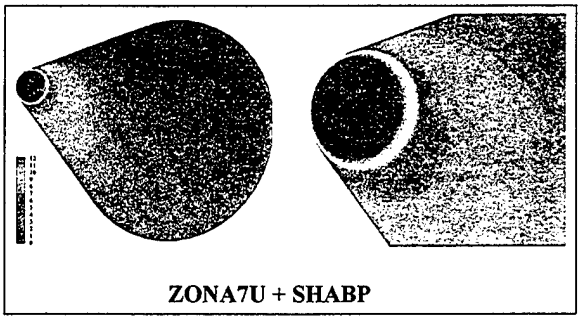

ZONA7U + SHABP

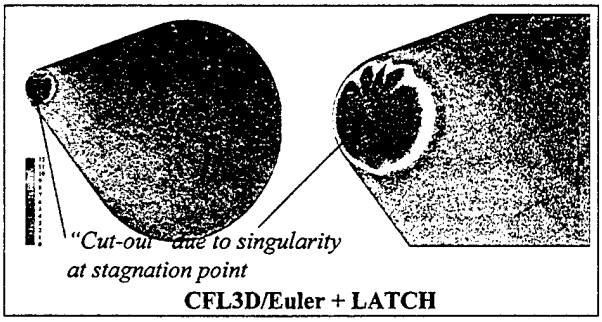

CFL3D/Euler + LATCH

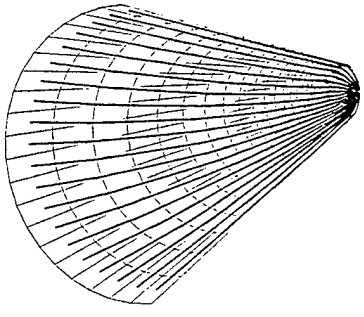

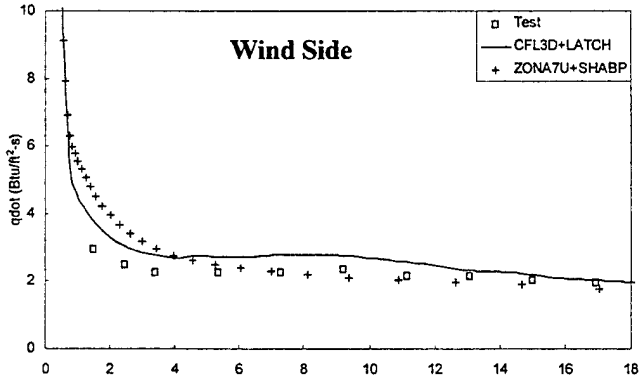

ZONA TECHNOLOGY

Laminar Heat Rate: 15° Blunt Cone

$M_\infty = 10.6, \alpha = 10°, P_\infty = 2.66\ lb/ft^2, T_\infty = 89.971°R, T_W = 540°R$

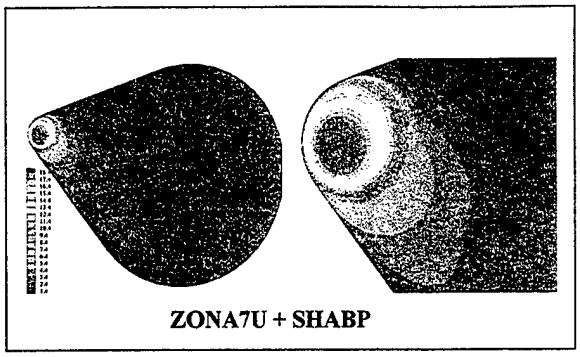

ZONA7U + SHABP

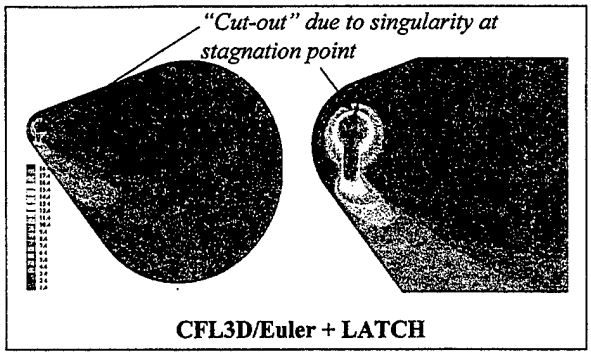

CFL3D/Euler + LATCH

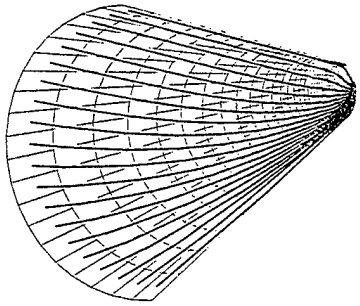

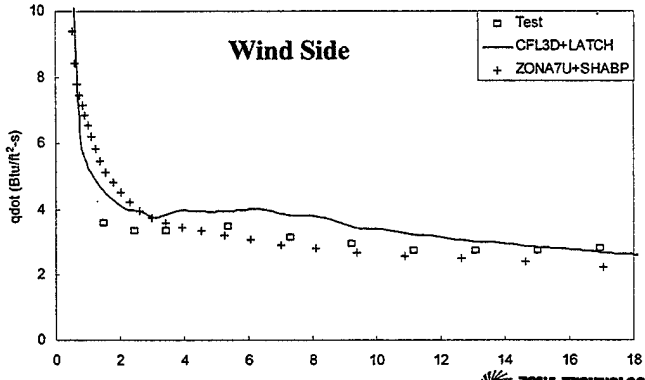

ZONA TECHNOLOGY

X-34 Wing-Body: Aerodynamics (I)

$M_\infty = 6.0, \alpha = 9°$

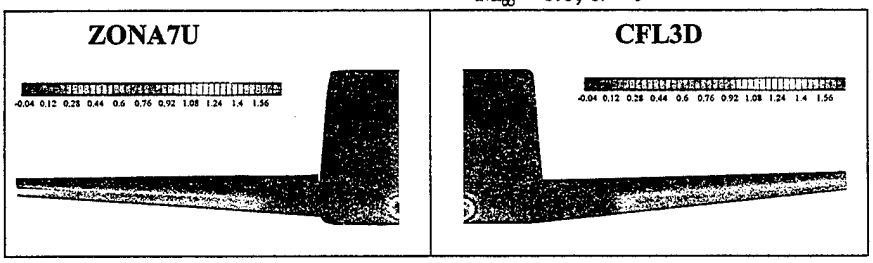

Front View

Wind-Side

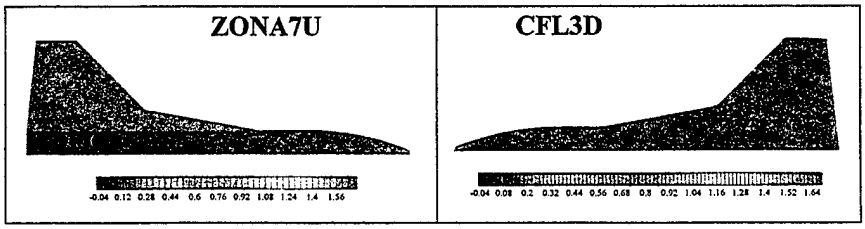

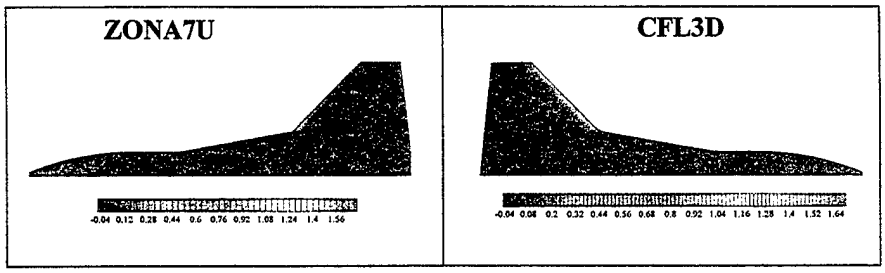

Lee-Side

ZONA TECHNOLOGY

X-34 Wing-Body: Aerodynamics (II)

$M_\infty = 6.0, \alpha = 15.22°$

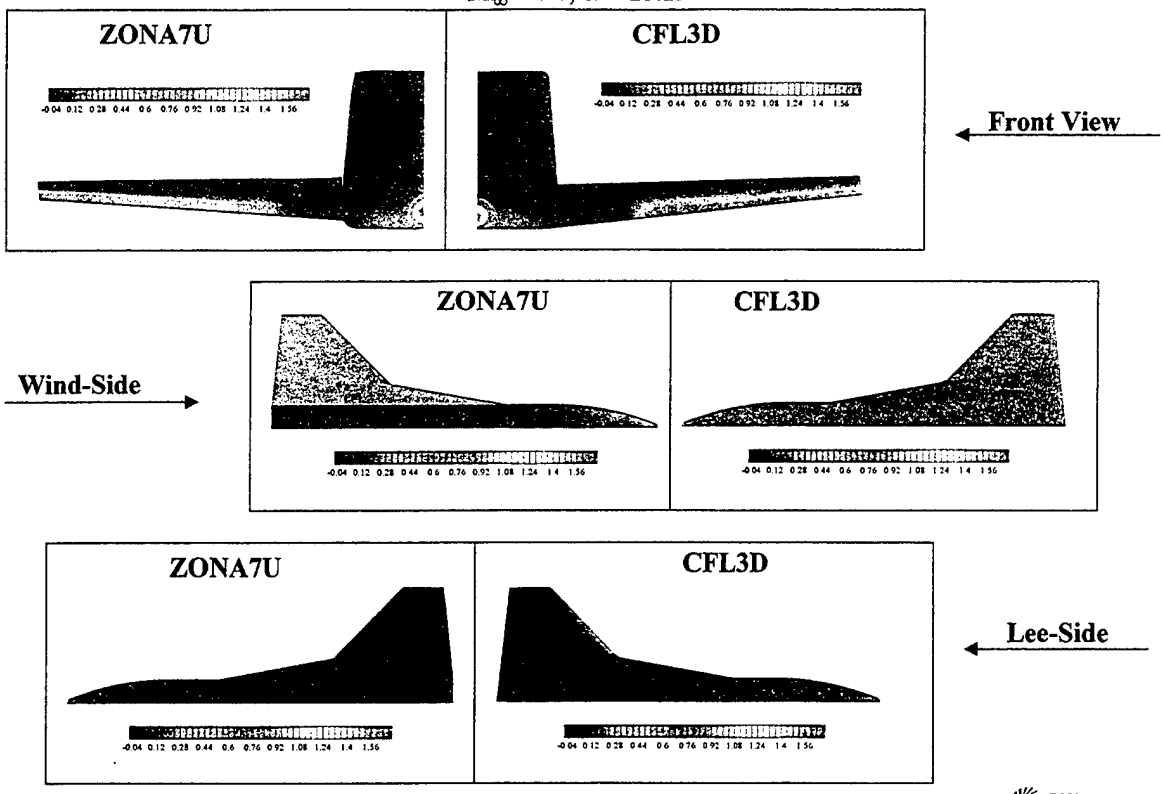

ZONA TECHNOLOGY

Sreamlines Computed by ZSTREAM on the X-34 at $M_\infty = 6$: $\alpha = 9°$, $\alpha = 15.22°$

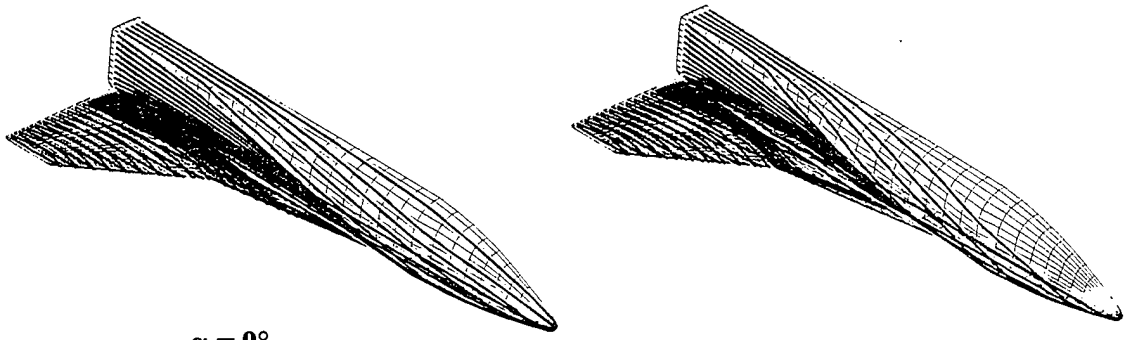

$\alpha = 9°$ $\alpha = 15.22°$

Aeroheating of X-34 (I)

M_∞ = 6.0, α = 9.0°, h = 183 Kft., Hot Wall, Emissivity = 0.8, Turbulent

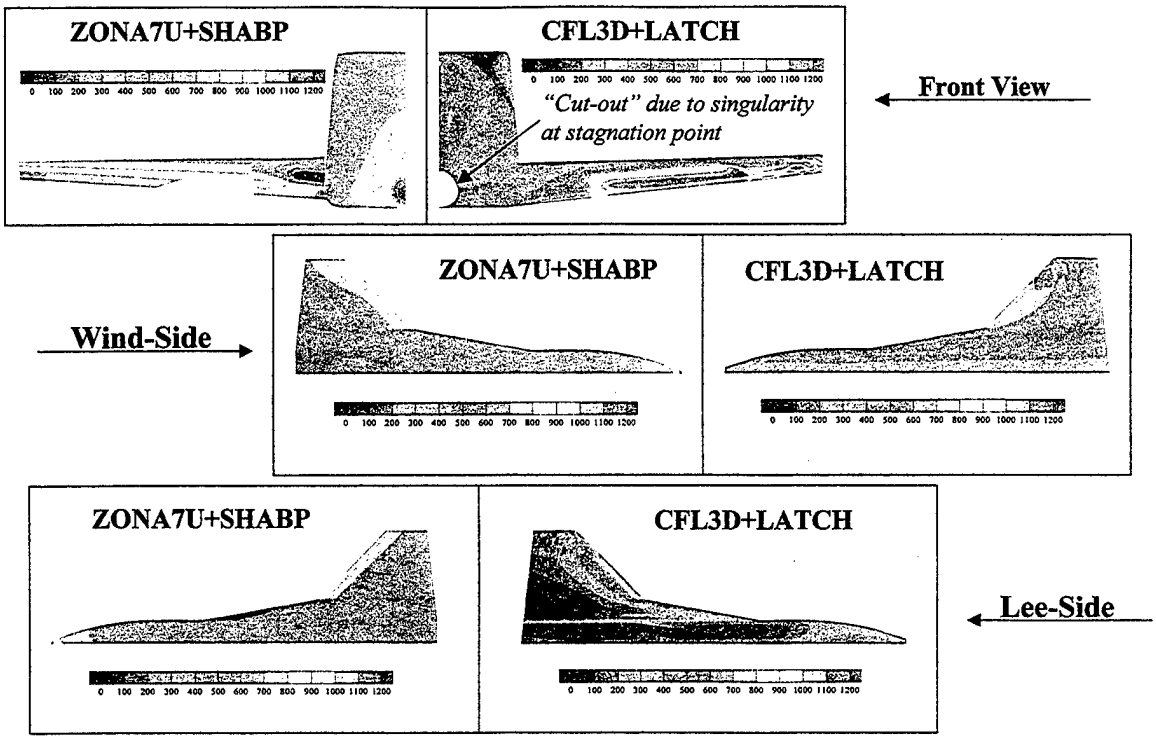

ZONA TECHNOLOGY

Aeroheating of X-34 (II)

M_∞ = 6.0, α = 15.22°, h = 112 Kft., Hot Wall, Emissivity = 0.8, Turbulent

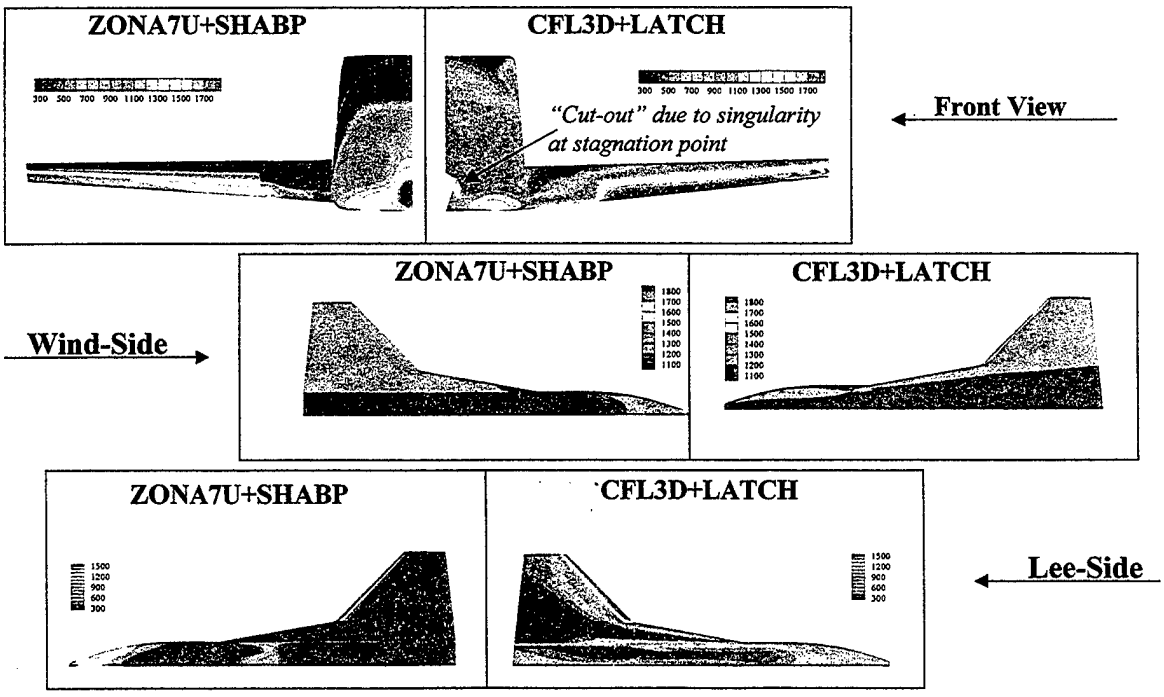

ZONA TECHNOLOGY

Aeroheating of X-34 Nose Stagnation Through Two Trajectories

X1004601/X1004701, Hot Wall Condition

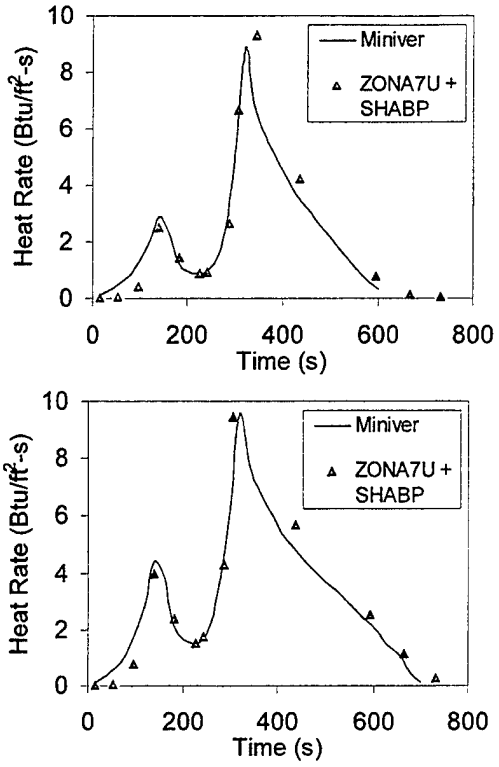

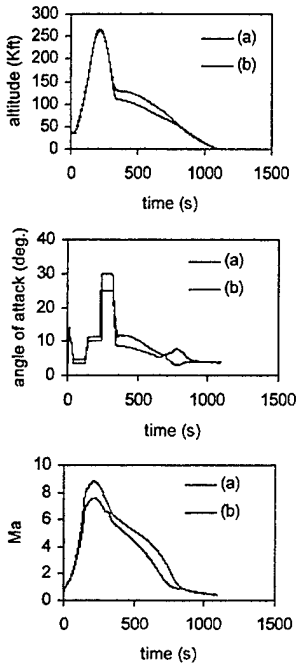

ZONA TECHNOLOGY

Elementary TPS Sizing of AFRSI

- **Heat Flux History**

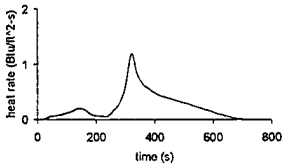

- TPS element on windward centerline of X-34 (L = 50'')
- "Maximum temperature" is determined by scanning all temperatures obtained throughout the trajectory history.
- ZONA7U+SHABP predicts correct peak $T_{outer/interior}$ at t = 340
- Thickness and Weight Solution of Layer (3)/AFRSI

Layer 3 material	Thickness	Normalized weight, TPS	Normalized weight, layer 3	Max T_{outer}	Max $T_{interior}$	Max T_{skin}
Felt insulation	0.456 in	1.000	1.000	708.7° F	696.4° F	300.3° F
Felt 3.5PCF	0.638 in	0.694	0.408	713.6° F	702.0° F	300.2° F
6LB Dynaflex	0.560 in	1.118	1.228	696.9° F	681.6° F	300.2° F

- **AFRSI Definition**

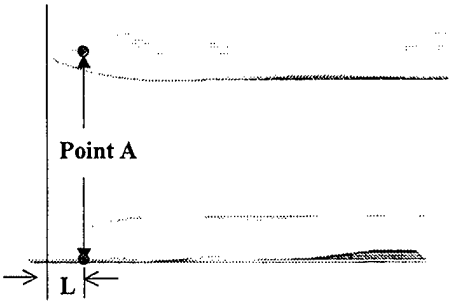

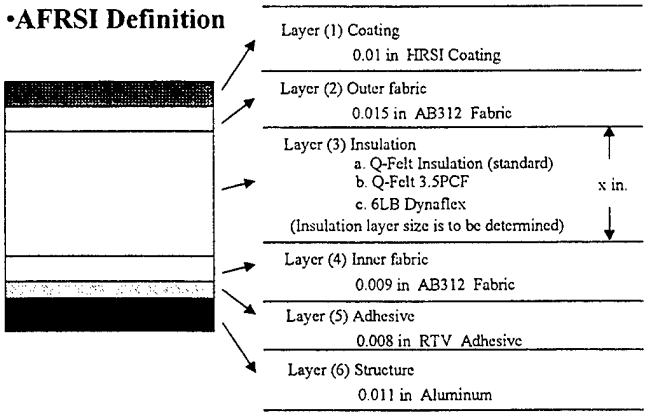

- *T_{outer} and $T_{interior}$ are the temperatures at the outer edge and interior of TPS. T_{skin} is the temperature at the nodes within the skin*

ZONA TECHNOLOGY

ASTROS* Engineering Modules

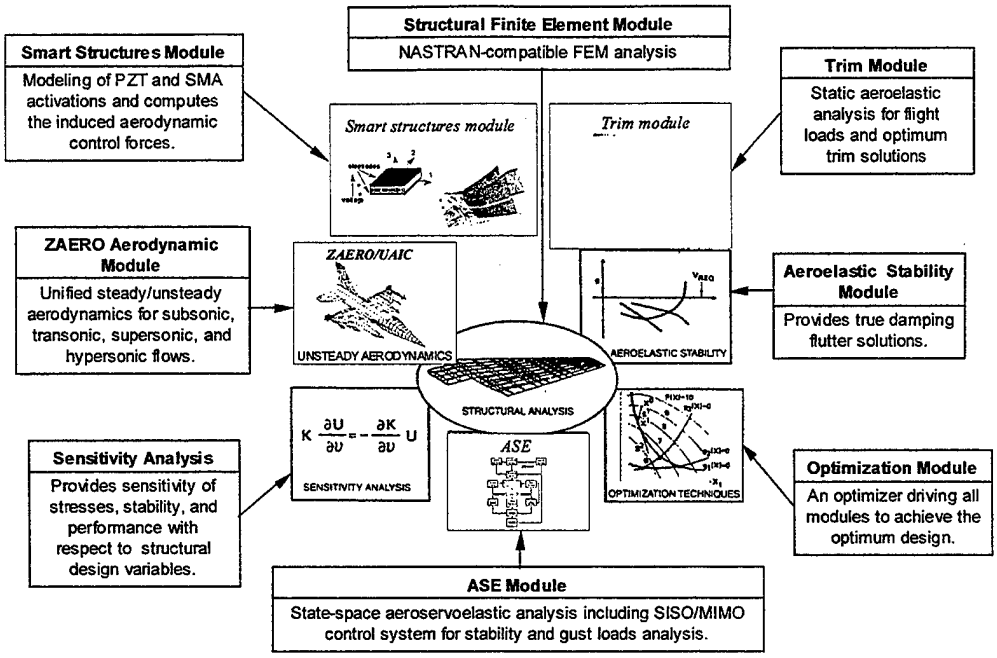

X-34 Trim Analysis Using ASTROS*

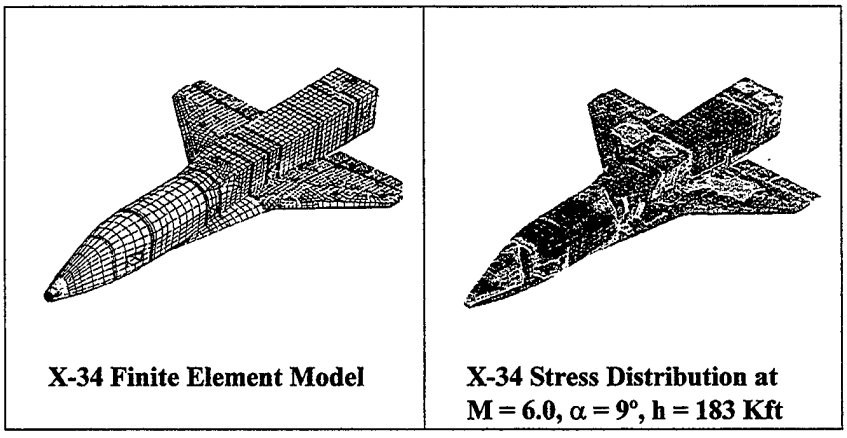

X-34 Finite Element Model

X-34 Stress Distribution at M = 6.0, α = 9°, h = 183 Kft

- X-34 ASTROS* FEM Model was converted from MCS/NASTRAN Model provided by Orbital/OSC
- TRIM condition is at M = 6.0, α = 9°, h = 183 Kft.
- TRIM results for total weight of 16,000 lbs.
  - $N_z = 0.97g$.
  - Trailing Edge Flap = 2.05°

Phase I Concluding Remarks and Recommendation for Phase II Tasks

- *Central Methodologies (Blocks 1-5)* required for aerothermodynamic optimization were individually developed and validated.
- Hypersonic Aerodynamics and Aerothermodynamic methodology for Blocks1/2 are aimed at replacing the high-level method CFL3D+LATCH and the low-level method MINIVER by a *mid-level method ZONA7U+ SHABP* which has been developed in Phase I.
- For ZONA7U+SHABP to generate one set of X-34 aerodynamic/heat rates typically requires *10 minutes on a 550 MHZ PC*, whereas for CFL3D+LATCH it requires 30 hours.
- *ZSTREAM* was developed in Phase I to replace the QUADSTREAM streamline generator of SHABP in that the latter, derived from the Newtonian flow consideration, has the a stagnation-point singularity in its streamline solution and it does not depend on freestream Mach number.
- Validation/verification of ZONA's aerothermodynamic method ZONA7U+SHABP suggests that further improvement is needed in the following: ZONA7U requires *higher-fidelity upgrade* in order to cope with the high AOA and the lee-side aerodynamics of SHABP needs to be replaced by the *AEROHEAT methodology* in order to further improve the local heat rate estimates.
- The TPS weight sizing example shows that the designed TPS weight can be further reduced if *an automated optimized scheme* can be developed. A *database of TPS material* in terms of their thermal and mechanical properties must be fully established in order to enhance the capability of the optimized scheme.
- *The trim solution of the X-34* in terms of the flight loads, input to the structural FEM within ASTORS*, will yield shear loads and shock loads which will result in strength constraint in the ASTROS* optimization procedure.
- Given trajectory inputs, ZONA7U+SHABP aeroheat solution at the nose of X-34 was verified with previous solutions obtained by NASA. *Total optimization loop including ASTROS** will be tested next using an X-34 example as a demonstration case.

Features of Improved ZONAIR: A High-Fidelity Unified Hypersonic/Supersonic Aerodynamic/Aerothermodynamic Tool

- Original ZONAIR is High-Order Panel, but only unified in supersonics/subsonics
- Incorporate Unified Hypersonic/Supersonic Methodology of ZONA7U into ZONAIR: Local Pulsating Cone Analogy
- Apply Perturbed Euler Formulation (PEF) to ZONAIR to account for:
  - Impinged shock strength and location
  - Cross-flow near-normal shock on Lee-side Flow
- Extend high AoA flow capability using L.E. vortex roll-up model to complex TAV configurations
- Extend ZONAIR to include two-body aerodynamics interference effect in hypersonic flow

ZONAIR (I): A High-Fidelity Supersonic/Subsonic Panel Method

- **Comparison of ZONAIR and PANAIR Paneling Schemes**

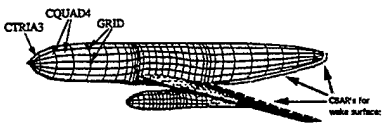

- Similar to structural FEM (MSC/NASTRAN), the entire configuration is defined by "grids".
- Only the starting lines of the wake need to be defined (via CBAR elements).
- PATRAN, FEMAP, etc., can be employed directly for pre- and post-processing.

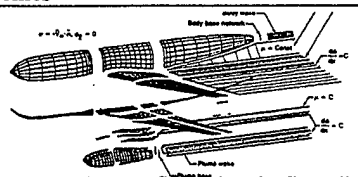

- The entire configuration is first divided into several "networks". Each network is further divided by m x n set of grids.
- The location of the wake surfaces must be explicitly defined.
- No commercially available software can be used directly for pre- and post processing.

- **Regular and Random Paneling of a Sphere at M = 0.0 and α = 0.0 deg.**

C_p on Regular Panels	C_p on Random Panels
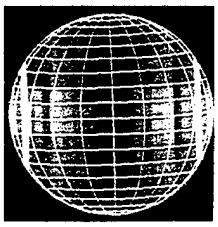	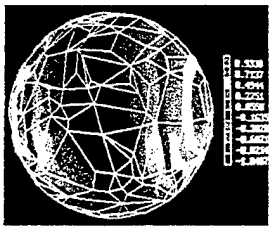

ZONA TECHNOLOGY

ZONAIR(II): Shock Location/Strength Correction by Perturbed Euler Formulation (PEF)

- **PEF for Shock Location/Strength Correction (Lighthill, 1960)**

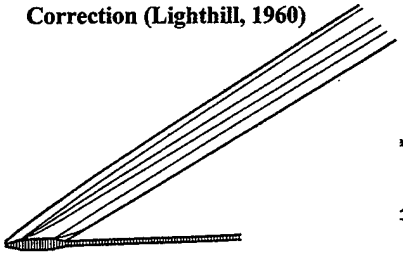

- **Oscillatory Shock of Panel Flutter due to PEF (Chavez & Liu, 1995)**

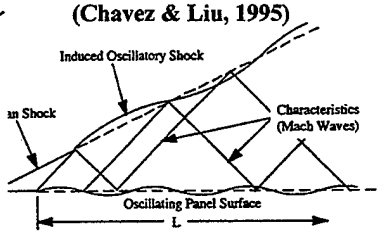

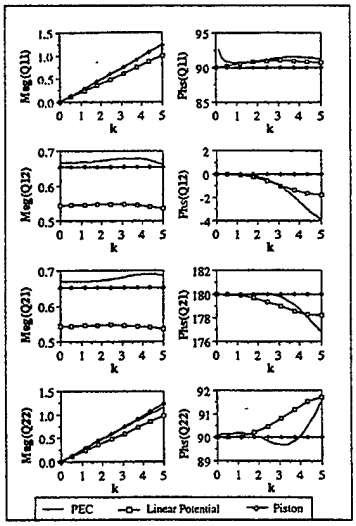

- **Solutions of Perturbed Euler Formulation (PEF) vs CFL3D (Liu & Tang, 2001)**

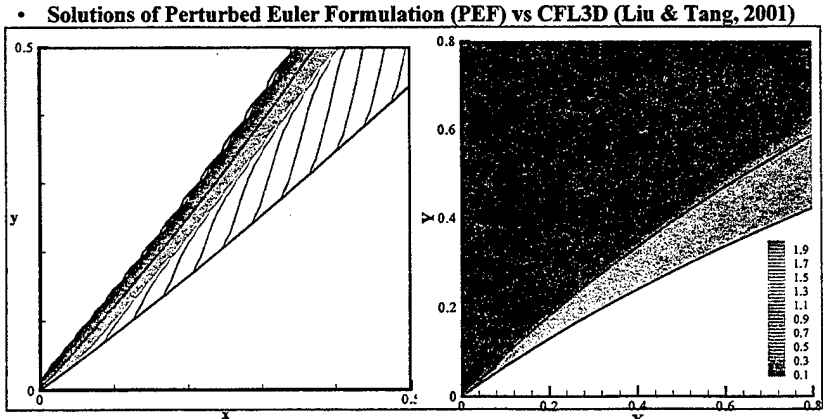

ZONA TECHNOLOGY

ZONAIR(III): ZONAIR Vortex Roll-Up for High Angles-of-Attack Aerodynamics

- Essential elements in ZONAIR for vortex roll-up modeling:
  - Vortex sheet emerging from the wing leading edge and tip (free vortex sheet)
  - Rolled-up core or spiral region (fed vortex sheet) fed by the leading-edge and tip-vortex sheets

Free/Fed Vortex Sheet Kinematics for Vortex Roll-Up

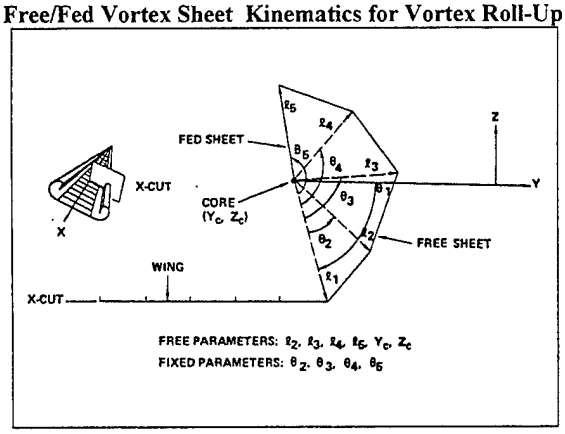

Force and Moment Coefficients of GAF vs Angle-of-Attack at M = 1.8

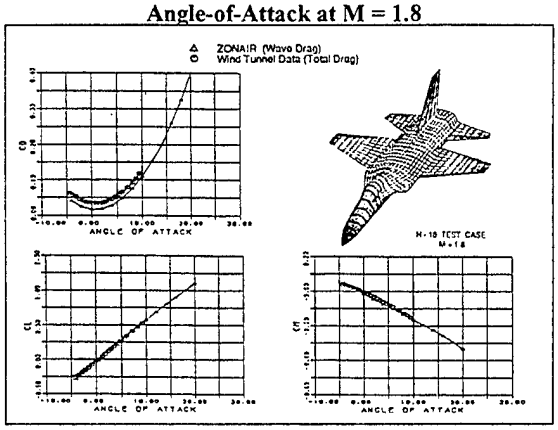

ZONA TECHNOLOGY

Capability Comparison: ZONAIR vs Other Aerodynamic Codes

Code	Method	Compu-tational Efficiency	Streamline Solution For Aeroheating	Hypersonic/ Supersonic/ Subsonic Mach No.	AIC for Structural FEM	Geometry High Fidelity	High AOA	2 Body Aero Inter-ference
CFL3D	Euler/N-S	30 hrs/ X-34	Yes	All	No	Yes	Yes	Yes
PANAIR	Potential	20 min/ X-34	No	Supersonic/ Subsonic	No	Yes	No	Yes
ZONAIR	Potential + PEF	20 min/ X-34	Yes	All	Yes	Linear-Order Panel	Yes	Yes
ZONA7U	Potential + PEF	10 min/ X-34	Yes	All	Yes	Constant-Order Panel	No	Yes
APAS	Potential + Empirical	< 10 min	Newtonian S.L.	Empirical for hypersonics	No	Low-Order Panel	No	Yes
MINIVER	Analytical/ Empirical	<< 10 min	No	No subsonics	No	No	No	No
DATCOM	Analytical/ Empirical	<< 10 min	No	All	No	No	Yes	No
AP98	Analytical/ Empirical	<< 10 min	No	All	No	No	Yes	No

AEROHEAT for Accurate Aerothermodynamic Analysis

- SHABP aeroheating analysis is based on empirical equations and is not accurate.
- AEROHEAT solves the convective-heating equations using an axisymmetric analogy that allows any axisymmetric boundary layer method to be applied along an inviscid surface streamline.
- Laminar and turbulent heating rates are calculated by relating the surface skin friction to the momentum thickness Reynolds number.
- the 3D effects of the AEROHEAT methodology is included through the streamline metric coefficients which can be accurately provided by the ZSTREAM code.
- The inviscid aerodynamic solutions required by AEROHEAT will be computed using ZONAIR.
- The integrated ZONAIR + ZATREAM + AEROHEAT computational procedure will be validated with the CFL3D + LATCH results of the CKEM body, 15° blunt cone and the X-34 wing-body configuration.

TPS Sizing Optimization Using Complex-Variable Differentiation Sensitivity

- TPS sizing will be automated by developing an optimization driver of the MINIVER/EXITS code.
- For a given heat flux $\dot{q}$ applied on the outer boundary, the objective is to minimize the total weight of the TPS system while keeping the temperature at each layer (T_i) below their respective maximum operational temperature, T_{oi}.
- Minimize: $W = \sum_{i=1}^{n} \rho_i h_i$ where ρ_i is the density of the i^{th} layer.

  Subjected to: $T_i < T_{oi} \qquad i = 1,2...n$

  Design variables: $h_i > 0 \quad i = 1,2...n$

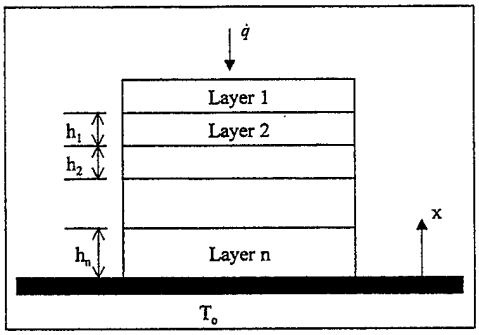

Typical TPS Sizing Problem

- The complex-variable differentiation can provide "numerically exact" derivatives of a complicated function.
  - -The variable h of a real function $T(h)$ is replaced by $h + i\Delta h$.
  - -For small Δh: $T(h+i\Delta h)=T(h)+i\Delta h\frac{\partial T}{\partial h}+\ldots$ Yields: $\frac{\partial T}{\partial h}=\frac{Im(T(h+i\Delta h))}{\Delta h}+0\left(\Delta h^2\right)$
- To incorporate the complex variable technique into the MINIVER/EXITS module for sensitivity analysis is straightforward simply by declaring all variables in the MINIVER/EXITS module as complex variables.
  - -The imaginary part of the thickness input of MINIVER/EXITS represents a small incremental thickness.
  - -The sensitivity is the imaginary part of the temperature output divided by the incremental thickness.

Temperature and Aeroloads Mapping from Aerodynamic to Structural Grids

- Displacement / forces mapping between FEM and aerodynamic grids is an existing capability in ASTROS*. Four spline methods are included:
  - infinite plate spline method
  - Thin plate spline method
  - Beam spline method
  - Rigid body attachment method
- Temperature mapping from aerodynamic to FEM surface grids will be developed using a finite-element-based mapping procedure
  - assumes a bilinear temperature distribution over the aerodynamic quadrilateral panel
  - Temperatures are defined at the corners of the panel and then mapped to the surface of the FEM model

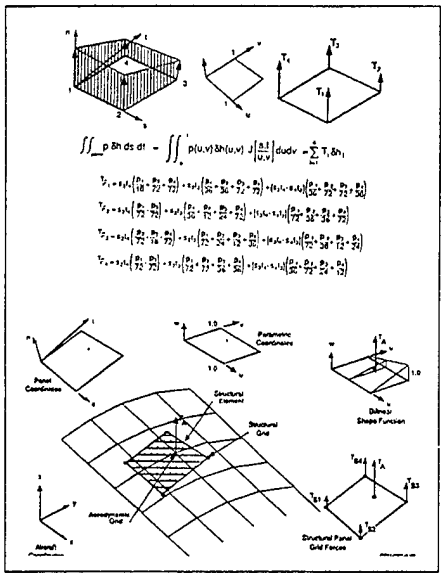

Temperature Mapping from Aerodynamic to Structure Grids

Automated Parametric Mesh Generation for ASTROS* and ZONAIR

- Automated parametric mesh generation for MSC/NASTRAN models is an existing capability in the Supersonic Hypersonic Vehicle Design (SHVD) system developed by LMCO/Technosoft.
- Because of the similarity between the MSC/NASTRAN and ASTROS*/ZONAIR bulk data cards. A mesh generator for ASTROS*/ZONAIR models can be developed with minor modification to the SHVD system.
- In order to monitor the progress of the ASTROS* optimization computation, a real-time graphical capability will be developed to display the design variables on the FEM model along with the active constraints at each optimization iteration.
- If an optimization solution cannot be achieved, the graphical capability will help the user to quickly identify the source of the problem and consequently modify the optimization problem statement until an optimum solution is obtained.

Test Beds of the Proposed Design Environment

- Hyper-X Configuration

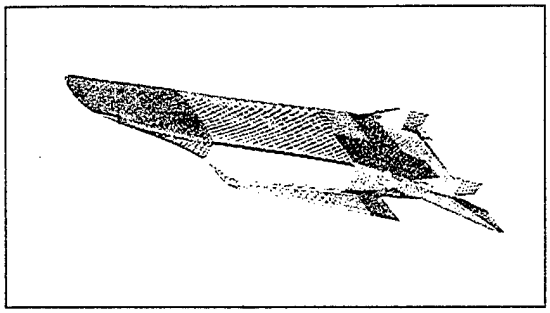

- A Reusable Military Launch System (RMLS)

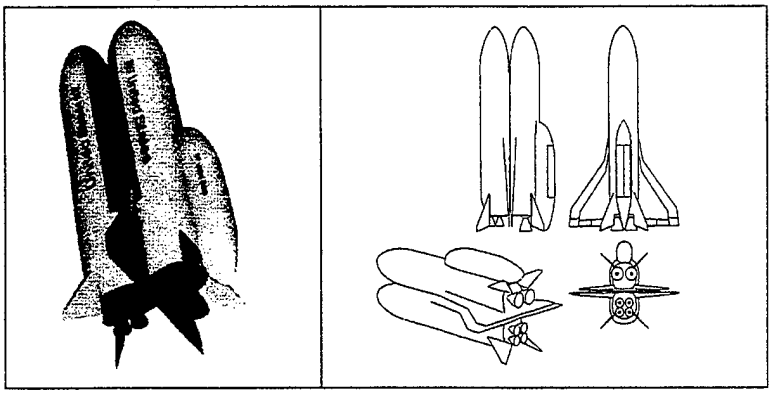

Demonstration of the Rapid Design Capability of the Proposed Design Environment

- Generate an *ASTROS** and *ZONAIR* model based on a set of initially guessed values of the geometric controlling parameters.
- Perform a *ZONAIR+ZSTREAM+AEROHEAT analysis* to establish the aerodynamic and aeroheating database.
- Obtain a trajectory of the initial design using *POST/OTIS*
- Conduct a *TPS* sizing over the entire vehicle based on the heat rate time histories computed by *POST/OTIS*
- Perform an *ASTROS** *optimization* computation for an optimum structural design
- Establish an updated weight of the vehicle and initiate a new trajectory analysis
- Repeat the above process until a converged solution is achieved
- Obtain a converged solution by defining a second set of geometric controlling parameters
- Compare the weight and performance of the two solutions for the sensitivity of the *RMLS* performance with respect to the geometric controlling parameters
- Graphically document all intermediate solutions during the iteration phase of the above two converged solutions
- Establish operational guidelines of the proposed design environment
- Conduct a final adjustment of the software system based on the experience gained during the *RMLS* design

Planned Program Schedule

Tasks	Yr 1 Quarter				Yr 2 Quarter				Performed by
	1	2	3	4	1	2	3	4	
1. Enhancement of ZONAIR for Hypersonic Aerodynamics									
• Incorporate the hypersonic methodology into ZONAIR									Z
• Validate the enhanced ZONAIR with the CFL3D results									Z
2. Integration of AEROHEAT into ZONAIR									
• Modify the AEROHEAT code to accept streamlines and inviscid pressures computed by ZSTREAM and ZONAIR									Z/D
• Validate the ZONAIR+ZSTREAM+AEROHEAT results with CFL3D+LATCH aeroheating results									Z
3. Development of Optimization for TPS Sizing									
• Incorporate the complex-variable differentiation sensitivity									Z
• Develop an optimization driver for TPS optimization									Z
4. Include TPS Mass and Stiffness Effects for Optimization of Main Structures									
• Develop an automated procedure to convert TPS stiffness/mass into equivalent composite laminate properties									Z
• Extract the inter-laminar shear stresses and shock loads from ASTROS* for detailed design of TPS structures									Z
5. Development of the Automated Parametric Mesh Generator for ASTROS* and ZONAIR									
• Modify the SHVD system for ASTROS*/ZONAIR meshes									T/Z
• Establish an automated procedure for defining the design variables and constraint functions.									Z/T
• Develop a real-time graphical capability to display the progress of the ASTROS* optimization computations.									Z
6. Development of Temperature Mapping Capability from Aerodynamic to Structural Grids									
• Establish a projection process to map the temperature distribution from the aerodynamic to structural grids									Z
• Output the mapping results in terms of NASTRAN or ASTROS* TEMP and TEMPD bulk data cards									Z
7. Demonstration of the Rapid Design Capability Using the Reusable Launch Vehicle (RLV) System as a Test Bed									
• Generate ASTROS*/ZONAIR model of the initial design									T/Z
• Perform a ZONAIR+ZSTREAM+AEROHEAT analysis									Z
• Obtain a trajectory of the initial design using POST/OTIS									Z
• Conduct a TPS sizing over the entire vehicle									Z
• Perform an ASTROS* optimization computation									Z
• Establish an updated weight of the vehicle									Z
• Repeat the above process for a converged solution									Z
• Obtain a converged solution by defining a second set of geometric controlling parameters									Z
• Compare the weight and performance of the two solutions for the sensitivity of the RLV performance									Z
• Graphically document all intermediate solutions									Z/T
• Establish operational guidelines									Z
• Conduct a final adjustment of the software system									Z/T
8. Documentation of the Proposed Design Environment									
Kick-Off Meeting	▲								
Final Oral Presentation									▲

Z = ZONA Technology; T = TechnoSoft; D = Dr. DeJarnette